Experimental Studies of Greenschist and Amphibolite Facies Metamorphism of Basic Rocks

by

Nicholas Francis Best B.A. (Oxon)

Thesis submitted for the degree of

Doctor of Philosophy

University of Edinburgh

1977

DECLARATION

I, hereby, declare that all work presented in this thesis is my own, except where specifically stated in the text, and that the thesis has been composed by myself.

N.F. BEST

ABSTRACT

The transition from the greenschist to the amphibolite metamorphic facies is essentially defined on the basis of changes in the mineral assemblages found in basic rocks. In broad terms, the change is from a chlorite - actinolite - albite - epidote - quartz - bearing assemblage to one dominated by hornblende and plagioclase. The reactions involved in the transition are complex, and are manifested in cryptic compositional variation in co-existing phases as much as in actual phase changes.

To appreciate the significance of these compositional variations, the nature of the solid solutions in the various minerals must be understood. In this work, the clinozoisite - epidote solid solution series has been explored in an unrealistic divariant reaction and in a naturalistic multivariant reaction, and it is shown that the former yields data with a wider field of application. A preliminary examination of the edenite - tremolite substitution in calcic amphiboles has also been undertaken, using a simple iron-free divariant reaction.

One of the major factors controlling greenschist facies metamorphism, and producing changes in the phase assemblage, is fluid phase composition. A mixed volatile model, simulating basic rocks in the system CAFMS - H_2O - CO_2 has been derived from field observations, and, in this thesis, is quantified experimentally, at 5 Kb, in an iron-free system. Subsequently, using both established and assumed solid solution properties for the various minerals, and phase chemical data from natural Dalradian metadolerites, several alternative 'real rock' models have been constructed, and are distinguished, and judged on field evidence, and independent experimental work on the various titanium minerals found in the metadolerites.

ABSTRACT CONTD.

The field of study is too large for a complete synthesis of the thesis work to be constructed, and so various convergent lines of research are suggested, to link the present isolated elements.

CONTENTS

CONTENTS CONTD.

CHAPTER 1

1) General Remarks:

Variations in the mineral assemblages found in metamorphic rocks of a given composition provide the basis for assessing changes in the physical conditions of metamorphism, and thereby give an indication of the conditions within the Earth's crust and mantle. Specific phases, and phase assemblages have been used empirically by geologists to characterize certain conditions of rock formation. Thus, Barrow (1893) developed the basis for the concepts of metamorphic grades and zones, by identifying a continuous series of changes in the mineral assemblages of pelites. Similarly, Eskola (1915, and subsequently) used the mineral assemblages in metabasalts to identify a series of metamorphic facies by which different patterns of regional metamorphism could be categorized. Within this basic framework, numerous petrographers have worked to increase the general awareness of the many mineral assemblages which reflect the physical conditions of metamorphism, in the varied chemistries of natural rocks.

Following this accumulation of information on natural rocks, laboratory experimental studies on mineral stabilities have provided a means of estimating the absolute values of the temperatures, pressures and fluid compositions in existence during the formation of rocks. This thesis represents such an experimental study on the mineral assemblages to be found in metabasic rocks in the greenschist, epidote-amphibolite, and amphibolite facies, erected by Eskola (1939). In broad terms, the change across these facies is from a chlorite - albite - actinolite - epidote - quartz assemblage to one dominated by

hornblende and plagioclase, which may also contain, either or both, epidote and garnet. The reactions involved in the transition are complex, and manifest themselves through cryptic variation in the compositions of co-existing phases, as well as through actual changes in the phase assemblage. Thus, although epidote disappears in the transition, the increase in calcium content of the plagioclase is a more sensitive indicator of the actual reactions in progress. Again, although garnet appears, through a complex of reactions centred around the breakdown of chlorite, the distribution of iron between chlorite and amphibole is more widely indicative of changing metamorphic conditions. (Miyashiro 1968, Harte and Graham 1975). In addition, the composition of the fluid phase, especially the H_2O and CO_2 content, exerts a strong influence over the mineral assemblages actually to be found in the field (Billings and White 1950, Harte and Graham 1975).

It is perhaps because the reactions involved are so complex, and their effects relatively inapparent that the greenschist to amphibolite facies transition has received much less experimental attention than the phase assemblage changes in pelitic rocks. Enough experimental data exists on the latter to construct extensive petrogenetic grids (Harte 1976). Using these data it is also possible to estimate the absolute physical conditions of metamorphism of metabasic rocks by comparison with associated metapelites. Thus, Turner (1968 esp fig 8-6), inter alia, has estimated the metabasic facies transition to cover the ranges 400°C - 600°C, 4-8 Kb. Liou et al (1974) support these estimates with hydrothermal experiments on natural metabasalts.

Using the disappearance of chlorite, and changes in amphibole and plagioclase composition as indicators, they find a transition range of 475 - 550°C at 2 Kb, and 500 - 575°C at 5 Kb. An alternative technique for the estimation of absolute physical conditions of metamorphism produces more precise values, but by a weaker theoretical argument. It depends upon the equation of a metamorphic facies boundary with the appearance or disappearance of a single phase, and employs mineral stability data to quantify the boundary. Thus, if the base of the greenschist facies can be equated with the appearance of the assemblage epidote plus actinolite, then the experimental data obtained by Nitsch (1971) on the reactions:

$$\text{pump} + \text{chlor} + \text{qtz} = \text{ep} + \text{act} + H_2O$$

and

$$\text{prehn} + \text{chlor} + \text{qtz} = \text{ep} + \text{act} + H_2O$$

can be used to locate the boundary at around 350°C. Similarly, if the highest grade of the greenschist facies is identified by the last occurrence of chlorite in the phase assemblage, the stability studies of Hsu (1968), and Fawcett and Yoder (1966) on Fe- and Mg-chlorite respectively, giving breakdown temperatures of around 600°C, may be relevant.

2) Objectives:

The objectives of this thesis are the complete experimental definition of reaction relationships across the wide range of greenschist, epidote - amphibolite, and amphibolite facies mineral

assemblages in metabasic rocks, and the simultaneous establishment of the temperature, pressure and fluid phase conditions for their respective stabilities. To avoid unnecessary restriction in applicability, simplified chemical systems have been adopted, with the intention of applying these to natural rocks by gradually increasing their complexity, and by combining the experimental data thermodynamically. In this fashion, it should be possible to model the conditions of metamorphism of any rock that has an essentially basic composition. Table 1:1 is a list of mineral abbreviations, and thermodynamic and algebraic terms used throughout the thesis.

The experimental work has fallen into two broad divisions. The first has involved the study of the stability and solid solution properties of individual minerals under greenschist to amphibolite facies conditions, in the presence of a pure H_2O (hydrous) fluid. The second part has been concerned with the development of a mixed (CO_2 - H_2O) fluid model for the entire greenschist facies.

a) Single mineral stabilities in a hydrous fluid:

The complex transition from greenschist to amphibolite facies can be resolved into a number of relatively simple, hypothetically separate reactions; e.g.

$$\text{chlor} + \text{qtz} = \text{gnt} + H_2O$$

$$\text{ab} + \text{act} = \text{eden} + \text{qtz}$$

$$\text{ab} + \text{ep} + \text{qtz} = \text{gnt} + \text{plag} + H_2O$$

The original intention of this part of the thesis was to investigate some of these basic reactions in simple chemical systems,

TABLE 1:1

MINERAL ABBREVIATIONS, AND THERMODYNAMIC AND ALGEBRAIC TERMS USED THROUGHOUT THIS THESIS

a_x^y	activity of endmember, or chemical component x, in phase or site y
ab	albite
act	actinolite
alm_x	almandine, mole fraction of almandine in garnet
amph	amphibole
an_x	anorthite, mole fraction of anorthite in plagioclase
and_x	andradite, mole fraction of andradite in garnet
ank	ankerite
biot	biotite
cc	calcite
cchlor	clinochlore
ch	no. of Al ions (VI + IV) per 6 octahedral chlorite sites
chl 2	chlorite with 2 Al ions (VI + IV) per 6 octahedral sites, i.e. clinochlore
chlor	chlorite
czo	clinozoisite
dol	dolomite
$eden_x$	edenite, mole fraction of edenite in amphibole
en	enstatite
ep	epidote
f_{O_2}	oxygen fugacity

TABLE 1:1 CONTD.

fo	forsterite
$G_f^{1,298}$	Gibbs' energy of formation at 1 bar, 298 K (25°C)
$\Delta G_R^{P,T}$	Gibbs' energy of reaction of P,T
$G^*_{H_2O}(P,T)$	Free energy of pure water at P,T
gnt	garnet
$gross_x$	grossular, mole fraction of grossular in garnet
HM	haematite-magnetite oxygen buffer
K	equilibrium constant
Kb	Kilobar
K_D	distribution coefficient, e.g. $(X^{M1}_{Fe}/X^{M1}_{Al})/(X^{M3}_{Fe}/X^{M3}_{Al})$
ky	kyanite
μl	microlitre 10^{-3} cm^3
ln	natural log
A_{M_x}, M^A_x	A co-ordinated site, containing ion x
msc	muscovite
mgs	magnesite
MH	haematite-magnetite oxygen buffer
MRK	modified Redlich-Kwong model for non-ideal mixing of gases
NNO	nickel-nickel oxide oxygen buffer
P	pressure
P_{CO_2}	of CO_2
P_{flu}	of fluid
P_{tot}	total pressure
(phase)	absent phase designation for invariant or univariant
plag	plagioclase

TABLE 1:1 CONTD.

prehn	prehnite
psi	pounds per sq. inch
ps_x, Ps_x	mole fraction of pistacite in epidote
pump	pumpellyite
pyroph	pyrophyllite
qtz	quartz
R	gas constant 1.987 cal/deg
rut	rutile
S_f^{298}	entropy of formation, at 298 K (25°C)
sid	siderite
sp	spinel
sph	sphene
system	
A	Al_2O_3
C	CaO
F	FeO , Fe_2O_3
M	MgO
N	Na_2O
S	SiO_2
T, T_C	Temperature, generally in K; critical temperature
tc	talc
tr, trem	tremolite
$\overline{V}^{1,298}$	molar volume, at 1 bar, 298 K (25°C)
ΔV^1_{sol} , ΔV^1_{a-b}	molar volume change of solids (a-b) in reaction, at 1 bar
W	interaction parameter for regular binary solid solution

TABLE 1:1 CONTD.

W_{xy}	interaction parameter for regular ternary solid solution
W_1, W_2	interaction parameters for subregular solid solution
x_c	critical composition on solvus
X_x^y	mole fraction of component of endmember x, in site or phase y
zo, zois	zoisite
Γ_{vol}	fugacity coefficient of volatile
γ_x^y	activity coefficient of component or endmember x, in site as phase y
μCO_2	chemical potential of CO_2

and then approximate more closely to natural rocks by gradually increasing the complexity of the chemical system. In view of previous experimental work (Newton 1966, Holdaway 1972, Liou 1973), it was possible to start experiments on the stability of epidote in the fairly complex NCAFS - H_2O system. These experiments are described in Chapter 2.

This approach subsequently became modified by the need for specific thermochemical data on several of the minerals exhibiting solid solution, and the realization that, once such data was available, it would be possible to model complex natural systems, thermodynamically, with only limited recourse to further experimentation. The study of epidote-clinozoisite solid solution which evolved from the epidote-albite study is detailed in Chapter 3. Since the edenite and tschermakite endmembers of the calcic amphiboles are unstable, reactions designed to elucidate amphibole solid solution must also permit the derivation of endmember thermochemical data. Chapter 7 describes a preliminary attempt to do this for the tremolite-edenite series, and it is hoped to continue this promising line of research.

b) Greenschist facies assemblages, in the presence of a mixed (H_2O - CO_2) fluid phase:

Chapters 4, 5 and 6 are concerned with the influence of fluid composition on mineral assemblages, and particularly, with the development of a model for greenschist mixed volatile (H_2O - CO_2) metamorphism. The model is based on field evidence (Billings and White 1950, Graham 1973, Harte and Graham 1975) and is quantified experimentally, at 5 Kb, in the simple system CAMS - H_2O - CO_2.

Recalculation of the data to model natural rock assemblages generates several alternative possibilities, which are subsequently distinguished on field evidence, and experimental data from other sources.

3) Experimental procedure - the high pressure equipment:

Standard fluid media pressure apparatus, as described by Edgar and Platt (1971) was used for all experiments. For runs up to 5 Kb and 750°C; which covers the conditions of all the mixed volatile data, most of the epidote-albite data, and about half the edenite-tremolite data, "Tuttle-type" coldseal pressure vessels were used. Temperatures were measured using platinum vs platinum/13% rhodium thermocouples. The uncertainty in temperature measurement associated with this apparatus is believed to be within $\pm$ 5°C (Ford 1972). Experiments above 5 Kb, and at high temperatures; that is the epidote-anorthite-kyanite series, and most of the tremolite-edenite series, were performed using internally heated gas vessels. Using the same type of thermocouples, temperature control with this equipment is to within $\pm$ 1°C.

On both systems, the pressure is measured using a single manganin gauge on the main pressure line, by equalizing the pressure in the line and the pressure vessel. This procedure is believed to involve a total uncertainty of $\pm$ 100 bars. (Ford, pers. comm.)

The temperature scales were calibrated up to 600°C against standard mixtures of NaCl and Na_2CO_3, using d.t.a. to determine the melting point (Ford 1972) during the period of the thesis experimental work. The pressure scale was calibrated using a mercury cell, in

November 1976. The freezing pressure of mercury at 0°C is an arbitrary fixed point on the pressure scale (Bridgeman 1911), which Newhall et al (1963) have located at 7565.4 bars (109760 $\pm$ 750 psi) using a manganin gauge. The pressure calibration bracketed it at 7590 $\pm$ 100 bar (110055 psi). (C. Begg, pers. comm.).

CHAPTER 2

STABILITY OF THE ASSEMBLAGE EPIDOTE-ALBITE

Introduction:

Between the upper greenschist and the higher grades of the amphibolite facies, the main calcium-bearing phase in metabasalts changes from epidote to plagioclase.

The breakdown of epidote-zoisite minerals, at high temperatures, in the presence of quartz, has been studied by several workers, in progressively more complex chemical systems. The simplest system in which zoisite can exist is CAS-H_2O, where its breakdown reaction is univariant:

$$4 \text{ zoisite} + \text{qtz} \longrightarrow \text{grossular} + 5\text{an} + 2H_2O$$

This reaction has been studied experimentally, using natural minerals, by Strens (1965) and Newton (1966). The latter obtained a curve which passes through 618°C at a pressure of 4.6 Kb (water saturated) and 765°C at 8 Kb (Table 2:2).

The addition of iron to the system creates an extra degree of freedom, which can be taken up by definition of the epidote composition. This is normally expressed in terms of solid solution between clinozoisite and the hypothetical endmember, pistacite ($Ca_2Fe^{III}_3Si_3O_{12}(OH)$, so that e.g. Ps_{24} represents the epidote $Ca_2(Al_{2.28}Fe^{III}_{0.72})_3Si_3O_{12}(OH)$. However, some German workers define epidote compositions in terms of the endmembers clinozoisite and $Ca_2Al_2Fe^{III}Si_3O_{12}(OH)$ (e.g. Raith 1976).

Two workers have published experimental data on the reaction in the CAFS-H_2O system. Liou (1973) studied the stability relations of epidote, in the presence of quartz, by recrystallizing an oxide mix of bulk compositions Ps_{33}, over a range of P-T-$^fO_2$ conditions. At low oxygen fugacities (around the NNO buffer, and below), he obtained multivariant assemblages which included epidote, iron spinels, garnet and pyroxene. At the MH buffer and above, with the iron predominantly ferric, the epidote broke down across a pseudo-univariant reaction giving anorthite and grossular-andradite garnet, the composition of which Liou has estimated to be about $gross_{30}$. Holdaway (1972) studied the specific reaction producing grandite garnet and anorthite, using natural minerals, at the MH buffer. In particular he showed that ps_{30} epidote equilibrated with a garnet of composition and$_{63}$ $gross_{34}$ alm_3. From this reaction data on epidote, and parallel studies involving natural zoisite (1966), Holdaway has estimated the zoisite-clinozoisite (ps_0) phase transition to be isothermal above 3 ± 1 Kb, at $635 \pm 75^{\circ}C$. (1972).

Experimental Work:

The presence of albite decreases the stability field of epidote, by stabilizing plagioclase in the breakdown assemblage (decreasing the activity of the anorthite component):

$$\text{albite} + \text{epidote} + \text{quartz} \longrightarrow \text{garnet} + \text{plag} + H_2O$$

A series of experiments have been conducted to explore this effect, by recrystallizing a nitrate gel (Biggar & O'Hara 1969) in the presence of albite and quartz (cf. Liou 1973). The phases used were:

epidote nitrate gel (Ps_{33})

natural quartz

natural low albite

synthetic high albite

The natural minerals were ground to an average size of 15μ, and the charges made up in the weight ratios:

N : 6 epidote : 3 low albite : 1 quartz

A : 6 epidote : 3 high albite : 1 quartz

Q : 7 epidote : 3 quartz

The proportion of albite was calculated to produce plagioclase compositions similar to those found in amphibolites, (an_{30}) when combined with the anorthite formed by the epidote breakdown. Two forms of albite were used, (natural, 99.9 per cent pure, from a low temperature blueschist assemblage, and synthetic, recrystallized from a gel at 900°C, P_{H_2O} = 2Kb, for 48 hours), in case the free energy difference between high and low albite was significant. On average, the high temperature assemblage crystallized better from the charges containing synthetic high albite (A series) than from those containing natural low albite (N series). However, no actual separation of reaction curves could be distinguished within experimental accuracy ($\pm$ 5°C; Ford, 1972). The albite-free charges were run as a check on Liou's (1973) data.

The charges were sealed, with excess water, in Ag_{70} Pd_{30} capsules (2 mm) and run in coldseal bombs, except for a couple of runs above 5Kb, for which internally heated vessels were required.

TABLE 2:1

EPIDOTE STABILITY: EXPERIMENTAL DATA FOR THE REACTIONS:

Q : $ep + qtz = gnt + an + H_2O$

A,N: $ep + qtz + ab = gnt + plag + H_2O$

Run	Vessel	P Kb	T °C	Durn. (hrs)	Buffer replacements	Products Q	A,N
H 2	coldseal	4	721	67	2	gnt	---
H 3	"	4.7	718	71	2	ep	---
H 4	"	4	681	72	2	ep	gnt
H 5	int. htd.	6	750	48	1	ep	gnt
H 6	"	6.2	710	50	1	---	ep
H 7	coldseal	4	654	106	3	---	ep
H 8	"	3	670	50	1	ep	gnt
H 9	"	3	690	72	1	gnt	---
H12	"	2	640	72	2	gnt	gnt
H14	"	3	605	85	3	---	ep
H15	"	2	591	85	3	ep	gnt
H17	"	5	703	72	2	---	ep
H19	"	4.5	691	60	2	ep	gnt
H25	"	4.51*	736	100	2	gnt	ep + gnt
H28	"	1.01	577	67	2	gnt	gnt
H30	"	3.51	700	94	2	gnt	---
H31b	"	3.52	688	125	3	ep	---
H32b	"	3.49	651	156	3	ep	gnt
H33	"	3.50	642	143	3	---	ep + gnt
H35	"	3.01	623	293	4	---	gnt
H36	"	2.01	615	260	2	ep + gnt	gnt
H26	"	4.48	688	96	2	ep	---

Reaction reversals (A,N only):

Run	Vessel	P Kb	T °c	Durn. (hrs)	Buffer replacements	Reaction direction
HR 1	int. htd.	5.01	716	68	3	ep → gnt
HR 3	coldseal	2.97	630	190	2	ep → gnt
HR 8	"	3.03	599	88	3	gnt → ep
HR 9	"	3.98	652	74	2	gnt → ep
HR10	"	5.01	695	48	2	gnt → ep

*Introduction of manganin pressure gauge, previously a bourdon-tube gauge was in use.

Figure 2:1 Equilibrium Curve for Reaction:

$$ep + qtz \longrightarrow gnt + an + H_2O$$

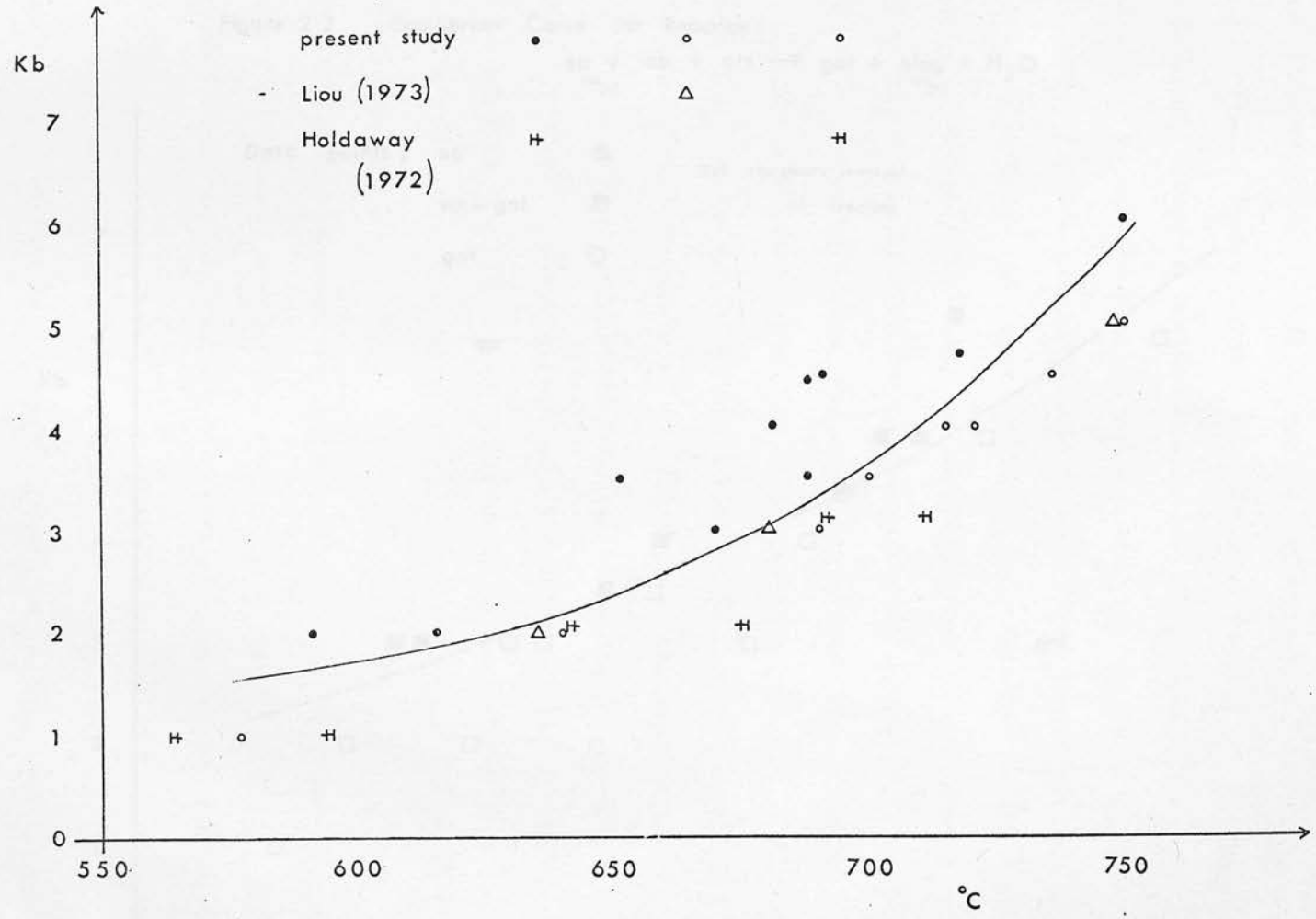

Figure 2:2 Equilibrium Curve for Reaction:

$$ep_{ps_{33}} + ab + qtz \longrightarrow gnt + plag_{an_{30}} + H_2O$$

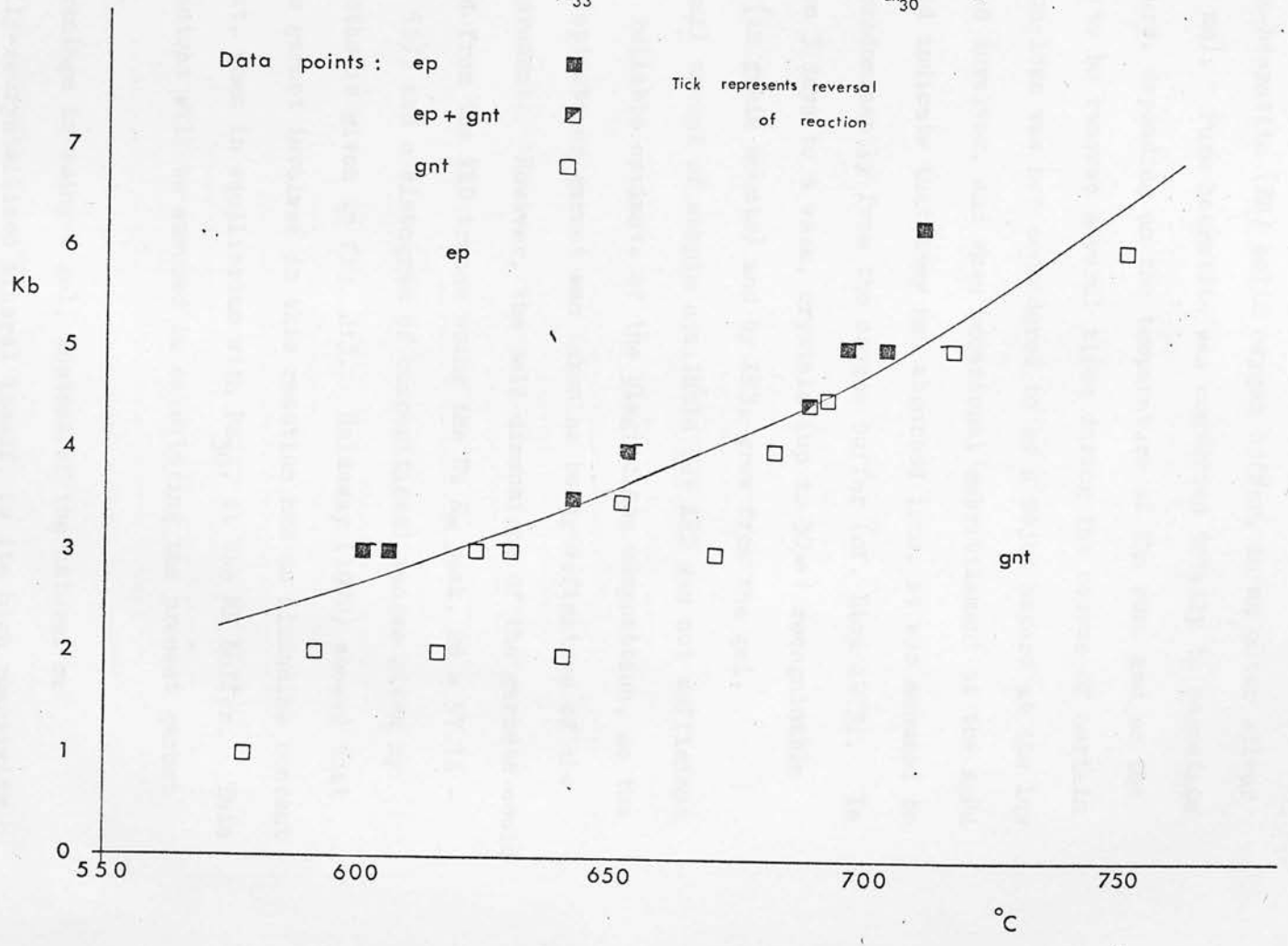

The oxygen fugacity was maintained by sealing the 2mm capsule, with a magnetite-haematite (MH) solid oxygen buffer, in an outer silver capsule (3 mm). Pure haematite was converted totally to magnetite in 6-48 hours, depending on the temperature of the run, and so the buffer had to be renewed several times during the course of certain runs. Iron-loss was not considered to be a major hazard at the low temperatures involved, and when occasional embrittlement of the AgPd capsules did indicate that they had absorbed iron, it was assumed to have come predominantly from the oxygen buffer (cf. Liou 1973). In runs of from 3 days to a week, crystals (up to 30μ) recognisable optically, (in grain mounts) and by XRD, grew from the gel.

The small amount of sample available for XRD was not sufficient to obtain a reliable estimate of the plagioclase composition, so the presence of epidote or garnet was taken as being definitive of the assemblage present. However, the cell dimensions of the garnets could be estimated from the XRD traces using the Cu K_α peak, $2\theta = 57.16 - 58.35^\circ$ (N = 56), and a histogram of compositional ranges given by the peak widths is given in fig. 2:3. Holdaway (1972) showed that the grandite garnet involved in this reaction has an almandine content of 3 per cent, when in equilibrium with Ps_{30}, at the MH buffer. This almandine content will be assumed in calculating the present garnet composition.

The advantage in using a gel, instead of the natural or hydrothermally-recrystallized mineral itself, is its high reactivity, which at, for example, temperatures of 6-700°C causes phases to recrystallize within a week or so; while under similar conditions,

Figure 2:3 Histogram of ranges in unit cell size of garnet from breakdown of ps_{33} at MH buffer, derived from XRD peak widths at CuK_α 2θ 57·16–58·35° (N = 56)

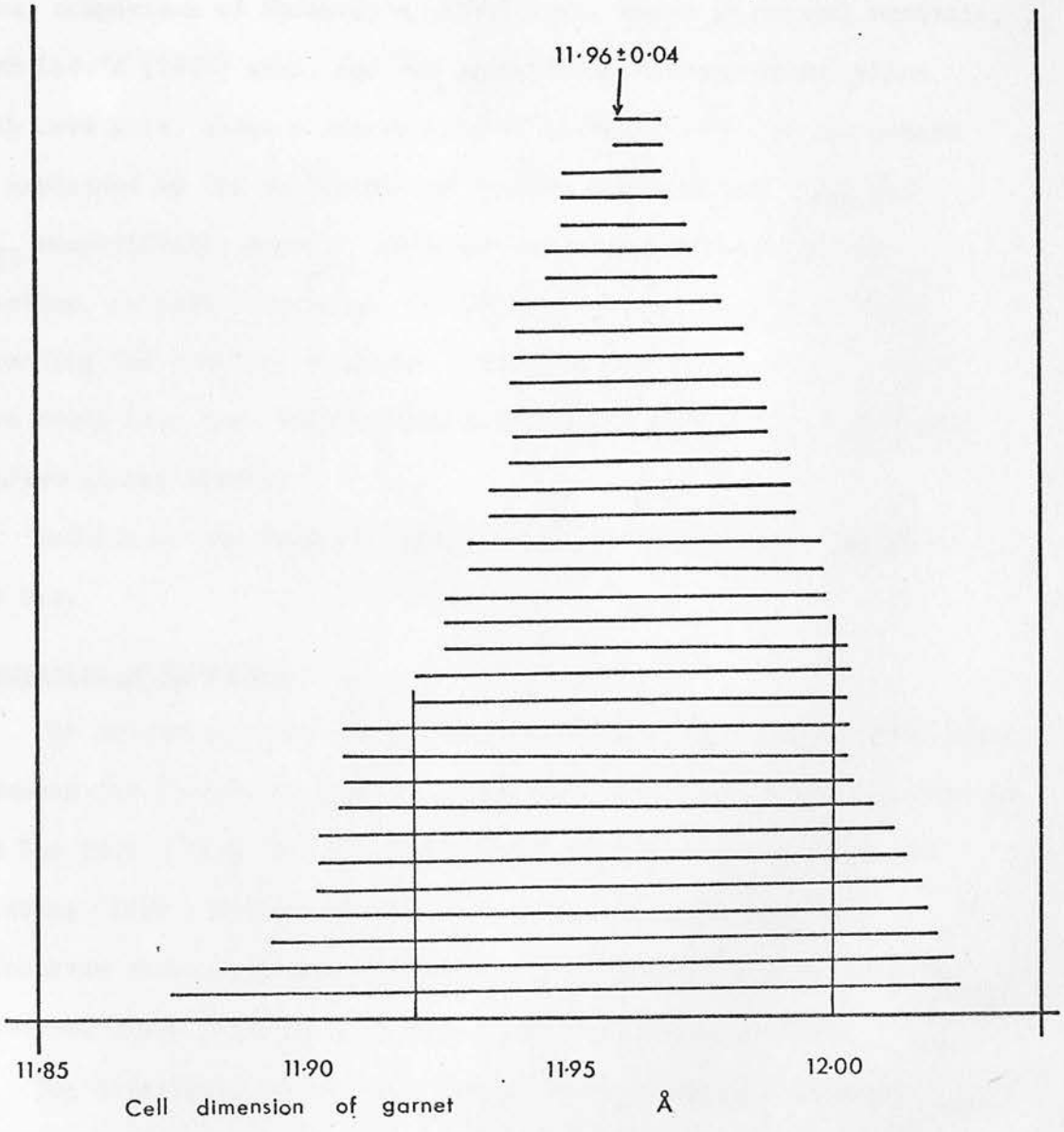

natural minerals would require runs of about a month to generate observable reaction. However, the great danger is that the results may represent a "synthesis curve" (Fyfe 1960), owing more to rates of nucleation and crystal growth, than to actual mineral stability. Thus, comparison of Holdaway's (1972) data, based on natural minerals, with Liou's (1973) work, and the present albite-free study, which both used gels, shows a discrepancy of at least 15°C - which cannot be explained by the difference in epidote compositions (Ps_{30} and Ps_{33} respectively) alone. Care has been taken to reverse the reaction, in both directions, in the albite-bearing system, by rerunning the reaction products. However, the subsequent value of this study (see next chapter) has not merited a re-evaluation using recrystallized phases.

Details of the runs are presented in Table 2:1, and figures 2:1 and 2:2.

Discussion of Results:

The univariant reaction studied by Newton (1966) can be calculated, assuming the Fisher-Zen approximation for dehydration reactions (Fisher and Zen 1971), from the thermochemical data published by Robie and Waldbaum (1968), and Zen (1972). As shown in Table 2:2, the calculated curve, and experimental data agree well. This is to be expected, since Newton's work was one of Zen's data sources.

The divariance of the reaction in the more complex chemical systems is dependent upon the activities of the various reacting endmembers; that is: grossular in grandite garnet, clinozoisite in epidote, and in the case of the albite-present study, anorthite

TABLE 2:2

A comparison of Newton's (1966) experimental data on the equilibrium:

$$4 \text{ zois} + \text{qtz} = \text{gross} + 5 \text{ an} + 2 H_2O$$

and the curve:

$$136330 - T(128.33) + 1.424P + 2G^*_{H_2O}(P,T) = 0$$

calculated from data published by Robie & Waldbaum (1968), and Zen (1972)

Newton's data		$G^*_{H_2O}$ cals	calculated data points	
T^oC	P Kb		G_R cals	T^oC
618	4.6	-33429	- 77	617
650	5.6	-31799	+500	658
670	6	-30906	+289	675
720	7.2	-29572	+249	725
765	8	-26607	-456	758

from Fisher & Zen (1971)

in plagioclase. Of these, data only exists for the last solid solution. Orville (1972) has estimated the activity of anorthite in plagioclase, empirically, at 700°C and 2Kb, from solution energy data. For plagioclases in the composition range an_{0-30} he obtains an activity coefficient of 1.28. The error involved in using this value lies mainly in its unknown pressure dependence.

In the absence of data on the other two solid solutions, and, indeed, the absence of data on clinozoisite itself, no extrapolation of these experimental data sets to natural rocks can be made, nor can their relative values be determined, although the raw experimental data and the techniques used give some indication of this.

In general, all that can be deduced from these studies is an estimation of the maximum temperature, and water pressure at which epidote ($Ps_{30,33}$) with or without albite can exist. As Liou (1973) points out, the stability field of epidote will be extended in f_{O_2} space, when it co-exists with Fe^{II}-bearing silicates, such as chlorite. However, these extensions may well be in temperature as well, so no predictions beyond the HM oxygen buffer can be made from the present data set.

CHAPTER 3

EPIDOTE ACTIVITY - COMPOSITION RELATIONSHIPS

Introduction:

The previous chapter on epidote-albite assemblage stability is a prime example of the experimental method which seeks to simulate natural assemblages by gradually increasing the complexity of a synthetic system. The approach was able to define the upper limit of the P-T stability field of epidote - ps_{33} and albite, at the MH oxygen buffer, fairly precisely, but even slight variations in epidote composition, or oxygen fugacity effectively invalidated the data. The complex simulation of a natural assemblage could be applied only to rocks for which identical conditions of equilibration could be assumed. Attempts to reduce the data to thermodynamic terms failed through lack of data on the individual minerals.

An alternative experimental approach is to try to obtain data on individual minerals, rather than on entire mineral assemblages, and then to use the data in theoretical syntheses of the natural assemblages. Then, a few experiments in the natural system are sufficient to confirm the extrapolation. Applying this approach to the problem raised in the last chapter, the major data gaps concern clinozoisite and the clinozoisite-epidote solid solution. A standard technique has been developed over the past few years for establishing the activity-composition relationships in a solid solution (Wood 1975). A univariant reaction is studied, firstly, in a chemical system which allows no solid solution in any of the phases involved; and then in a

system which permits solid solution only in the phase of interest. Departure from the univariant is, then, wholly attributable to that solid solution. For epidote, such a reaction is:

$$2\ czo + ky + qtz = 4\ an + H_2O$$

since epidote is the only phase to show extensive solid solution in the system $CAF^{III}S\text{-}H_2O$. Chinner et al (1969) do quote iron contents in Dalradian kyanites of up to 1%, so this possibility must be included as a minor source of uncertainty in any end-product solution model. One advantage of this approach is that the stability of the other component in the solid solution (in this case, pistacite) is irrelevant, unless its breakdown phases (magnetite and anorthite) form solid solutions with the other phases in the reaction.

Experimental:

1) Previous Work:

No experimental data on the reaction:

$$2\ czo + ky + qtz = 4\ an + H_2O$$

has been published. However, Newton (1966) has bracketed the equivalent reaction, involving zoisite and sillimanite, metastably, in the kyanite field, at 550°C, 7.2 $\pm$ 0.1 Kb, and 650°C, 8.85 $\pm$ 0.15 Kb. Boettcher (1970), in a broad survey of the system $CAS\text{-}H_2O$, has located the zoisite-kyanite reaction at 12.7 Kb, 760°C; and adjusting Newton's data by 270 bars, as a correction to kyanite, arbitrarily accepts the datapoint at 650°C, but not that at 550°C. (fig 3:1)

Figure 3:1 Base Univariant Reaction

$$2zo + ky + qtz \longrightarrow 4an + H_2O$$

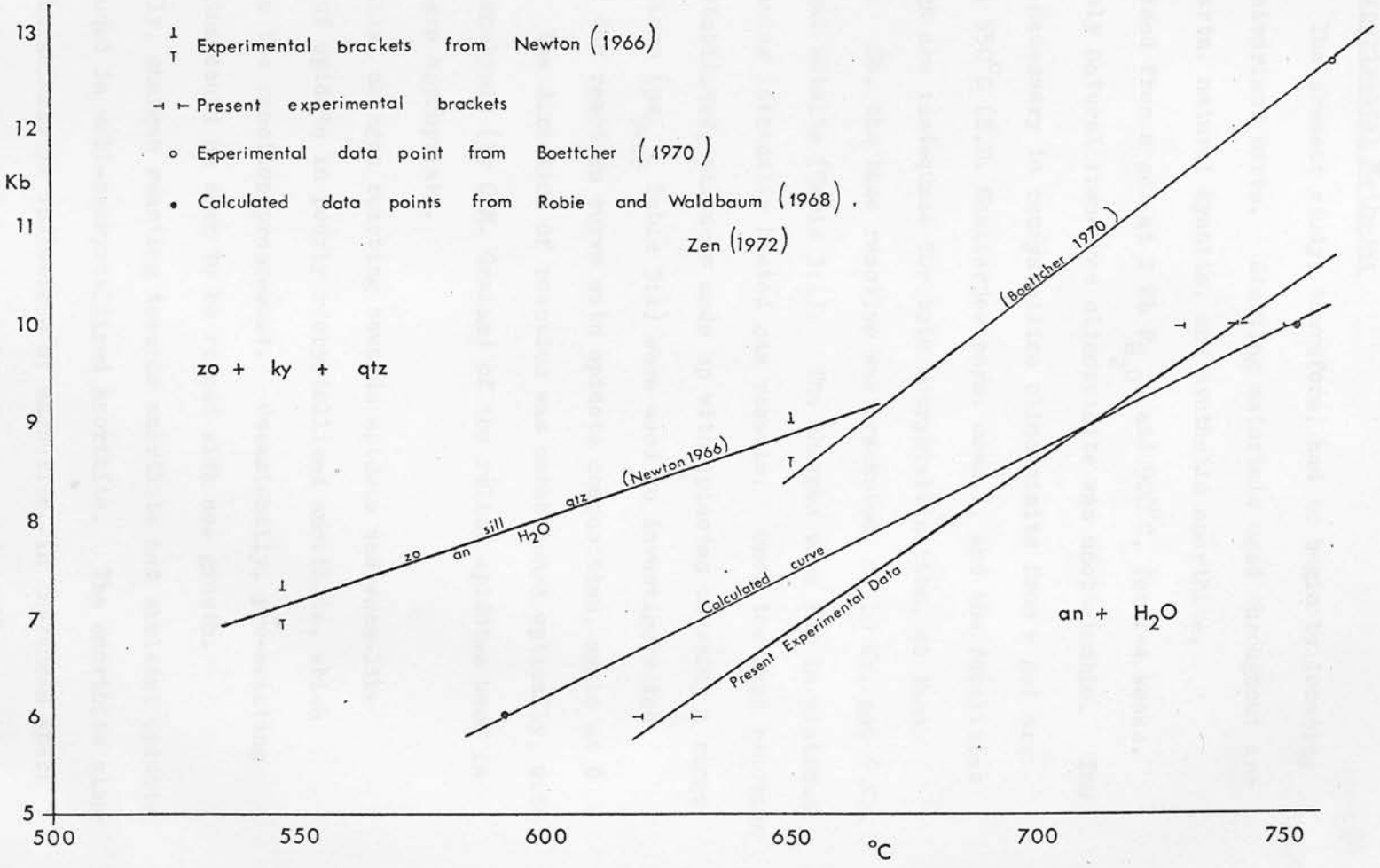

2) Experimental Methods:

The present study, therefore, had to begin by locating the base univariant curve. Starting materials used throughout are natural quartz, natural kyanite, and synthetic anorthite, recrystallized from a gel at 1 Kb P_{H_2O}, and 900°C, for 1-4 weeks. Unfortunately natural iron-free clinozoisite was unobtainable. The conditions necessary to recrystallize clinozoisite from a gel are 15 Kb P_{H_2O}, 550°C (N.D. Chatterjee pers. comm.), and the facilities at Edinburgh are inadequate for bulk recrystallization, at these conditions. So, the base reaction was bracketed, at 10 Kb, and 6 Kb, using natural zoisite (Table 3:1). The charges were run in platinum capsules, using internally heated gas vessels. Once the base reaction has been established, mixtures made up with epidotes covering a range of compositions (ps_{9-29} Table 3:1) were used to investigate the movement of the reaction curve with epidote composition, again at 6 and 10 Kb. The direction of reaction was established optically, with microprobe analysis (by C.M. Graham) of the relict epidotes used in support, where appropriate.

Typically, charges reacting towards epidote had worm-like inclusions of epidote in poorly recrystallized anorthite, which coalesced as the reaction progressed. Occasionally, pre-existing epidote grains could be seen to be rimmed with new growth. Alternatively, charges reacting towards anorthite had skeletal epidote grains included in well-recrystallized anorthite. The anorthite also contained characteristic inclusions of magnetite, in instances where smaller epidote grains had been completely consumed. The reaction towards anorthite involves dehydration, so these latter exothermic

TABLE 3:1

LEGEND:

[1]zoisite + 1.7 mole quartz, from Vermont, collector J. Rosenfeld, XRF analysis G.R. Angell

[2]clinozoisite (14309), from Grantown on Spey, Grant Institute Departmental Collection

[3]clinozoisite (74-20), from San Gabriel Mtns., Calif., collector C.M. Graham

[4]epidote (D 45), from Dorfer Tal, Osttirol, Austria, collector M. Raith, quoted as $ps_{20.3}$ by Langer and Raith, 1974.

[5]epidote (70-2), from Troodos Massif, Cyprus, collector T.H.E. Heaton

Data on the iron-bearing epidotes, and clinozoisites are partial microprobe analyses, by C.M. Graham.

*total Fe

**assumed, and backcalculated.

***variation due to zoning.

TABLE 3:1

ANALYSES OF ZOISITE, CLINOZOISITE, AND EPIDOTES

	zo[1]	ps$_9$[2]	ps$_{13}$[3]	ps$_{20}$[4]	ps$_{29}$[5]
SiO_2	49.4	***38.16 ± .23	38.37 ± .46	37.67 ± .25	37.23 ± .19
TiO_2	0.24	--	--	--	--
Al_2O_3	25.8	29.38 ± .71	27.35 ± .76	25.39 ± 1.4	21.61 ± .76
Fe_2O_3*	1.55	4.70 ± .28	7.21 ± .87	10.44 ± 1.9	14.31 ± 1.0
Mn_2O_3	--	0.18	0.31	--	0.20
MgO	1.0	--	--	--	--
CaO	19.6	23.96 ± .13	23.58 ± .05	23.09 ± .34	23.48 ± .17
K_2O	0.20	--	--	--	--
P_2O_5	0.36	--	--	--	--
H_2O**	1.57	1.99	1.99	1.96	1.93
TOTAL	99.72	98.37	98.81	98.55	98.76
	to 2 Ca		to 12 (O) anhydrous		
Si	4.70	2.87	2.90	2.88	2.90
Al	2.89	2.61	2.44	2.29	1.98
Fe(III)	0.11	0.27	0.41	0.60	0.84
Mn(III)	--	0.01	0.02	--	0.01
Ca	2.00	1.93	1.91	1.89	1.96
OH**	1.00	1.00	1.00	1.00	1.00
	ps$_3$	ps$_{9.3}$cz$_{90.4}$	ps$_{14.3}$cz$_{85.1}$	ps$_{16-28}$	ps$_{29.6}$cz$_{70.0}$
		***av.10 anal.	av. 2 anal.	av. 12anal	av. 8 anal.

reaction textures tended to be rather more obvious than the textures produced by the endothermic hydration reaction. Kyanite and quartz are not modally abundant in the stoichiometric reaction mixtures, but corrosion, and overgrowth, on these rarer grains indicated that both were participating in the reaction in both directions.

All the iron-bearing runs were performed using a MH oxygen buffer, with an additional capsule containing Co_2O_3, included in the furnace assemblage, to act as a hydrogen absorbant. This simple technique nearly triples the life of the haematite buffer, at 800°C. In instances where the buffer did fail, the epidote rapidly broke down to anorthite and magnetite.

The microprobe analyses indicated unexpectedly low pistacite contents for epidotes that broke down above 800°C, although stable epidotes at these temperatures generally retained their predicted pistacite contents. This pattern of results was interpreted as indicating that iron-loss can only occur after the epidote breaks down, iron cannot escape directly into the platinum from the epidote structure. (cf Liou 1973). Subsequent to this discovery, runs were performed in gold capsules, to inhibit iron-loss. However the dependence of iron mobility upon epidote stability should mean that the earlier results remain valid. Certainly no discrepancy in the phase relations observed was noted between the runs in gold, and those in platinum, although the agreement of the microprobe analyses improved with the introduction of gold capsules.

The experimental data is presented in Table 3:2, and figures 3:1, 3:2 and 3:3.

Figure 3:2 P-T Diagram of present experimental data

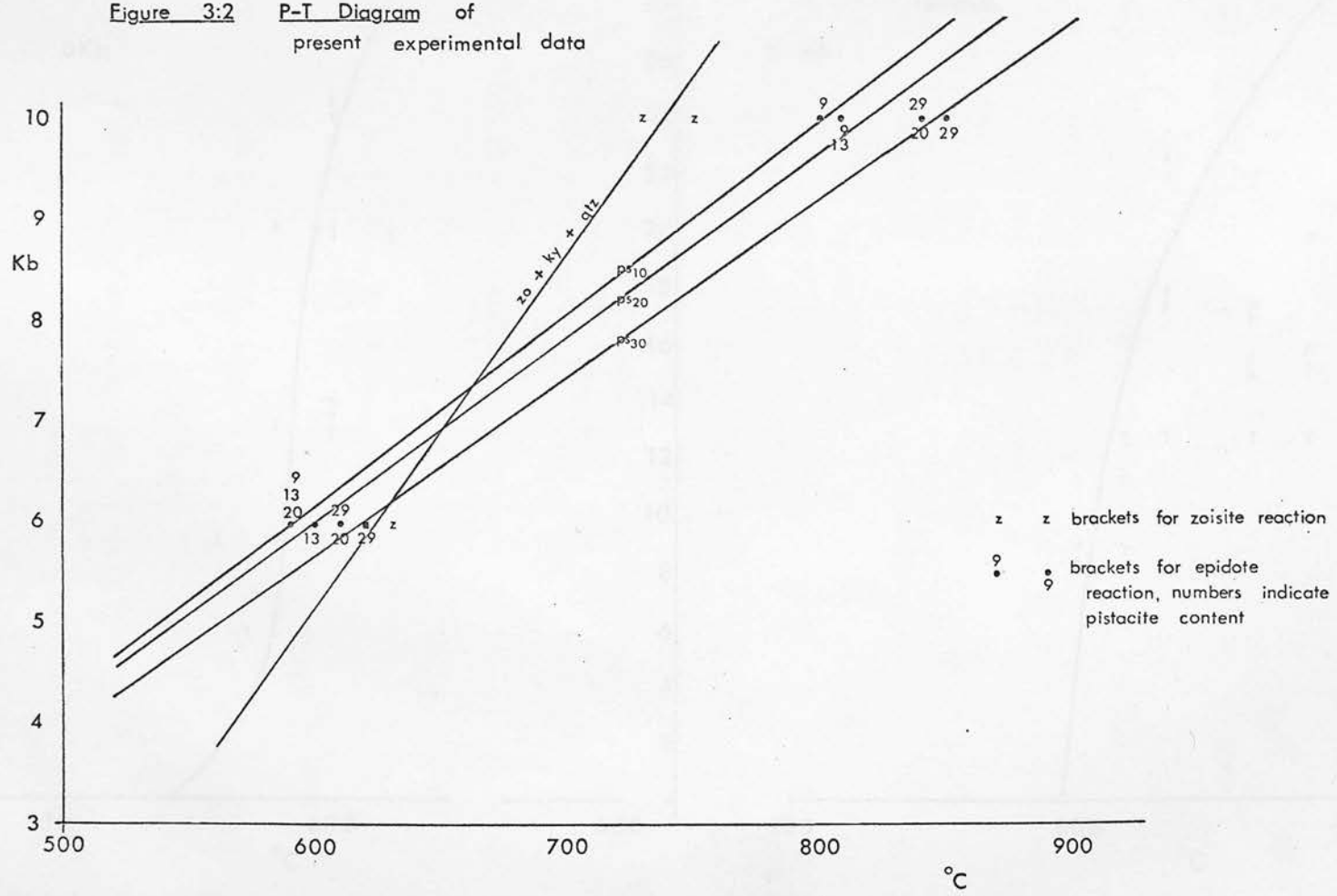

Figure 3:3 T-X Diagrams of present experimental data

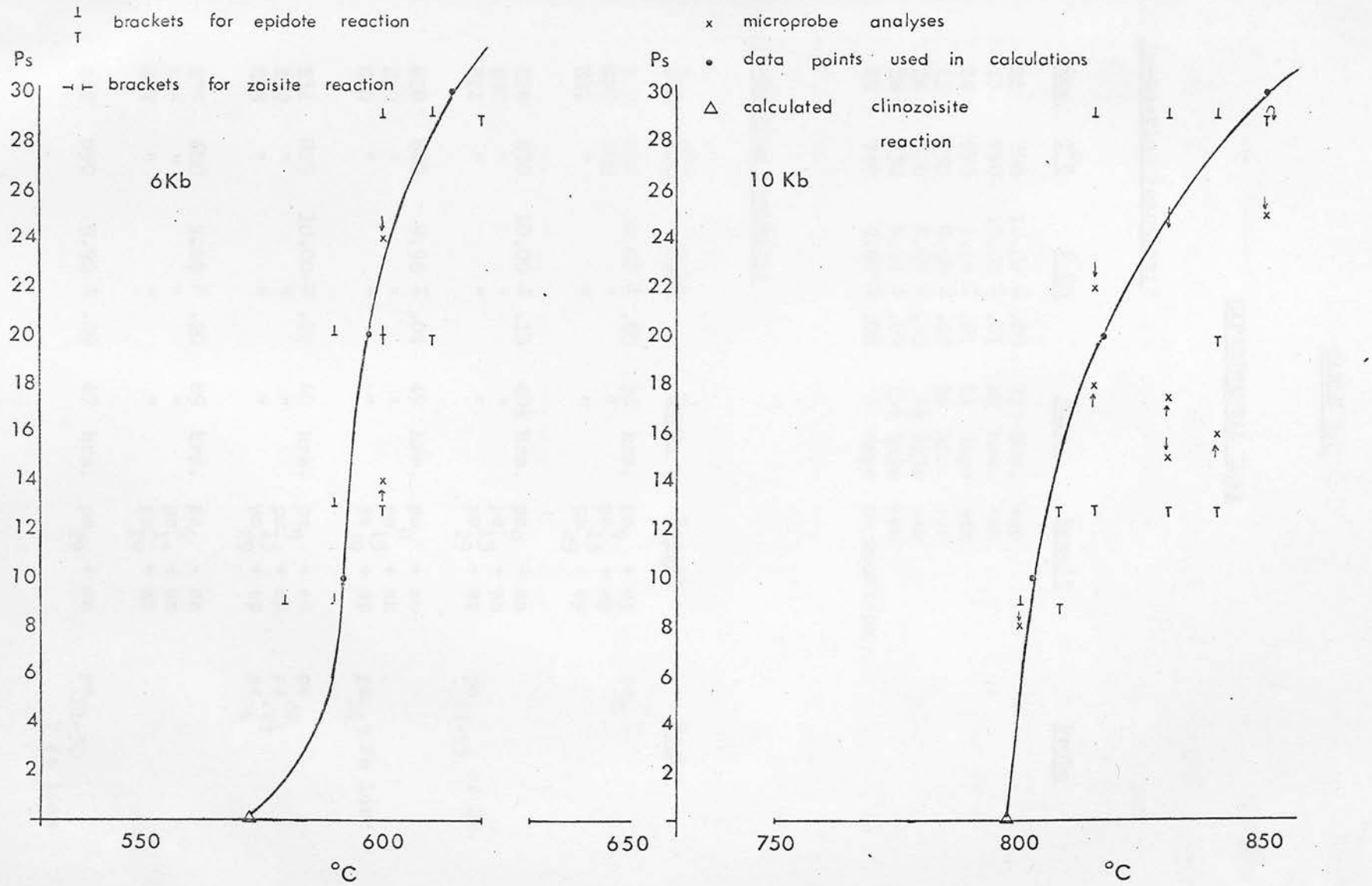

TABLE 3:2

EXPERIMENTAL DATA

Zoisite-bearing reaction:

Run	T°C	P Kb	Durn.	Result	Probe
Z1	700	10.02 ± .08	72 hrs.	+zo	
Z3	750	10.00 ± .01	48 hrs.	+an	
Z4	650	5.96 ± .04	14 days	+an	
Z5	730	9.98 ± .06	96 hrs.	+zo	
Z6	620	5.99 ± .10	9½ days	+zo	
Z8	630	5.94 ± .09	13½ days	+an	
Z9	740	9.96 ± .06	6 days	no reaction	

Epidote-bearing reaction:

Run	T°C	P Kb	Durn.	Result	Probe
E 9	800	10.03 ± .05	36 hrs.	ps_9 + ep	ps_8
E10	800	"	"	ps_{13} + ep	
E11	"	"	"	ps_{29} + ep	
E19	830	10.00 ± .13	40½ hrs.	ps_9 + an	
E20	"	"	"	ps_{13} + an	
E21	"	"	"	ps_{29} + ep	ps_{17-25} av 22
E28	840	9.96 ± .04	49 hrs.	ps_9 + an	
E29	"	"	"	ps_{13} + an	
E30	"	"	"	ps_{29} + ep	ps_{15} ? Fe loss
E31	825	10.00 ± .02	60 hrs.	ps_9 + an	ps_{29}
E32	"	"	"	ps_{13} + an	$ps_{17\frac{1}{2}}$
E33	"	"	"	ps_{29} + ep	ps_{26}
E35	680	5.89 ± .20	89 hrs.	ps_9 + an	
E36	"	"	"	ps_{13} + an	
E37	"	"	"	ps_{29} + an	
E47	850	9.92 ± .09	47 hrs.	ps_{29} + an	ps_{21-30} ? Fe loss

TABLE 3:2 CONTD.

Epidote-bearing reaction contd.:

Run	T°C	P Kb	Durn.	Result	Probe
E52	620	5.94 ± .13	154 hrs.	ps_9 + an	
E53	"	"	"	ps_{13} + an	
E54	"	"	"	ps_{29} + an	
E55	840	9.99 ± .05	78 hrs.	ps_{13} + an	ps_{14-21} av 16
E56	"	"	"	ps_{20} + an	
E57	"	"	"	ps_{29} + ep	ps_{20-29} av 25
E58	600	5.96 ± .09	190 hrs.	ps_{13} + an	ps_{13-15}
E59	"	"	"	ps_{20} no reaction	
E60	"	"	"	ps_{29} + ep	ps_{15-27} av 24
E61	580	5.92 ± .17	190 hrs.	ps_9 + ep	ps_{8-13}
E62	"	"	"	ps_{13} + ep	
E63	"	"	"	ps_{20} + ep	
E65	808	9.98 ± .04	71 hrs.	ps_9 + an	
E66	"	"	"	ps_{13} + an	
E67	610	5.91 ± .18	141½ hrs.	ps_{13} + ep	
E68	"	"	"	ps_{20} + ep	
E70	591	5.98 ± .10	223 hrs.	ps_9 + ep	
E71	"	"	"	ps_{13} + ep	

Modelling of Results:

1) Establishment of the Base Reaction:

The aparallelism of the zoisite, and several epidote reaction curves (fig. 3:2) indicates that the simple substitution of zoisite for clinozoisite is an inadequate approximation. However, in the absence of either experimental or thermochemical data on clinozoisite, the zoisite curve can be used as the base reaction, provided parameters for the unknown enthalpy, entropy and molar volume change of the phase change are included in the model. Fisher and Zen (1971) have shown that, for a dehydration reaction, it is a valid approximation to assume that only the thermochemical parameters of water change with pressure and temperature. They have combined all the free energy terms for water into a single variable $G^*_{H_2O}(P,T)$, such that, for a reaction:

$$A_{xtln} \longrightarrow B_{xtln} + H_2O \text{ fluid}$$

the free energy equation approximates to:

$$\Delta G^{1,298}_{f,\ B-A} - \Delta S^{298}_{f,B-A}(T-298) + \Delta V^{1,298}_{B-A}(P-1) + G^*_{H_2O}(P,T) = 0$$

where the temperature is in degrees absolute, and the pressure in bars. Assuming this approximation, and a molar volume change (ΔV_s) of 1.516 cal/bar for the reaction calculated from the data sets published by Robie and Waldbaum (1968), and Zen (1972), the two brackets on the reaction curve fit a linear equation:

$$86050 - 104.5(T-25) + 1.516P + G^*_{H_2O}(P,T) = 0$$

where T is in ^oC. The uncertainty on the formational free energy

term is ± 5909, and on the entropy ± 9.2. The values for these terms, as calculated from the thermochemical data of Robie and Waldbaum, and Zen, are 71542 ± 3126 cals and 83.03 ± 4.92 cal/deg, respectively. Thompson (1974) has calculated a data set, which incorporates Boettcher's (1970), and Newton's (1966) experimental data, and this gives values of 66646 ± 5421 cals, and 83.03 ± 4.92 cal/deg respectively. The divergence between the present data, and both sets of published data is unfortunate, but underlines the continuing uncertainty in the thermochemistry of aluminous phases. The absolute position of the base reaction involving zoisite is unimportant in the present calculations, since the phase inversion difference terms will compensate for variations between any assumed zoisite thermochemical data, and the clinozoisite data will remain constant, depending only upon the epidote reaction data.

2) Crystal chemistry of clinozoisite-epidote minerals:

Site occupancy analysis by electron diffraction and ^{57}Fe Mössbauer spectrometry (Dollase 1971, 1973) has been used to show that the Fe^{III} in epidotes resides predominantly in the $^{VI}M_3$ site, with a small proportion in the $^{VI}M_1$ site, while aluminium, alone, occupies the least distorted $^{VI}M_2$ site. Dollase (1973) has gone further, and attempted to discover whether the iron-aluminium distribution on the sites varies with temperature and composition, by analysing a range of epidotes of varying compositions and parageneses, and also some synthetic, and artificially heated specimens. His data is not sufficiently accurate to quantify any trends, but there is a distinct

increase in the proportion of iron entering the M_1 site with increasing temperature. The distribution coefficient:

$$K_D = (X^{M1}_{Fe}/X^{M1}_{Al}) \div (X^{M3}_{Fe}/X^{M3}_{Al})$$

appears to be independent of composition.

Allowing for substitution on two sites, the activity of clinozoisite can be written:

$$a^{ep}_{cz} = (X^{M3}_{Al} \cdot \gamma^{M3}_{Al}) \cdot (X^{M1}_{Al} \cdot \gamma^{M1}_{Al}) \qquad (1)$$

If epidote is assumed to have two basic site-types; M_3 and M_2, then M_1 sites can be considered as a combination of, say, c M_3 sites and (1-c) M_2 sites. In this case:

$$a^{ep}_{cz} = (X^{M3}_{Al} \cdot \gamma^{M3}_{Al}) \cdot (X^{M3^c}_{Al} \cdot \gamma^{M3^c}_{Al}) \cdot (X^{M2(1-c)}_{Al} \cdot \gamma^{M2(1-c)}_{Al})$$

$$= (X^{M3(1+c)}_{Al}) \cdot (\gamma^{M3(1+c)}_{Al}) \qquad (2)$$

Assuming that the composition and activity coefficient terms are entirely separate attributes of the site and comparing equations (1) and (2):

$$X^{M1}_{Al} = (X^{M3}_{Al})^c$$

$$\gamma^{M1}_{Al} = (\gamma^{M3}_{Al})^c$$

$$c = \ln (X^{M1}_{Al}) / \ln (X^{M3}_{Al}) = \ln (\gamma^{M1}_{Al}) / \ln (\gamma^{M3}_{Al})$$

X^{M1}_{Al} and X^{M3}_{Al} can be calculated from the known epidote bulk composition, and estimated values of K_D, the site distribution coefficient, although they cannot be isolated from the equations:

$$X^{M1}_{Al} = 3X^{ep}_{cz} - X^{M3}_{Al} - 1$$

$$K_D (3X^{ep}_{cz} - X^{M3}_{Al} - 1)(1 - X^{M3}_{Al}) = X^{M3}_{Al} (2 - 3X^{ep}_{cz} + X^{M3}_{Al})$$

Models have been calculated, initially, for values of K_D of 0.01, and 0.05, bracketing the range estimated by Dollase (1973), and allowing for a large increase as the temperature rises to 800°C. The real values of X_{Al}^{M1} and X_{Al}^{M3} at these K_D values, and also for $K_D = 0.02$, and 0.03, for epidote compositions ps_{10}, ps_{20}, and ps_{30} are presented in Table 3:3.

3) Choice of solution model:

The epidote solvus (Raith 1976) is highly assymmetric, with its crest at around ps_{19}, so a subregular solution model in the binary form:

$$RT \ln\gamma_1 = X_2^2 \left(W_1 + 2(1 - X_2)(W_2 - W_1)\right)$$

is more appropriate than a regular solution model, and even this may be an oversimplification, since the interaction parameters, undoubtedly, overstep the limits:

$$0.5 \leqslant W_1/W_2 \leqslant 2 \qquad \text{(Powell 1974)}$$

However the complexities of the various alternatives; Green's assymmetric quasichemical model, the Van Laar model, or a three coefficient Margules' fit, are considered to outweigh their increased precision, in this instance. The solution model will be fitted in terms of site occupancies, (X_{Al}^{M3}), taking note of the crystal chemistry of epidote.

4) Calculation of model:

The entire equilibrium equation for the epidote reaction studied can be written:

$$\Delta G_{R(zo)}^{P,T} = -2RT\ln\mathfrak{a} + 2\Delta G_{f,czo-zo}^{1,298} - 2(T-298)\Delta S_{f,czo-zo}^{298} + 2P\Delta V_{czo-zo}^{1,298}$$

Table 3:3

Distribution of aluminium between the M1 and M3 sites in epidote

Composition K_D*		Ps_{10}	ps_{20}	ps_{30}
0.01	X_{Al}^{M1}	0.996	0.986	0.947
	X_{Al}^{M3}	0.704	0.414	0.153
	c**	0.0119	0.0159	0.0288
0.02	X_{Al}^{M1}	0.992	0.974	0.918
	X_{Al}^{M3}	0.708	0.426	0.182
	c	0.0238	0.0311	0.0502
0.03	X_{Al}^{M1}	0.998	0.963	0.895
	X_{Al}^{M3}	0.712	0.437	0.205
	c	0.0355	0.0458	0.0696
0.05	X_{Al}^{M1}	0.981	0.944	0.862
	X_{Al}^{M3}	0.719	0.456	0.238
	c	0.0586	0.0737	0.1034

*$K_D = (X_{Fe}^{M1}/X_{Al}^{M1}) \div (X_{Fe}^{M3}/X_{Al}^{M3})$

**$c = \ln(X_{Al}^{M1})/\ln(X_{Al}^{M3})$

where T is in degrees absolute, and:

$$\ln K = - \ln a_{cz}^{ep} = - (1+c) \ln(X_{Al}^{M3} . \gamma_{Al}^{M3})$$

$$c = \ln (X_{Al}^{M1}) / \ln(X_{Al}^{M3})$$

Values of X_{Al}^{M1} and X_{Al}^{M3} for the range of conditions of interest are presented in Table 3:3

In keeping with the Fisher-Zen approximation, the entropy and formational free energy of the zoisite-clinozoisite phase inversion are assumed to be relatively temperature independent. If the two interaction parameters are also assumed to be temperature independent, then there are only five unknowns involved in the equation: W_1; W_2; $\Delta G_{f,czo-zo}^{1,298}$; $\Delta S_{f,czo-zo}^{298}$; and $\Delta V_{czo-zo}^{1,298}$. The experimental data can be considered to bracket the reaction plane at three compositions, approximating to ps_{10}, ps_{20}, and ps_{30}, at both 6Kb, and 10Kb. This gives six distinct data points, and hence six equations which are simultaneous, if the above assumptions are correct. The solution is presented in Table 3:4, for K_D values of 0.01 and 0.05.

If the rather high phase inversion data are subtracted from the present experimental zoisite base reaction, and the resulting clinozoisite curve compared with the calculated curve, from Robie & Waldbaum (1968), and Zen (1972), then more reasonable values, of about +11.4 cal/deg, and 4500 cals for the entropy and formational free energy, appear. Holdaway (1972) has made some semiquantitative estimates for the molar volume change, and entropy of the zoisite-clinozoisite inversion from parallel sets of reaction data, involving the two polymorphs. He quotes the molar volume change at about 0.2 ± 0.1 cm^3 (0.048 cal/bar), which is about an order of magnitude less

Table 3:4

Model assuming interaction parameters to be independent of temperature

Experimental data:

	Epidote composition	T °C	P Kb
1	ps_{30}	850	10
2	ps_{30}	614	6
3	ps_{20}	817	10
4	ps_{20}	598	6
5	ps_{10}	802	10
6	ps_{10}	592	6

Thermochemical parameters:

K_D	0.01	0.05	
$\Delta S^{298*}_{f,czo-zo}$	6.15	11.72	cal/deg
$\Delta V^{1,298}_{czo-zo}$	-0.47	-0.17	cal/bar
$\Delta G^{1,298*}_{f,czo-zo}$	7881	9138	cal
W_1	3468	2928	cal
W_2	2588	3164	cal

Predicted temperatures for the clinozoisite reaction:

K_D	0.01	0.05
6 kb	571°C	571°C
10 Kb	798°C	798°C

*relative to experimentally determined zoisite base reaction

than the present estimate; and the entropy at 6 ± 5 cal/deg, which just overlaps the present data.

5) The epidote-clinozoisite solvus - a test for the solution model.

As has been shown by Guggenheim (1949: eqns 5:53:1,2), the activity coefficient of a solution model is related to the critical composition on the solution solvus by the expressions:

$$\frac{\partial(\ln\gamma)}{\partial x_c} = \frac{1}{(1-x_c)}$$

$$\frac{\partial^2(\ln\gamma)}{\partial x_c^2} = \frac{1}{(1-x_c)^2}$$

For a subregular solution model, these reduce to:

a) $2x_c(2E_2 - E_1) + 3x_c^2(2E_1 - 2E_2) = 1/1(1-x_c)$

b) $2(2E_2 - E_1) + 6x_c(2E_1 - 2E_2) = 1/(1-x_c)^2$

where $E = W/RT_c$

Raith (1976) has studied co-existing clinozoisites and epidotes in a prograde greenschist - amphibolite sequence in the Tauern Window (Eastern Alps). He estimates that the miscibility gap closes at about 550°C, Ps_{19-20}. Assuming a critical composition of Ps_{19}, the above relationships, when solved in sequence a), b) give critical temperatures:

	K_D	0.01	0.05
from	W_1	962 K	757 K
	W_2	611 K	778 K

These indicate that, if Raith's estimates are correct, then a K_D value of 0.05 is more realistic at greenschist to epidote-amphibolite conditions, and that the critical temperature is about 500°C.

Development of the Epidote - Albite Data:

The development of a solution model for epidote-clinozoisite minerals permits a more quantitative interpretation of the various epidote breakdown data sets (Chapter 2). As has previously been described, a full thermodynamic analysis of the reaction:

$$ep + ab + qtz = plag + gnt + H_2O$$

is inhibited by the lack of thermochemical data on clinozoisite, or on any of the three solid solutions involved. However, using the present data on epidote solid solution, and assuming that Orville's (1972) plagioclase activity data is applicable to P-T conditions other than 2Kb, 700°C; only one unknown, the nature of grossular-andradite solid solution, remains. This can, therefore, be derived. Although the accuracy of the data will only improbably produce a reasonable result, the coherence of the various data sets will give a fair idea of their relative validities. Using a Fisher - Zen (1971) approximation, the free energy curve for the iron-soda-free reaction can be calculated from Robie & Waldbaum 1968, Zen 1972 and present data:

$$128730 - 124.33(T - 298) + 0.77P + 2\,G^{*}_{H_2O}(P,T) = 0$$

Addition of the two omitted chemical components introduces an equilibrium constant term:

$$K = (a^{gnt}_{gross}) \cdot (a^{plag}_{an})^5 / (a^{ep}_{czo})^4$$

From Orville (1972), for the range an_{0-30};

$$a^{plag}_{an} = 1.28\, X^{plag}_{an}$$

at 2Kb, 700°C, and, for present purposes, at all P-T conditions.

The epidote solid solution, as has been shown in this chapter, fits a subregular solution model on the M3 site, for a binary Fe-Al epidote:

$$a^{ep}_{czo} = (X^{M3}_{Al})^{(1+c)} \cdot (\gamma^{M3}_{Al})^{(1+c)}$$

$$\text{where } c = \ln(X^{M1}_{Al}) / \ln(X^{M3}_{Al})$$

$$K_D^{M1-M3} = 0.05$$

$$\text{and } RT\ln(\gamma^{M3}_{Al}) = (X^{M3}_{Fe})^2 (2928 + 472\, X^{M3}_{Al})$$

The activity of the grossular can be written:

$$a^{gnt}_{gross} = X^{gnt}_{gross} \cdot \gamma^{gnt}_{gross}$$

Although the mole fraction term can be split up:

$$X^{gnt}_{gross} = (X^{A}_{Ca})^3 \cdot (X^{B}_{Al})^2$$

the accuracy of the present data does not warrant calculation of activity coefficients for the different octahedral sites (A,B) in garnet. However, examination of the values obtained for the free energy discrepancy, which could be attributed to grossular-andradite non-ideality, shows both published data sets giving negligibly small differences. The two present data sets give no coherent picture; the albite-free study can be disregarded as a 'synthesis curve', if necessary, while the albite-present data suffers from inaccurate plagioclase activity data, and suspect phase composition determinations. Therefore disregarding the present data sets, it can be claimed that within experimental error, grossular-andradite can be considered as an ideal solution.

Table 3:5

Calculations on the reaction data for:

$$4\ ep \pm ab + qtz = 5\ an\ \underline{or}\ plag + gnt + 2\ H_2O$$

$$128730 - 124.33(T-298) + 0.77 + 2G^{*}_{H_2O} = -RT\ln\left(\frac{a^{gnt}_{gross} \cdot (a^{plag}_{an})^5}{(a^{ep}_{czo})^4}\right)$$

Source*	T K	P Kb	$G^{*}_{H_2O}$ +	$G^{P,T}_{R}$ + RTlnK
Holdaway (1972)	863	1.034	-36827	17
	923	2.068	-33999	516
	973	3.102	-31650	815
Liou (1973)	908	2	-34522	75
	953	3	-32278	79
	1021	5	-28862	514
Present albite-free study	953	3	-32278	900
	983	4	-30760	1230
	1008	5	-29293	2038
Present albite-bearing study	888	3	-34471	4399
	938	4	-32202	5341
	981	5	-30189	5954

* cf figures 2:1,2

+from Holloway (1976, pers. comm.)

CHAPTER 4

MIXED VOLATILE EQUILIBRIA IN GREENSCHIST FACIES METABASALTS

Introduction:

The behaviour and composition of the fluid phase during metamorphism has been the subject of intense investigation, since Yoder's seminal paper in 1952. Early models assumed "perfect mobility" of the fluid component e.g. for pure water (Thompson 1957), and for a H_2O-CO_2 fluid, at $P_{flu} = P_{tot}$ (Wyllie 1962, Greenwood 1962). In the latter instance, the interdependence of the partial pressures of the fluid components means that they must have "perfect mobility" independently, since variation in the chemical potential of one, will vary the chemical potential of the other.

The common occurrence of carbonates as accessory phases, in otherwise identical assemblages, at constant metamorphic grade (Tilley 1923, 1938, Billings and White 1950, Miyashiro 1958, de Waard 1959, and Holdaway 1965) indicates a variation in μ_{CO_2} which could only be caused by incomplete diffusion of carbon dioxide through the rock. This is confirmed by Graham (1973) from observations on dolerite sills intruded into calcareous country rock in the Dalradian of the S.W. Highlands. Here the greenschist assemblages were found to be carbonate-rich at the edges of the sills, and carbonate-free in the interiors. The fact that these assemblages were zoned rather than gradational, indicates the critical control was a mechanical diffusion rate, rather than a chemical buffering process. There was also a strong positive correlation between the degree of shearing in the

rock, and its carbonate content, but the causal relationship between these two is uncertain.

Billings and White (1950), in a study of metabasic greenschists from the Woodsville Quadrangle, Vermont and New Hampshire, discovered a range of assemblages:

chlor - act
chlor - act - cc
chlor - cc
chlor - ankerite

+ qtz - ep - ab

at the same metamorphic grade. They interpreted them as representing a gradual increase in the CO_2 content of the same bulk rock composition. The first ion to leave the silicate lattice is calcium, and only at relatively high molar carbon dioxide proportions (X_{CO_2}) do magnesium and iron form carbonates. Harte and Graham (1975) have shown that, in the system CAFMS-H_2O-CO_2, these assemblages can be related by the reactions:

(1) act + ep + CO_2 + H_2O = chl + cc + qtz

(2) act + ep + CO_2 + H_2O = chl + ank + qtz

(3) chl + cc + CO_2 = ank + ep + qtz + H_2O

(4) act + cc + CO_2 = ank + qtz + H_2O

Assuming constant aluminium, and iron-magnesium distributions, these reactions are divariant, and so may be arranged, according to Schreinemakers' rules (Zen 1966) about a single isobaric invariant point in T-X_{CO_2} space (fig. 4:1). The basic shapes of the curves can be deduced from the positions of the volatile in the reaction, as described by Greenwood (1967). Those with CO_2 and H_2O on the same

FIGURE 4:1

Schematic analysis of relationships in isobaric T - X_{CO_2} section of quartz-, epidote-, and fluid-bearing greenschist facies basic assemblages in the system CA(FM)S - H_2O - CO_2. The sequence of changes occurring in natural assemblages with increasing X_{CO_2}, at constant T is indicated by the dashed arrows, with characteristic assemblage types I, II, III, IV, and V.

Phase abbreviations used are:

act	actinolite
ep	epidote
chl	chlorite
cc	calcite
ank	ankerite
qtz	quartz

(after Harte & Graham 1975)

Basic composition fall consistently in the epidote-bearing fields, so the empirical model does not distinguish between the two compatability triangles possible in the field 'Assemblage III'.

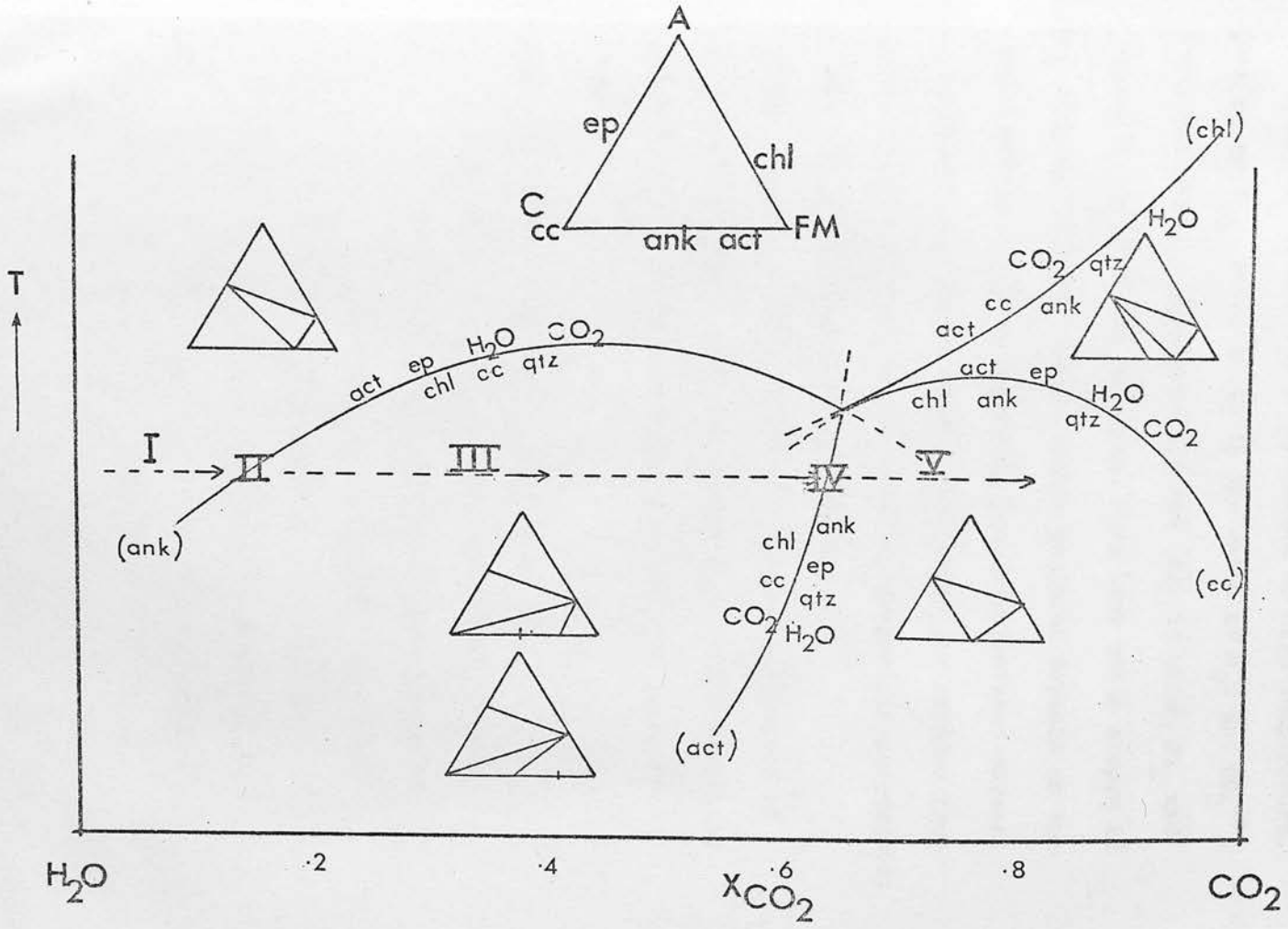
A
ep
chl
C
cc
ank act
FM
T
I
II
III
IV
V
(ank)
act ep chl cc
H2O CO2
qtz
(chl)
CO2 qtz
cc ank
act
H2O
act ep
chl ank
H2O
qtz
CO2
(cc)
chl ank
cc ep
qtz
CO2 H2O
(act)
H2O
·2
·4
·6
·8
XCO2
CO2

side of the reaction ((1) and (2)) are convex to high temperature, with a maximum at an X_{CO_2} value equal to the ratio of H_2O and CO_2 involved in the reaction. Equations (3) and (4), in which CO_2 and H_2O are on opposite sides of the reaction, have very steep slopes in $T\text{-}X_{CO_2}$ space, with an inflexion point, whose position depends on the entropy of the reaction. Three remaining pseudo-univariant curves (the fluid-, epidote-, and quartz-absent reactions) are omitted from the model, since epidote and quartz are normally present in greenschist metabasalts, and the model assumes fluid saturation.

An isothermal section across the model produces a sequence of qtz-ab-ep-bearing assemblages, with increasing X_{CO_2}, which parallels Billings' and White's (1950) observations, and predicts an extra assemblage (Type IV):

Assemblage Type I: chlor-act; unbuffered CO_2

Type II: chl - act - cc; buffered CO_2, but a common natural assemblage because of the increase in variance associated with aluminium, and iron content variation in natural amphiboles, and the geometry of the reaction curve in $T\text{-}X_{CO_2}$ space.

Type III: chlor - cc; unbuffered CO_2

Type IV: chlor - cc - ank; buffered CO_2, unrecorded in the literature, rarer than II because the near-constant aluminium content of metabasalt

chlorites, and the geometry of the reaction curve combine to inhibit any possible widening of the reaction zone in natural assemblages.

Type V: chlor - ank; unbuffered CO_2.

Experimental:

The experimental purpose of this section of the thesis is to quantify the Harte - Graham mixed volatile model, at 5Kb, in the iron-free CAMS-H_2O-CO_2 system, as a basis for extrapolation to natural rocks. Following the assumption that all the assemblages to which the model applies contain quartz, epidote, and fluid during metamorphism, the reactions from which these phases are absent have not been investigated. Furthermore, if the amphibole is non-aluminous tremolite, the chlorite- and zoisite-absent reactions degenerate to the experimentally well-defined reaction:

$$cc + trem + CO_2 = dol + qtz + H_2O$$

in the CMS-H_2O-CO_2 system (Skippen 1971, reaction 19; inter alia). Thus, attention has been focussed on the three reactions; dolomite-, tremolite-, and calcite-absent.

Although natural chlorites in greenschist metabasalts are fairly consistently clinochlore, with a tendency towards more aluminous compositions; two synthetic chlorites representing the extremes in natural alumina content, penninite and amesite, were used in the experimental study. This was done in order to provide a broad data set, from which chlorite data could be interpolated, rather than risk

the rather more uncertain extrapolation from a single data point. The amphibole used was an "alumina-free" sample of Gouverneur Tremolite (anal. Table 4:1, provided by A.E.J. Engel), which was supplied as a very fine powder (5-10μ needles). The validity of the assumption that the tremolite remains non-aluminous is not certain, particularly in the reactions involving amesite. Jasmund and Schäffer (1972) have recrystallized amphiboles from gels with compositions on the tremolite-tschermakite join, containing as much as 30 mole % tschermakite, at 500°C and P_{H_2O} = 2Kb. However this probably represents a "synthesis curve" (Fyfe 1960), and, taking into account the problems with aluminous enstatites synthesized by different techniques (Macgregor 1974, Howells and O'Hara 1975 and Howells 1976) can only be a very generous estimate of the maximum tschermakite content under equilibrium conditions. Probe analysis of the amphiboles in the present study was impossible because of the extra-ordinarily fine-grained starting material. However, the amesite experimental data set does not show any divariance, relative to the penninite data, within experimental error, so the assumption of non-aluminous tremolite is considered justified by the end-result.

The chlorites were recrystallized from nitrate gels, at 650°C, P_{H_2O} = 4Kb, for 10 days, after which time, strong chlorite peaks, with a trace of septechlorite, were all that showed on the XRD charts, and optical grain mounts showed well-recrystallized, if fine-grained, chlorite. The other phases used were:

natural zoisite, admixed with quartz - anal. Table 4:1

natural quartz

and analar calcium carbonate

TABLE 4:1

ANALYSES OF INITIAL PHASES

wt %	Gouverneur Tremolite	Zoisite
SiO_2	57.76	49.4
Al_2O_3	0.64	25.8
TiO_2	0.05	0.24
Fe_2O_3	0.00	1.55 (total Fe)
FeO	0.14	---
MnO	0.16	0.00
MgO	24.73	1.0
CaO	13.27	19.6
Na_2O	0.29	0.00
K_2O	0.09	0.20
H_2O	2.38	1.57*
F	0.26	---
P_2O_5	---	0.36
TOTAL	99.67	99.72
	to 24(O,OH,F)	to 2Ca
Si	7.84	4.72
Al (tet)	0.10	
Al (oct)		2.91
Fe	(II) 0.02	(III)0.09
Mn	0.01	
Mg	5.03	0.14

TABLE 4:1 CONTD.

Ca	1.94	2.00
Na	0.08	
K	0.02	0.02
OH	2.14	1.00*
F	0.06	
P		0.03

wet chemical analysis — A.E.J. Engel

XRF analysis — G.R. Angell

1 mole zo: 1.7 moles qtz

*assumed, and backcalculated

The zoisite and quartz were ground to an average grain size of about 20μ. The carbon dioxide source used was silver oxalate, supplied by Engelhard, Cinderford, Glos., (code 3256, batch 750172), with a quoted purity of only 71%. Capsules containing silver oxalate, alone, run at 5Kb and 500°C, yielded about 70% of the calculated weight of gas, assuming 100% pure silver oxalate. It was concluded that the impurities were non-volatile, probably silver, and could therefore be simply compensated for. Dolomite was grown "in situ", in the charges, from a mixture of:

10 analar $CaCO_3$: 4 analar MgO : 3 71% silver oxalate

by weight, after trial runs had shown that such a mixture is converted totally to dolomite and silver, within a week, at 500°C, 5Kb, under X_{CO_2} conditions ranging from 20-70%.

For each reaction, charges were made up in the stoichiometric proportions of the phases involved, since these compositions will be most sensitive to changes in phase proportions. As both chlorite compositions were used for each reaction, six different bulk compositions were used in all.

The X_{CO_2} of the runs was fixed by adding a weighed amount of silver oxalate to the charge, and then making it up with the appropriate proportion of water. For carbon dioxide contents up to 20 mole %, about 10 mg of silver oxalate per charge were used; for values from 20-70% about 20 mg; and for X_{CO_2} values above 70%, about 30 mg of silver oxalate were necessary to maintain the same degree of precision. The weight of the solid phases in each charge was about 10-15 mg.

Charges were run in 3mm platinum capsules, three to a coldseal pressure vessel, for about a month. Temperatures were checked daily, and pressures weekly. The precision of the coldseal apparatus is considered to be about $\pm 5^{o}C$, and ± 100 bars (Ford 1972, pers. comm). The gas compositions of two early runs, at $450^{o}C$, were analysed by gas chromatography (by D.H. Eggler and T.C. Hoering), with the following results:

Run	Intended X_{CO_2} mole %	vol CO_2	vol CH_4	% *	vol N_2	% *
16I	7%	276 µl	19.5 µl	0.49	3 µl	0.08
16L	60%	2750 µl	6.7 µl	0.16	58.5 µl	1.36

*The percentages were calculated assuming a CO_2 content coincident with the intended X_{CO_2} value. Carbon monoxide was not detected. The nitrogen probably represents air trapped in the capsule, subsequently capsules were crimped flat before sealing. By way of comparison, Greenwood (1967) has recorded gas chromatography data from his parallel study in the system CMS-H_2O-CO_2, at around $500^{o}C$, and 5Kb. He finds methane contents of about 0.04%, with a maximum of 0.60%, and fails to detect carbon monoxide.

The gas compositions of the other runs were checked by the method described by Johannes (1969). This involves the weighing of capsules before and after puncturing, and before and after drying, and assumes that the gas is pure CO_2, and the liquid pure H_2O. Johannes estimates that an error of 1-2 moles % in X_{CO_2} is involved in the assumption. 3mm platinum capsules have a rupture pressure of about 200-300 bars (C.E. Ford pers. comm.), so that this is the maximum pressure in the capsule, immediately before being punctured.

FIGURE 4:2

EXPERIMENTALLY DETERMINED T - X_{CO_2} SECTION

at 5 Kb P_{flu}

for the phase assemblage including

penninite chlorite (chl 1)

⊢—⊣ error bars in X_{CO_2} space

⟶ arrow indicates direction of reaction

⊢⊖⊣ indicates no reaction

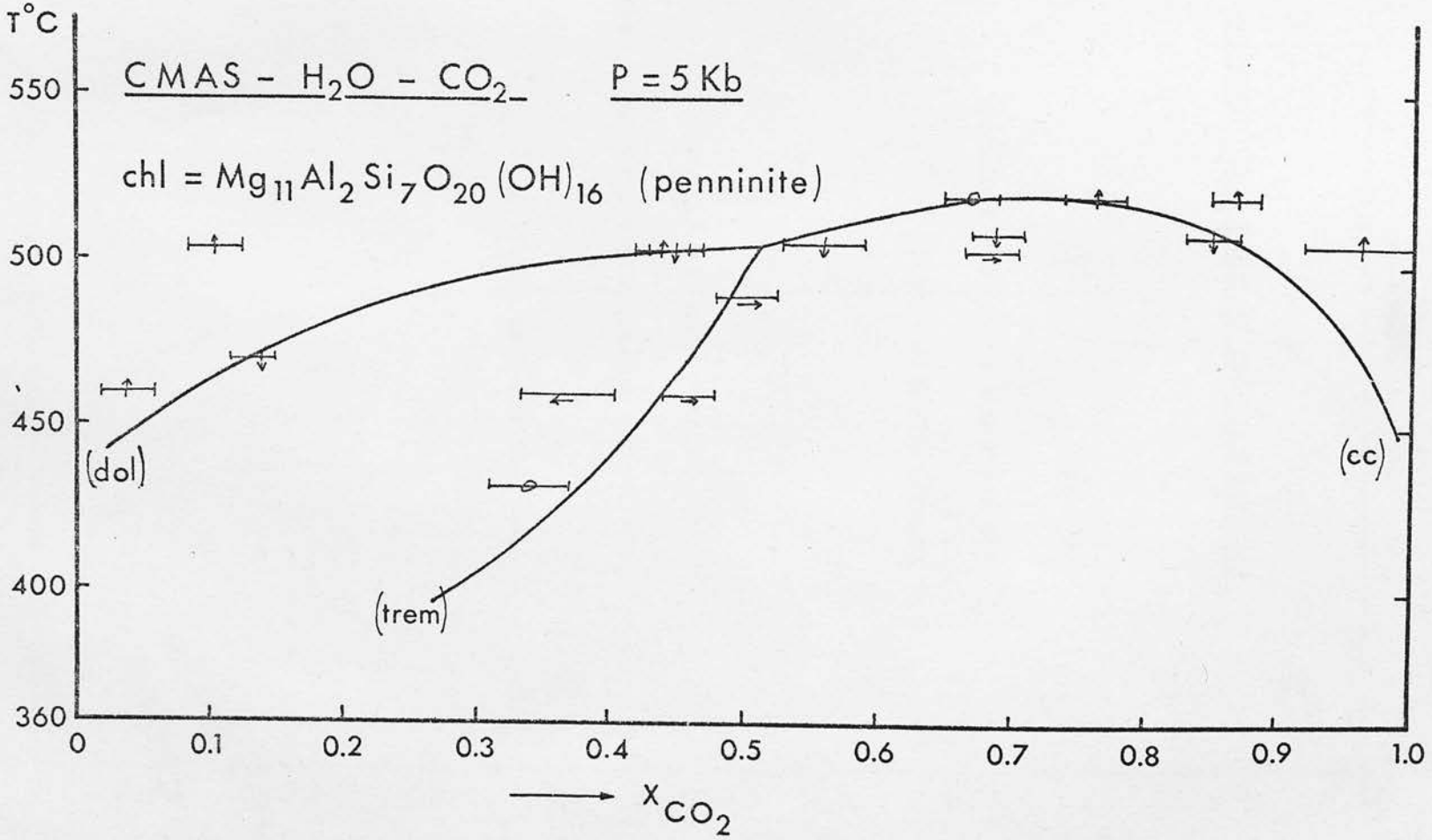
T°C
CMAS - H2O - CO2_
P = 5 Kb
chl = Mg11Al2Si7O20(OH)16 (penninite)
550
500
450
400
360
(dol)
(trem)
(cc)
0
0.1
0.2
0.3
0.4
0.5
0.6
0.7
0.8
0.9
1.0
XCO2

FIGURE 4:3

EXPERIMENTALLY DETERMINED T - X_{CO_2} SECTION

at 5 Kb P_{flu}

for the phase assemblage including

amesite chlorite (chl 4)

⊢—⊣ error bars in T - X_{CO_2} space

← arrow indicates direction of reaction

⊢0⊣ indicates no reaction

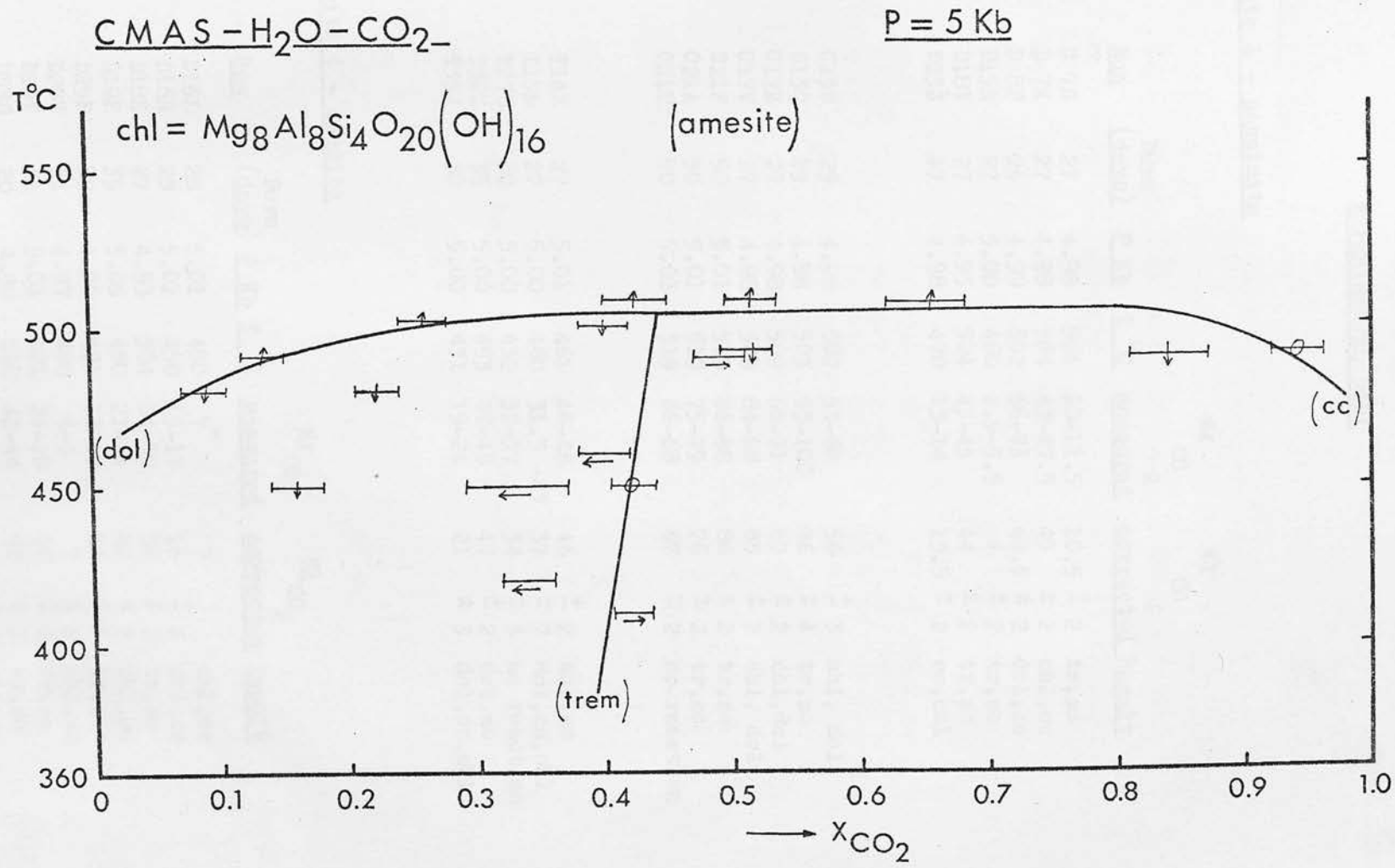
CMAS – H2O – CO2 –
P = 5 Kb
T°C
chl = Mg8Al8Si4O20(OH)16
(amesite)
550
500
450
400
360
(dol)
(cc)
(trem)
0
0.1
0.2
0.3
0.4
0.5
0.6
0.7
0.8
0.9
1.0
XCO2

TABLE 4:2

EXPERIMENTAL DATA

Chlorite 1 - penninite

Reaction	Run	Durn (days)	P Kb	T °C	%X CO_2 measured	%X CO_2 corrected	Result
dolomite -absent	D 7S	27	4.98	504	10-11.5	10.5 ± 2	tr,zo
	D 7Z	27	4.98	504	43-47.5	45 ± 2	chl,cc
	D 8P	26	4.99	502	66-71	68.5 ± 2	dol,zo
	D15B	27	5.00	460	2.5-5.5	4 ± 2	tr,zo
	D18Y	27	4.93	504	43-45	44 ± 2	tr,zo
	D23Z	47	4.98	470	13-14	13.5 ± 2	cc,chl
calcite -absent	C13B	29	4.98	502	53-60	56 ± 3	chl, dol
	C13Q	29	4.98	503	93-100	96 ± 4	tr,zo
	C17Z	27	4.98	509	68-71	69 ± 2	chl,dol
	C17V	27	4.98	509	84-88	85 ± 2	chl, dol
	C21F	50	5.01	519	86-88	86 ± 2	tr,zo
	C21A	50	5.01	519	75-79	76 ± 2	tr,zo
	C21P	50	5.01	519	66-68	67 ± 2	no reaction
tremolite -absent	T14Z	27	5.01	461	46-48	46 ± 2	dol,zo
	T15&	27	5.00	460	31.5 -43	37 ± 7	dol,cc,chl
	T27L	30	5.00	432	32-37	34 ± 3	no reaction
	T32Z	35	5.00	493	47-49	47 ± 2	dol,zo
	T35J	30	5.00	431	19-24	21 ± 3	dol,cc,chl

Chlorite 4 - amesite

Reaction	Run	Durn (days)	P Kb	T °C	%X CO_2 measured	%X CO_2 corrected	Result
dolomite -absent	D16I	28	5.01	450	7*	7	chl,cc
	D16B	28	5.01	450	15-17	16 ± 2	chl,cc
	D18Z	27	4.93	504	54-55	54 ± 2	tr,zo
	D19P	35	5.05	480	21-24	22 ± 2	chl,cc
	D25P	39	4.99	491	13-19	16 ± 3	tr,zo
	D28V	35	4.97	480	6-9	7 ± 2	chl,cc
	D29V	31	5.01	501	24-28	26 ± 2	tr,zo
	D33S	20	4.90	510	42-44	42 ± 2	tr,zo
	D29L	31	5.01	501	39-43	40 ± 2	chl,cc

TABLE 4:2 CONTD.

Chlorite 4 - amesite contd.

Reaction	Run	Durn (days)	P Kb	T °C	$\%X_{CO_2}$ measured	$\%X_{CO_2}$ corrected	Result
calcite -absent	C26P	37	5.00	492	82-87	84 ± 3	dol,chl
	C26Z	37	5.00	492	50-53	51 ± 2	dol,chl
	C30B	32	4.98	507	63-68	65 ± 3	tr,zo
	C30S	32	4.98	507	48-51	49 ± 2	tr,zo
	C32S	35	5.00	493	94-95	94 ± 2	no reaction
tremolite -absent	T16L	28	5.01	450	60*	60	dol,zo
	T20B	27	4.96	449	30-41	33 ± 4	chl,cc
	T20Q	27	4.96	449	42-46	42 ± 2	no reaction
	T25X	39	4.99	491	48-52	49 ± 2	dol,zo
	T27H	30	5.00	432	49-51	49 ± 2	dol,zo
	T31V	37	5.00	411	41-42	41 ± 2	dol,zo
	T35X	30	5.00	431	18-24	20 ± 3	cc,chl
	T35F	30	5.00	431	32-36	34 ± 2	cc,dol,chl
	T36A	30	5.00	459	21-25	22 ± 3	cc,chl
	T36B	30	5.00	459	40-41	40 ± 2	cc,dol,chl

*runs used for gas chromatography analysis

According to Wiebe and Gaddy (1939), the solubility of CO_2 in water, at room temperature, and this pressure range, is about $28cm^3$ CO_2 (STP equivalent) per gram H_2O, or about 2.3×10^{-2} moles/mole. Recent data, at lower pressures (e.g. Enns et al 1965) support this estimate. The partial pressure of water at room temperature, assuming ideal mixing of gases is negligible in total pressures of hundreds of bars. The net effect, therefore, of using Johannes' method is to produce a systematic bias towards H_2O-rich compositions, amounting to about 2 mole % in X_{CO_2} in H_2O-rich fluids, and about 0.1% in X_{CO_2} in CO_2-rich fluids. This bias has been compensated for in the corrected X_{CO_2} values in the data table (4:2).

The direction of reaction was determined optically, from phase growth and corrosion, taking care to note whether all the phases present were participating in the reaction. The identities of the carbonate phases were established by XRD. The experimental data is presented in Table 4:2, and in figures 4:2, 3.

Resolution of data:

Apart from calorimetry, the main source of thermochemical data is experimentally determined reaction data. The reduction of experimental data to thermodynamic parameters dependent upon single phases provides a data base which permits extrapolation over a wider range, and with a firmer theoretical basis, than the direct application of the original experimental data to natural assemblages. When much of the thermodynamic data is already available, the best modelling technique is to adjust the values of the least certain parameters in

the calculated curve to maximize the fit to the experimental data.

Development of the present data will proceed in a number of stages. In the rest of this chapter, the experimental reaction curves will be resolved to thermodynamic equations, and thermodynamic data on the chlorites will be extracted. In the two subsequent chapters, models involving intermediate chlorite compositions will be calculated, in the iron-free system, and then mineral data, from natural greenschist metadolerites in the Dalradian (Graham 1973) will be included, and a model for the natural rock system constructed.

The Fisher-Zen (1971) approximation for dehydration reactions can also be applied to reactions involving other volatiles, e.g. decarbonation processes, if the free energy term G^* for the volatile is known. This can be calculated:

$$G^*_{volat} = G^{1,T}_{f,\,volat} + RT\ln(P.\Gamma_{vol}.X_{vol}.\gamma)$$

where P is the total fluid pressure; Γ_{vol}, the fugacity coefficient; X_{vol}, the mole fraction of the volatile in the fluid; and γ the fluid mixing parameter.

For a reaction:

$$A = B + mCO_2 + nH_2O$$

the free energy equation can be approximated:

$$\Delta G^{1,298}_{f,sol} - \Delta S^{298}_{f,sol}(T - 298) + \Delta V^{1,298}_{sol}(P-1) + mG^*_{CO_2}(P,T,X) + nG^*_{H_2O}(P,T,X) = 0$$

where T is in degrees absolute. Holloway (1976) has calculated the thermodynamic parameters of several gases, over a wide range of

pressure and temperature, using a modified Redlich-Kwong equation of state (de Santis et al, 1974). This equation takes the form:

$$P = (RT/(\overline{V} - b)) - (a(T)/T^{\frac{1}{2}}\overline{V}(\overline{V} + b))$$

where a and b are parameters characteristic of the molecular species involved, and $\overline{V}$ is the molar volume. For simple molecules a and b can be derived from corresponding state theory, but for more complex molecules, they must be obtained by fitting the equation to empirical data. Thus, the simple model fits Burnham and Wall's (unpublished) CO_2 data to within $\pm 2\%$ relative, but the parameters quoted by de Santis et al (1974) for water, have to be adjusted before the equation fits Burnham et al's (1969) high pressure data. The model also allows the generation of data on gas mixtures, the molecular parameters being combined:

$$b_{mix} = \Gamma_1 . X_1 . b_1 + \Gamma_2 . X_2 . b_2$$

$$a_{mix} = \Gamma_1 . X_1 . a_1 + \Gamma_2 . X_2 . a_2 + X_1 . X_2 . a_{12} . \Gamma_1 . \Gamma_2$$

where a_{12} is a mixing term resulting from interactions between dissimilar molecules. For an H_2O - CO_2 mixture, the expression:

$$a_{12} = (a^o_{H_2O} . a^o_{CO_2})^{\frac{1}{2}} + R^2 . T^{(5/2)} . k$$

where a^o is the temperature-independent term in a, has been assumed by de Santis et al (1974) as a first order approximation. Very little data on the compressibility of CO_2 - H_2O mixtures exists in the literature, but the MRK model fits Greenwood's (1969) data to $\pm 5\%$, and Franck and Todheide's (1959) data to $\pm 6\%$. Holloway (pers. comm.) has written a computer programme which tabulates the thermodynamic

parameters of the gas mixtures (inter alia). Using the pressure and composition dependent free - energy term, RTln a_{volat}, thus computed, in combination with the temperature dependent formational free energy values published by Wagman et al (1945), values for $G^*_{CO_2}(P,T,X)$ and $G^*_{H_2O}(P,T,X)$ can be obtained. Some of these are included in Table 4:4, for the alternative assumptions of ideal mixing of gases, and MRK non-ideal mixing, and the two sets of calculations run in parallel from this point.

The accuracy of the Fisher-Zen approximation decreases considerably if volatiles are present on both sides of the reaction. However, for the reactions under consideration, the variations in the free energy of the solid phases with pressure and temperature probably do not amount to more than 2% of the difference in the equivalent net free energy variations of CO_2 and H_2O.

The thermochemical data used in this study have been taken from Robie and Waldbaum (1968), and Zen (1972) and are presented in Table 4:3. The data extracted by Zen is derived from limited experimental data, by a phase elimination process (Zen 1969, 1971). The relatively large errors on the zoisite data thus reflect the uncertainties associated with the thermochemical data on grossular. The data on clinochlore is derived from only two experimental points (Fawcett and Yoder, 1966), so no error can realistically be estimated for them. By way of comparison, Zen quotes the only other published value of $G_f^{1,298}$ for clinochlore: -1958400 cals (Helgeson 1969). It is, therefore, the chlorite data which will be modified in the present study, and the well-established (Skippen 1971) chlorite -

TABLE 4:3

THERMOCHEMICAL DATA USED IN CALCULATIONS

T = 298.15 K

Phase	$-G_f^{1,298}$ cal	$-S_f^{298}$ cal/deg	$V^{1,298}$ cal/bar
quartz	204646 ± 410	43.616 ± .05	0.5423
zoisite*	1552700 ±1400	319.5 ±3.4	3.262
tremolite*	2775200 ±2600	582.92 ± .94	6.5228
clinochlore*	1974000	523	4.9425
dolomite	518734 ± 530	130.402 ± .22	1.5377
calcite	269908 ± 330	62.65 ± .32	0.8827
spinel	522961 ± 510	100.082 ± .54	0.94909
enstatite	349394 ± 450	69.584 ± .45	0.75215
forsterite	491938 ± 530	95.362 ± .62	1.0466

*from Zen (1972), the rest from Robie and Waldbaum (1968)

zoisite - absent reaction will serve as an indicator of the limiting precision of the data. Zen's (1972) data on aluminous minerals is preferred to that of Thompson (1974), on the grounds that the latter has used reaction data on zoisite, from Boettcher (1970), and Newton (1966), both studies with which the present work disagrees (Chapter 3).

For a chlorite composition:

$$0.5(Mg_{12-x}Al_{2x}Si_{8-x}O_{20}(OH)_{16}) \quad - \quad (\text{chl } x)$$

the three reactions investigated can be written:

$$(\text{trem})\ 6\ \text{chlor} + (36 + x)\text{cc} + (9x - 24)\text{qtz} + (36 - 7x)CO_2 = 2x\ \text{zo} + (36 - 3x)\ \text{dol} + (24 - x)\ H_2O$$

$$(\text{dol})\ 30\ \text{chlor} + (72 + 14x)\text{cc} + (168 + 21x)\ \text{qtz} = (36 - 3x)\text{trem} + 10x\ \text{zo} + (72 + 14x)CO_2 + (84 - 2x)\ H_2O$$

$$(\text{cc})\ 18\ \text{chlor} + (72 + 14x)\ \text{dol} + (216 + 35x)\ \text{qtz} = (36 + x)\text{trem} + 6x\ \text{zo} + (144 + 28x)\ CO_2 + (36 - 4x)\ H_2O$$

For the purposes of calculation, five definitive points on the isobaric univariant reaction curves at 5 Kb have been selected, and are included in Table 4:4. For each reaction, free energy equations of the form:

$$A - cG^{1,298}_{f,chl} - (T - 298)\ (B - cS^{298}_{f,chl}) + P\ V^{1,298}_{sol} + a\ G^{*}_{CO_2}(P,T,X) + b\ G^{*}_{H_2O}(P,T,X) = 0$$

have been set up, using the molar volume of clinochlore for all chlorites. For a given chlorite, the linear equations in $G^{1,298}_{f,chl}$ and $S^{298}_{f,chl}$ from the five data points are, in theory, simultaneous.

The three data points on the tremolite-absent curve cover the broadest temperature range, and having the same coefficient for $G^{1,298}_{f,chl}$, are the most convenient for solving for $S^{298}_{f,chl}$; so these were used to derive the entropy first, which was, in turn, used to calculate the formational free energy. This method was used in preference to a least squares fit where an arbitrary weighting would be necessary to accentuate the greater temperature range covered by the tremolite-absent reaction data. The solutions for both ideal and MRK non-ideal mixing are presented in Table 4:4.

The uncertainties involved in these calculations are considerable, and fall into two main groups; the uncertainties associated with the source data, and the uncertainties implicit in the methodology. The first group can be subdivided into two: the uncertainties in the thermochemical data, which are quoted by both Zen (1972), and Robie and Waldbaum (1968) at two standard deviations; and the uncertainties in the experimental data. The uncertainties in the actual measurements are about $\pm 5^{o}C$, ± 100 bars (Ford 1972; and Chapter 1) and ± 2 mole% in X_{CO_2} (this chapter), on top of which must be added the uncertainty in positioning the reaction curves between the brackets. The MRK non-ideal model fits Greenwood's (1969) molar volume data to $\pm 6\%$ relative (Holloway 1976), which if taken to be the arithmetical uncertainty on the model, can be transferred to the log activity term according to the relationship:

$$P \overline{V}_{gas} = RT \ln a_{gas}$$

The ideal mixing model can be assumed to have an arithmetical uncertainty deriving from the fits of the several calculated fugacities

TABLE 4:4

1) Experimental data points used in calculation
2) Associated $G^*_{H_2O}$ and $G^*_{CO_2}$ values, and
3) Calculated thermodynamic parameters for chlorites

$P_{CO_2} + P_{H_2O} = P_{flu} = 5$ Kb

a) Ideal mixing:

Chlorite 1 - penninite:

Reaction	T °C	X_{CO_2}	$G^*_{CO_2}$	$G^*_{H_2O}$	$S^{298}_{f,chl}$	uncertainty	$G^{1,298}_{f,chl}$	uncertainty
(trem)	505 ± 1	0.515	-79542	-38240				
	440 ± 3	0.40	-80984	-40159	-540.88	± 20.17 calc* ± 12.95 expt**		
	405 ± 5	0.30	-81945	-41192	cal/deg		-1975025	
(dol)	505 ± 1	0.515	-79542	-38240			-1972222	
(cc)	518 ± 1	0.7	-78845	-38559			-1969234	
						mean	-1972000	± 9667 calc ± 2921 expt cals

*theoretically derived uncertainty

**internal consistency of data

TABLE 4:4 CONTD.

P_{flu} = 5 Kb

b) MRK non-ideal mixing:

Chlorite 1 - penninite:

Reaction	T °C	X_{CO_2}	$G^*_{CO_2}$	$G^*_{H_2O}$	$S^{298}_{f,chl}$	uncertainty	$G^{1,298}_{f,chl}$	uncertainty
(trem)	505 ± 1	0.515	-79097	-37730				
	440 ± 3	0.40	-80275	-39714	-582.11	± 20.19 calc ± 7.01 expt		
	405 ± 5	0.30	-80867	-40857	cal/deg		-1994497	
(dol)	505 ± 1	0.515	-79097	-37730			-1988902	
(cc)	518 ± 1	0.7	-78667	-37787			-1986487	
						mean	-1990000	± 9676 calc ± 4114 expt

TABLE 4:4 CONTD.

P_{flu} = 5 Kb

a) Ideal mixing contd:

Chlorite 4 - amesite:

Reaction	T °C	X_{CO_2}	$G^*_{CO_2}$	$G^*_{H_2O}$	$S^{298}_{f,chl}$	uncertainty	$G^{1,298}_{f,chl}$	uncertainty
(trem)	505 ± 1	0.44	-79786	-38017				
	465 ± 3	0.425	-80475	-39543	-534.20	± 35.32 calc		
	400 ± 5	0.40	-81636	-41580	cal/deg	± 11.89 expt	-2007839	
(dol)	505 ± 1	0.44	-79786	-38017			-2007267	
(cc)	505 ± 1	0.44	-79786	-38017			-2006245	
								± 16826 calc
						mean	-2007000	± 855 expt
							cals	

TABLE 4:4 CONTD.

P_{flu} = 5 Kb

b) MRK non-ideal mixing:

Chlorite 4 - amesite:

Reaction	T °C	X_{CO_2}	$G^*_{CO_2}$	$G^*_{H_2O}$	$S^{298}_{f,chl}$	uncertainty	$G^{1,298}_{f,chl}$	uncertainty
(trem)	505 ± 1	0.44	-79181	-37613				
	465 ± 3	0.425	-79846	-38906	-529.85	± 35.33 calc ± 1.51 expt		
	400 ± 5	0.40	-80925	-41063			-2005200	
(dol)	505 ± 1	0.44	-79181	-37613			-2001575	
(cc)	505 ± 1	0.44	-79181	-37613			-1995104	
						mean	-2000600 ± 16834 calc; ± 5114 expt	

to their respective empirical data; $\pm 2\%$ for CO_2 relative to Burnham and Wall's (unpublished) data, and $\pm 1.3\%$ for H_2O relative to Burnham et al's (1969) data (Holloway 1976). The uncertainties in the molar volume data only affect the fourth decimal place, and are insignificant compared with the systematic error involved in using the molar volume of clinochlore for the whole range of chlorite compositions. The difference in chlorite molecular weights across the range of aluminium contents is only about 0.6%, so this systematic error is, in turn, swamped by the 4% uncertainty in the pressure measurement. The combination of these uncertainties is cartooned in figure 4:4.

The systematic error deriving from the Fisher-Zen approximation has already been shown to reach a maximum of no more than 2%, when the volatiles are on opposite sides of the reaction. The methodological error in assuming either the ideal, or the MRK non-ideal mixing model is indeterminate from the present data, but the reversal of either set of calculations, and of the Fisher-Zen technique to calculate $T\text{-}X_{CO_2}$ models will reverse any systematic biases due to these assumptions. Table 4:4 includes the formational free energy and the formational entropy of both chlorites, together with errors deriving from data inconsistency (non-simultaneity of equations), and uncertainties from the calculation method. The latter is dominated by the uncertainties on the thermochemical source data, the exceptionally high uncertainties on the amesite data being due to the higher proportions of zoisite involved in these reactions. The theoretically derived uncertainties may be inflated by combination of interdependent errors on the source data, and so may, in fact, be smaller than stated here (Anderson, 1977).

FIGURE 4:4 CONTD.

ALLOCATION OF UNCERTAINTIES

For a series of equations:

$$A_s\, x + B_s\, y + K_s = 0$$

with known values of A_s, B_s, and error $\pm d_s$ on K_s; the uncertainty on x and y; x_e and y_e respectively, can be expressed:

$$A_s\, x_e + B_s\, y_e = d_s$$

if:

$$a^2 = \sum_{s=1}^{n} d_s^2 / (n-2)$$

then:

$$x_e^2 / \sum_{s=1}^{n} B_s^2 = y_e^2 / \sum_{s=1}^{n} A_s^2 = a^2 / \Delta$$

where:

$$\Delta = \begin{vmatrix} \sum_{s=1}^{n} A_s^2 & \sum_{s=1}^{n} A_s B_s \\ \sum_{s=1}^{n} A_s B_s & \sum_{s=1}^{n} B_s^2 \end{vmatrix}$$

FIGURE 4:4

SUMMATION OF UNCERTAINTIES

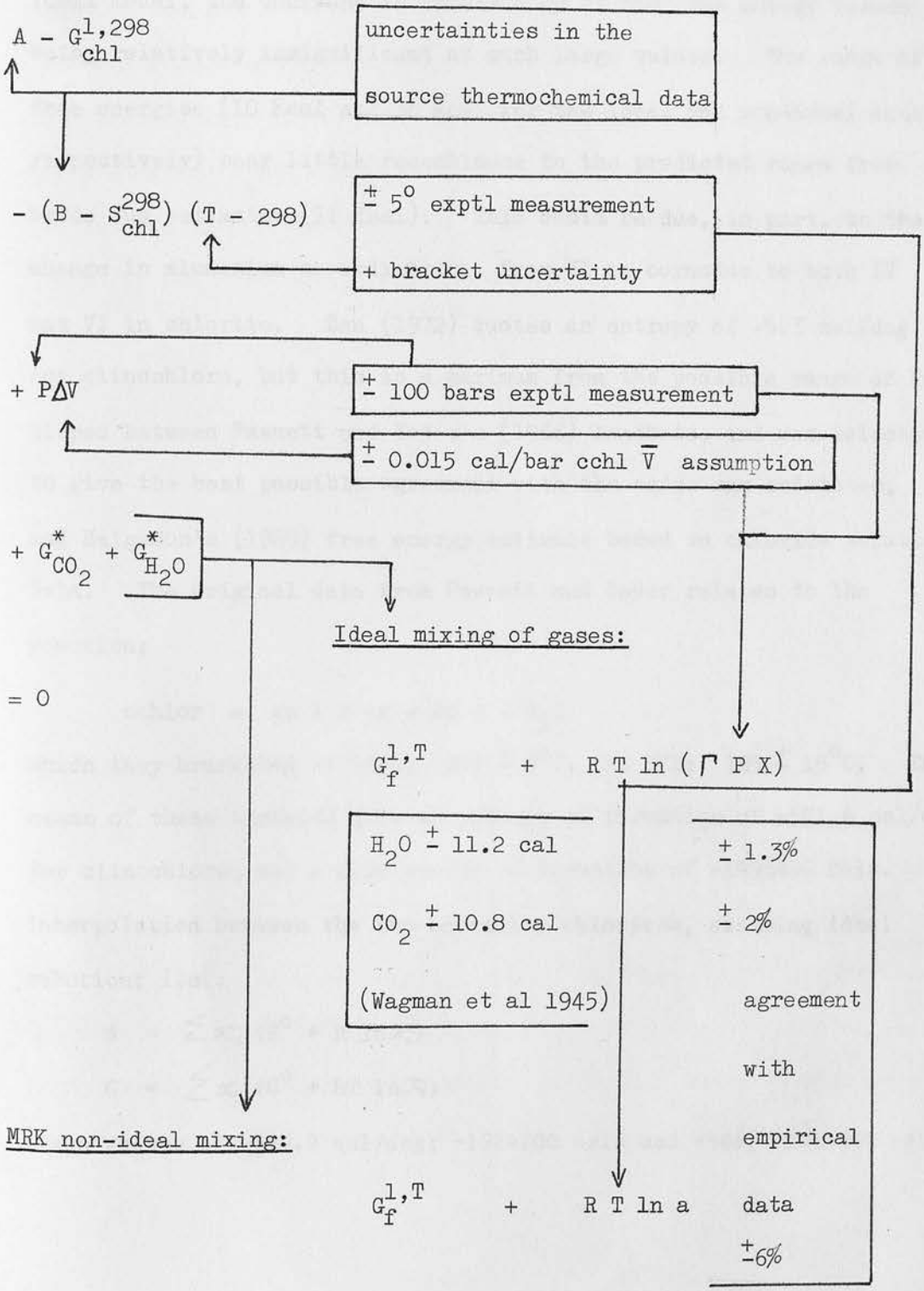

The internal consistency of the data sets indicate that the calculated values are probably more meaningful than the derived uncertainties would allow. In particular, the consistency of the entropy data calculated in the non-ideal model favours it against the ideal model, the decrease in consistency of the free energy values being relatively insignificant at such large values. The range of free energies (10 Kcal and 36 Kcal for the ideal and non-ideal models respectively) bear little resemblance to the predicted range from oxide sum estimates (51 Kcal). This could be due, in part, to the change in aluminium co-ordination, from VI in corundum to both IV and VI in chlorite. Zen (1972) quotes an entropy of -523 cal/deg for clinochlore, but this is a maximum from the possible range of P-T slopes between Fawcett and Yoder's (1966) brackets, and was selected to give the best possible agreement with the oxide sum estimates, and Helgeson's (1969) free energy estimate based on chloride solution data. The original data from Fawcett and Yoder relates to the reaction;

$$\text{cchlor} = \text{sp} + 2\ \text{en} + \text{fo} + 4\ H_2O$$

which they bracketed at 10Kb; 831 $\pm$ 6°C, and 5Kb; 785 $\pm$ 15°C. The means of these brackets give an entropy of formation of -551.6 cal/deg for clinochlore, and a free energy of formation of -1996400 cals. Interpolation between the two endmember chlorites, assuming ideal solution; i.e.:

$$S = \sum x_i (S^\circ + R \ln x_i)$$

$$G = \sum x_i (G^\circ + RT \ln x_i)$$

gives values of -539.9 cal/deg; -1984200 cals and -566; -1993900 cals

from the ideal and non-ideal gas mixing models respectively. The reasonable agreement between the experimental data sets indicates that the aluminium substitution in chlorites could be near ideal, and, at least within experimental error, this form of interpolation of chlorite data is a fair approximation. However the field evidence shows a predominance of aluminous clinochlore over other chlorites in the greenschist facies which could indicate a slight negative deviation from ideality. For the present, nevertheless, the substitution will be assumed ideal, and the preferred data set will be that deriving from the MRK non-ideal mixing model.

CHAPTER 5

DEVELOPMENT OF THE MIXED VOLATILE MODEL: I

Context of the basic isobaric invariant bundle in the system CAMS - H_2O - CO_2:

1) Introduction:

No experimental work in the full CAMS - H_2O - CO_2 system, at the P-T conditions of interest, has been published, but data exist for the two subsystems CMS - H_2O - CO_2, and CAS - H_2O - CO_2.

The "siliceous dolomite", CMS - H_2O - CO_2 system has been thoroughly studied, particularly since Metz and Trommsdorf's (1968) synthesis of experimental and field data, in the light of phase equilibrium theory. By 1971, enough experimental data existed for Skippen to be able to calculate, with reasonable accuracy, the curves of all possible isobaric univariant reactions involving the phases qtz - cc - dol - tc - trem - diop - fo - en - fluid, without recourse to calorimetric data. As far as the present study is concerned, the location of the isobaric invariant point involving tc - cc - qtz - trem - dol - fluid, by Slaughter et al (1975) is of primary importance. At 5Kb P_{flu}, this invariant point exists at $460 \pm 15^{\circ}C$, 20 mole % X_{CO_2}.

In the system CAS - H_2O - CO_2, Storre and Nitsch (1972) have studied the reaction:

$$2zo + CO_2 = 3an + cc + H_2O$$

and have determined that, at 5 Kb, total fluid pressure, it lies at a

virtually constant X_{CO_2} of about 6%, over the temperature range 570-670°C. However, if the present study has located the cc - dol - chl - zo - trem - qtz - fluid isobaric invariant point accurately, the zoisite breakdown reaction must undergo a severe inflexion in $T-X_{CO_2}$ space, between 530-600°C, which casts doubt on the lower end of the stability range determined by Storre and Nitsch. Glassley (1974) comes to a similar conclusion in his study of the prehnite-pumpellyite facies.

Two workers have published theoretical reaction networks, in the CAMS - H_2O - CO_2 system, which include the phases under discussion. Watts (1973 a,b) has calculated $\mu_{CO_2} - \mu_{H_2O}$ grids involving the phases an - zo - cc - chl - qtz - trem - tc - mgs - dol - fluid, at two temperatures; 152°C, and 427°C. Glassley (1974) has calculated $T-X_{CO_2}$ sections modelling the prehnite - pumpellyite facies at 1Kb and 2Kb, involving the phases prehn - pump - cc - chl - qtz - trem - tc - dol - zo - gross - fluid. Both these studies are at somewhat lower temperatures than the present work; in addition the former is at lower fluid pressures, and the latter at lower total pressures. However they may be linked by the $T-X_{CO_2}$ grid constructed in the next section.

2) Schreinemakers' Grid Construction:

The CMS - H_2O - CO_2, and CAS - H_2O - CO_2 experimental data may conveniently be incorporated into the present study by considering a network of reactions involving the phases qtz - cc - dol - tc - trem - zo - chl - an - fluid in the system CAMS - H_2O - CO_2. The $T-X_{CO_2}$ grid

FIGURE 5:1

PHASE POLYGON: ACM DIAGRAM PROJECTED FROM

SiO_2, CO_2, and H_2O

Chlor 1 - penninite

Chlor 2 - clinochlore

Chlor 3 - ripidolite/sheridanite

Chlor 4 - amesite

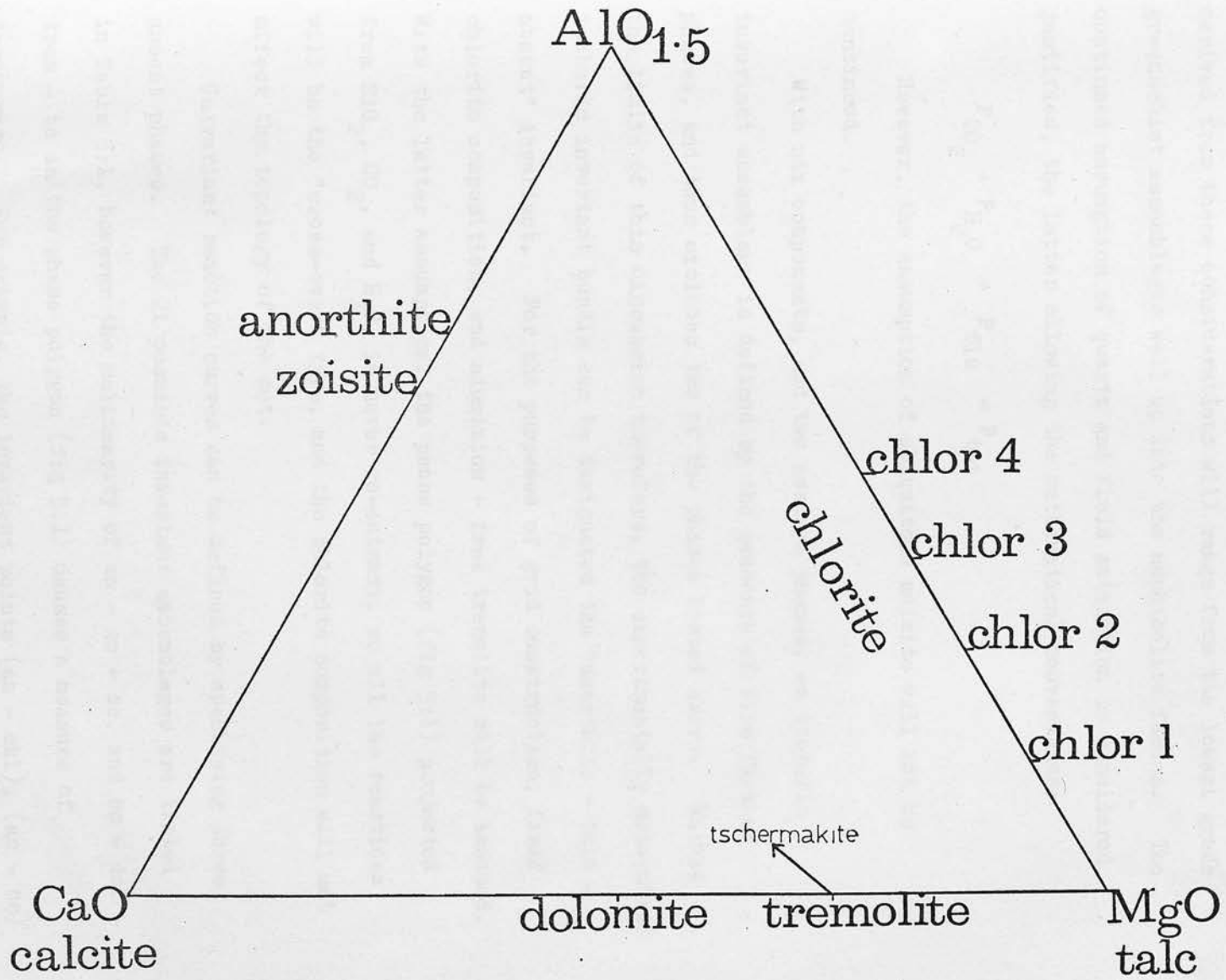
AlO1·5
anorthite
zoisite
chlor 4
chlorite
chlor 3
chlor 2
chlor 1
tschermakite
CaO
calcite
dolomite
tremolite
MgO
talc

derived from these considerations will range from the lowest grade greenschist assemblages well up into the amphibolite facies. The continued assumption of quartz and fluid saturation is considered justified, the latter allowing the mathematical convenience:

$$P_{CO_2} + P_{H_2O} = P_{flu} = P_{tot}$$

However, the assumption of ubiquitous zoisite will not be continued.

With six components, and two assumed phases, an isobaric invariant assemblage is defined by the presence of five further phases, and thus excludes two of the phases listed above. Within the limits of this discussion therefore, the experimentally determined isobaric invariant bundle can be designated the "anorthite - talc - absent" invariant. For the purposes of grid construction, fixed chlorite composition, and aluminium - free tremolite will be assumed. With the latter assumption, the phase polygon (fig 5:1) projected from SiO_2, CO_2, and H_2O, is never re-entrant, so all the reactions will be the "cross-over" type, and the chlorite composition will not affect the topology of the net.

Univariant reaction curves can be defined by specifying three absent phases. The 21 possible invariant assemblages are listed in Table 5:1, however the colinearity of an - zo - cc, and cc - dol - trem - tc in the phase polygon (fig 5:1) causes a measure of degeneracy. For example, the invariant points (an - chl), (an - cc) and (cc - chl) degenerate to the CMS - H_2O - CO_2 invariant located by Slaughter et al (1975). Pairs of invariant points are linked by

TABLE 5:1

EXPLANATION OF COMPATABILITY RELATIONS

Each univariant reaction defined by three absent phases links three invariant points defined by the pairs of absent phases permutable from the univariant designation. In the table, opposite, the column 'compatability dependence' contains invariants linked in this way.

The instances where only one linked invariant appears in the column, are restricted by the assumption of the reality of the degenerate invariant (zo-an-chl) (Slaughter et al 1975). In these cases, the two linked invariants have opposing stabilities. The remainder of the invariants are shown as being dependent upon two linked invariants. In these cases, if the stability states of the two linked invariants are the same, the third invariant is metastable, if they are opposite, then the third invariant is stable.

TABLE 5:1

COMPATABILITY RELATIONS FOR THE INVARIANT BUNDLES, IN THE ISOBARIC SYSTEM CAMS-H_2O-CO_2, INVOLVING THE PHASES:

anorthite	dolomite	clinochlore	
zoisite	tremolite	quartz + fluid	assumed ubiquitous
calcite	talc		

Invariant	Phase-absent univariant reaction zo	an	cc	dol	tr	tc	cchl	Compatability dependence	Actual stability
1 (zo-an)	/	/	+	±	+	+	x	(zo-chl)	stable
2 (zo-cc)	/	+	/	*	*	*	+	(an-cc)	stable
3 (zo-dol)	/	+	*	/	*	*	+	(an-dol)	m/stable
4 (zo-tr)	/	+	*	*	/	*	+	(an-tr)	m/stable
5 (zo-tc)	/	+	*	*	*	/	+	(an-tc)	m/stable
6 (zo-chl)	/	x	+	+	±	+	/	(zo-an)	m/stable
7 (an-cc)	+	/	/	*	*	*	+	(zo-cc)	m/stable
8 (an-dol)	+	/	*	/	*	*	+	(zo-dol)	stable
9 (an-tr)	+	/	*	*	/	*	+	(zo-tr)	stable
10 (an-tc)	+	/	*	*	*	/	+	(zo-tc)	stable
11 (an-chl)	x	/	+	±	+	+	/	(zo-chl),(an-zo)	stable
12 (cc-dol)	*	*	/	/	*	*	*	(zo-cc),(zo-dol)	stable
13 (cc-tr)	*	*	/	*	/	*	*	(zo-cc),(zo-tr)	stable
14 (cc-tc)	*	*	/	*	*	/	*	(zo-cc),(zo-tc)	stable
15 (cc-chl)	+	±	/	*	*	*	/	(zo-chl),(zo-cc)	m/stable
16 (dol-tr)	*	*	*	/	/	+	±	(zo-dol),(zo-tr)	m/stable
17 (dol-tc)	*	*	*	/	+	/	+	(zo-dol),(zo-tc)	m/stable
18 (dol-chl)	+	+	*	/	+	±	/	(zo-dol),(zo-chl)	m/stable
19 (tr-tc)	*	*	*	+	/	/	+	(zo-tr),(zo-tc)	m/stable
20 (tr-chl)	+	±	*	+	/	+	/	(zo-tr),(zo-chl)	stable
21 (tc-chl)	+	±	*	+	+	/	/	(zo-tc),(zo-chl)	stable

*normal univariants

+degenerate univariants

xdoubly degenerate univariants, linking degenerate invariants

univariant reactions with an absent phase common to both points. Thus, any one univariant reaction defined by three absent phases will pass through only three invariant points, unless degeneracy occurs. Since each univariant reaction changes its stability state on passing through a stable invariant point, and can only appear stable in a continuous curve, this places restrictions on the compatability of the 21 isobaric invariant assemblages. These compatability relations are included in Table 5:1.

The concepts behind all three sets of experimental data discussed in this section are firmly rooted in field evidence, so it is fair to assume that all the experimental data relates to stable, rather than metastable reactions. A further restriction on the combination of invariant bundles is imposed by the characteristic shapes of H_2O - and CO_2 - bearing reaction curves in $T\text{-}X_{CO_2}$ space as described by Greenwood (1967). Taking these restrictions into consideration, the isobaric invariant bundles can be constructed, and linked according to Schreinemakers' rules (Zen 1966) to produce the unique grid presented as figure 5:2.

3) Discussion:

Although the Schreinemakers' net is fairly extensive in $T\text{-}X_{CO_2}$ space, the assumptions made during its construction restrict its applicability considerably. Since, assuming non-aluminous tremolite, the phase polygon is non-reentrant whatever chlorite composition is assumed, the arrangement of the univariant reaction curves in each invariant bundle is fixed. However relative movement of the

FIGURE 5:2

SCHREINEMAKERS' WEB

in T - X_{CO_2} space;
for the chemical system CAMS - H_2O - CO_2;
involving the phases:
an anorthite zo zoisite
cc calcite dol dolomite
tr tremolite tc talc
chl chlorite + quartz, fluid.
The isobaric invariant points are numbered according to Table 5:1.

At 5 Kb, invariant point (1) has been located at 460 $\pm$ 15°C, 20 mole $\%X_{CO_2}$ (Slaughter et al 1975); and invariant point (10) at 505 $\pm$ 5°C, 0.48 $\pm$ .10 X_{CO_2} (present work, Chapter 4).

All experimentally determined reaction curves are represented by heavier lines.

pseudo-invariant bundles themselves, is possible with chemical (Fe - Mg, Al - Fe) and physical (pressure) variations. The former is well-demonstrated in the next chapter, in which natural mineral data will be incorporated into the single invariant model.

The network for pressures other than 5Kb varies considerably, particularly in cases where either or both the assumptions:

$$P_{CO_2} + P_{H_2O} = P_{flu} = P_{tot}$$

do not hold. For example, Ferry (1976) has studied some calcareous pelites in the Waterville - Vassalboro area of South-Central Maine, which have undergone metamorphism at an estimated 3.5Kb, total pressure, by contact with a wet granite intrusion. The combined pressures of CO_2 and H_2O at low grades (c 380°C), he calculates at 1.8Kb, while at higher grades (520°C max), the combined pressure reaches about 3.3Kb. He explains this by considering the granite as a source of both heat and water, and defines three isograds in this unusual form of metamorphism:

R1: msc + ank + qtz + H_2O = biot + chlor + cc + CO_2

R2: intermed. plag + cc + chl + qtz = Ca amph + calcic plag + H_2O + CO_2

R3: calcic plag + cc + H_2O = zo + intermed. plage + CO_2

R1 is a complex version of the dolomite breakdown reaction, and is common in metapelite sequences; R2 is an equivalent of the dolomite-absent reaction in the present experimental study, and R3, is the zoisite - calcite - anorthite reaction studied by Storre and Nitsch (1972). However the sequence of isograds is totally different from

that predicted using the Schreinemakers' net, and probably reflects the relatively low fugacities of both CO_2 and H_2O, and the lower overall pressure.

Further distortion of the net occurs when it overlaps with prehnite- or pumpellyite-bearing assemblages which were not considered in its construction. Nitsch (1971) has shown that both prehnite and pumpellyite can be involved in breakdown reactions to actinolite plus chlorite at around 350°C, effectively independent of pressure over the range of interest. However Hashimoto (1972) has described two metamorphic sequences in which pumpellyite-bearing assemblages are interwoven with typical greenschist assemblages to be found on the grid. In the Permian greenstones of the Tamba region of Kyoto, he has observed a series of assemblages which can be interpreted by the reaction sequence:

1) CO_2 + pump + qtz = cc + ep + chl + H_2O

2) cc + chl + qtz = ep + act + H_2O + CO_2

While at higher pressures (the lower part of a blueschist series) in the Oozu-Nomura region of the Chichibu belt, W. Shikoku, the sequence had changed to:

3) cc + chl + qtz = pump + act + H_2O + CO_2

4) pump + chl + qtz = ep + act + H_2O

If Nitsch's (1971) data is correct, this 'overlap' of the greenschist and pumpellyite facies with increasing pressure is caused solely by movement of the present set of pseudo-invariant bundles in

P-T-X_{CO_2} space. As far as the stability of prehnite, in the presence of CO_2 is concerned, Glassley (1974) estimates that it breaks down at a maximum temperature of around 400°C; above X_{CO_2} = 0.1 at 2Kb, and above X_{CO_2} = 0.25 at 1 Kb.

Within the assumed restrictions of pressure and fluid composition, the net predicts credible assemblages for typical greenschist and amphibolite facies sequences, such as the Dalradian, and the arbitrary adjustment of Storre and Nitsch's (1972) experimental data on the zo - cc - an reaction is justified by the relatively common occurrence of the assemblage epidote + dolomite in the amphibolite facies, (Graham pers. comm.) although not in the metadolerites themselves. The one exception to this realism is the somewhat overfrequent prediction of talc-bearing assemblages, when the mineral is only common in ultrabasic rocks, and siliceous dolomites. At high X_{CO_2}, talc reacts with CO_2 to form magnesite and quartz (Greenwood 1967), with a reaction curve that, at 2Kb, passes through 60% X_{CO_2} at 300°C, and approaches the T-axis at X_{CO_2} = 1, assymptotically above 450°C. Since, in the ACM projection in use, the reaction is quasi-isochemical, this reaction has been omitted, with the result that talc appears on the grid instead of magnesite at CO_2-rich conditions.

However, the most blatantly unfulfilled prediction of the model, is the appearance of zo- chl - tc, and zo - trem - tc assemblages in preference to zo - chl - trem under very H_2O-rich conditions. Glassley (1974) found a similar problem which he solved by claiming that tremolite rather than talc was stable in the presence of pumpellyite + prehnite. A parallel interpretation in the present

situations would be to note that serpentine, rather than talc, is stable in iron-bearing systems. The higher water content of serpentine will generate slight differences in the characteristic shapes of the reaction curves; in particular, moving the dolomite - calcite - absent invariant (12) on the T-axis. However, the distribution of the reaction curves in each invariant bundle will be unchanged, since the form of the phase polygon (fig 5:1), again, remains unaltered. A further explanation, for the absence of both talc and serpentine could lie with the rocks. The epidote - chlorite - actinolite (Type I) assemblages described by Graham (1973), and Harte and Graham (1975), typically contain relict pyroxenes altering to the amphibole, indicating a failure to reach equilibrium even at this stage of hydration, while serpentine is virtually restricted to veining in the rocks. A third possible factor working against the appearance of talc, or serpentine, could be the absolute geometry of the net; the position of invariant point 8 (dol - an - absent) may be very close to the 'X_{H_2O} = 1' T-axis, so that, unless the metamorphic fluid was pure water, neither talc nor serpentine would appear.

The limited number of phases used in net construction leads to further failures in its realism. Thus the omission of alumino-silicates means, for example, that a chlorite breakdown reaction of the form:

chlor + CO_2 = Al silic + magnesite - siderite + qtz + H_2O

does not appear on the net, although the characteristic assemblage; mgs-sid - ky - pyroph - qtz without chlorite appears in the

greenschist calc-pelites on Islay (Burgess, Graham and Harte, in ppn). Omission of grossular and pyrope from the phases used limits the upper part of the net, just as the omission of prehnite and pumpellyite has been shown to limit the lower part. However limits must be set, and omission of these particular phases sets limits coinciding with accepted facies boundaries. Thus, within the pressure and fluid composition limits, and the other shortcomings described, the net is valid from the base of the greenschist facies to the epidote-amphibolite facies.

CHAPTER 6

DEVELOPMENT OF THE MIXED VOLATILE MODEL: II

Application to natural rocks:

1) Model construction:

This section of the thesis is concerned with the extrapolation of the experimentally quantified mixed volatile model to natural greenschist assemblages. For this purpose, the Dalradian greenschist metadolerites will be assumed to be a typical example of the facies, and rocks collected from Knapdale, by C.M. Graham (1973) will be used to supply the necessary phase chemical data. For the complete calculation of the three major reaction curves in the model, the calcite-, tremolite- and dolomite-absent reactions, chemical data on the epidote, chlorite, and amphibole are required. The carbonates can be assumed to be relatively pure endmembers (but see 6:3 - carbonate geothermometry). Thus, of the series of assemblages classified by Harte and Graham (1975), only Types I and II, epidote - chlorite - amphibole - $\pm$ calcite, are appropriate as data sources. Three rocks have been selected, and are referred to by their Edinburgh University Geology Department catalogue numbers. All three were collected from immediately below the garnet isograd; 25005 represents the most magnesian composition found, 25006, the most iron-rich, (apart from some anomalous Keratorphyres), and 25105 represents an average composition tending towards the iron-rich. The analyses of the phases of interest, in the three rocks are

TABLE 6:1

PHASE CHEMISTRY OF AMPHIBOLE, CHLORITE, AND EPIDOTE

IN SELECTED GREENSCHIST METADOLERITES

(extracted from microprobe data, by Graham 1973)

Rock 25005

Amphibole (to 23(0) anhydrous)			chlorite (to 28(0) anhydrous)
0.03-0.25	0.14	Al^{VI}	2.60
1.39-1.28	1.33	Fe	3.32
3.66-3.36	3.51	Mg	6.05
.03	0.03	$misc^{VI}$	0.05
2.00	2.00	Ca	--
0.03-0.18	0.11	alk	--

$a^{amph}_{trem} = X^{A}_{l-alk} . (X^{M4}_{Ca})^2 . (X^{M1,2,3}_{Mg})^5$

$= 0.89 . 1^2 . 0.70^5$

$RT\ln a^{amph}_{trem} = 3.767\ T$

(1) $a_{chlor} = (X^{VI}_{Mg})^{6-(ch/2)}$

$= (0.636)^{4.75}$

$RT\ln a_{chlor} = -4.27\ T$

Epidote

$Ps_{12.9}$ Ps_{13}

$X^{M3}_{Al} = 0.638$

$(1+c)RT\ln X^{M3}_{Al} = -0.949T$

$(1+c)RT\ln \gamma^{M3}_{Al} = 450$

(2) $a_{chlor} = (ch/2z)^3 . (X^{Tcl,2}_{Mg})^3$

$= (0.962)^3 . (0.44)^3$

$RT\ln a_{chlor} = -5.13\ T$

TABLE 6:1 CONTD.

PHASE CHEMISTRY OF AMPHIBOLE, CHLORITE, AND EPIDOTE IN SELECTED GREENSCHIST METADOLERITES

Rock 25006

Amphibole (to 23(0) anhydrous)		Chlorite (to 28(0) anhydrous)
0.74	Al^{VI}	2.46
2.69	Fe	5.09
1.78	Mg	4.46
0.09	$misc^{VI}$	0.13
1.75	Ca	--
0.63	alk	--

$a^{amph}_{trem} = X^{A}_{l-alk} \cdot (X^{M4}_{Ca})^2 \cdot (X^{M1,2,3}_{Mg})^5$

$= 0.62 \cdot 0.87^2 \cdot 0.34^5$

$RT\ln a^{amph}_{trem} = -12.22\ T$

(1) $a_{chlor} = (X^{VI}_{Mg})^{6-(ch/2)}$

$= (0.463)^{4.75}$

$RT\ln a_{chlor} = -7.28\ T$

Epidote Ps_{26} (assumed)

$X^{M3}_{Al} = 0.317$

$(1+c)RT\ln X^{M3}_{Al} = -2.484\ T$

$(1+c)RT\ln \gamma^{M3}_{Al} = 1518$

(2) $a_{chlor} = (ch/2z)^3 \cdot (X^{Tcl,2}_{Mg})^3$

$= (1.02)^3 \cdot (0.15)^3$

$RT\ln a_{chlor} = -11.20\ T$

TABLE 6:1 CONTD.

PHASE CHEMISTRY OF AMPHIBOLE, CHLORITE, AND EPIDOTE IN SELECTED GREENSCHIST METADOLERITES

Rock 25105

Amphibole (to 23(0) anhydrous)		chlorite (to 28(0) anhydrous)
0.41	Al^{VI}	2.56
2.12	Fe	5.01
2.44	Mg	4.35
0.05	$misc^{VI}$	0.13
1.89	Ca	--
0.26	alk	--

$a^{amph}_{trem} = (X^{A}_{l-alk}).(X^{M4}_{Ca})^2.(X^{M1,2,3}_{Mg})^5$ (1) $a_{chl} = (X^{VI}_{Mg})^{6-(ch/2)}$

$= 0.85.\ 0.945^2.\ 0.486^5$ $= 0.456^{4.75}$

$RT\ln a^{amph}_{trem} = -7.716\ T$ $RT\ln a_{chl} = -7.41\ T$

Epidote Ps_{17} (2) $a_{chl} = (ch/2z)^3.(X^{Tcl,2}_{Mg})^3$

$X^{M3}_{Al} = 0.532$ $= 0.98^3.\ 0.15^3$

$(1+c)RT\ln X^{M3}_{Al} = -1.339\ T$ $RT\ln a_{chl} = -11.47\ T$

$(1+c)RT\ln \gamma^{M3}_{Al} = 774$

presented in Table 6:1. 25006 contains no epidote so the composition of the epidote in a comparable rock has been assumed.

The incorporation of the natural mineral data into the T-X_{CO_2} model derived from the present experimental data (Chapter 4) demands several assumptions regarding the mixing properties of various solid solutions. Since many of the alternative assumptions cannot be distinguished in the light of the present experimental data, parallel alternative models must be generated from each indeterminate nexus, and the endproducts judged on field evidence, and the experimental data of other workers. The derivation of the alternative models is presented in flow diagram form as figure 6:1. The various stages in the development are denoted by the Roman numerals in the lefthand column, and the three alternate endproduct models, at each pathend, are derived from the three rock compositions employed.

The calculation of T-X_{CO_2} sections throughout this chapter has been performed using a Fisher - Zen (1971) equation:

$$\Delta G^{1,298}_{f,sol} - (T - 298)\Delta S^{298}_{f,sol} + P\Delta V^{1}_{sol} + nG^{*}_{CO_2}(P,T) + mG^{*}_{H_2O}(P,T) = - RT\ln a^{n}_{CO_2} \cdot a^{m}_{H_2O}$$

with T in degrees absolute, and

$$G^{*} = G^{1,T}_{f} + RT\ln f$$

For the model assuming ideal mixing of gases:

$$a_{CO_2} = X_{CO_2} \quad ; \quad a_{H_2O} = X_{H_2O}$$

while, for the MRK non-ideal mixing model, Holloway's computer programme tabulates gas activities:

FIGURE 6:1

FLOW CHART OF ALTERNATIVE T-X_{CO_2} MODELS

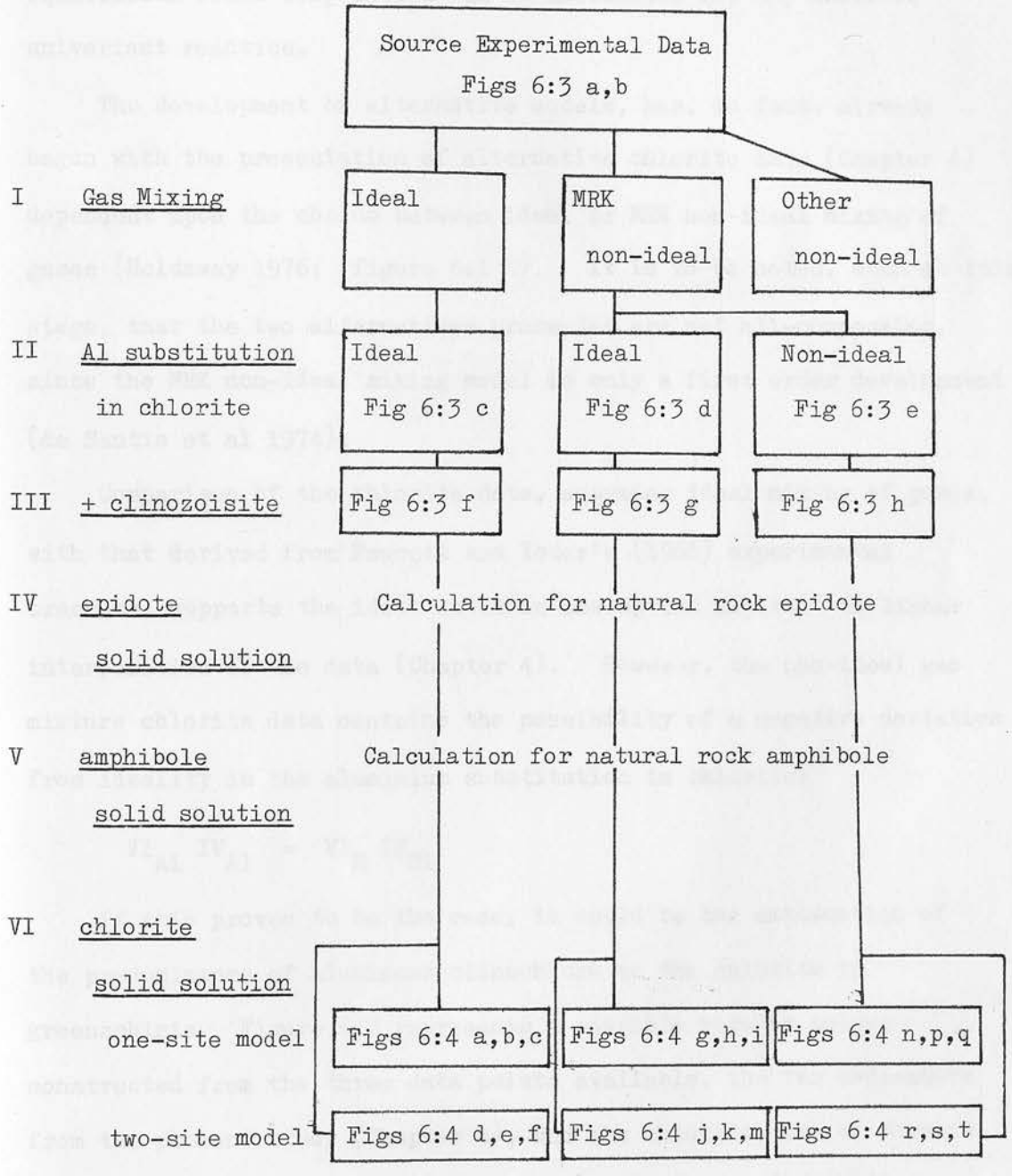

Each group of three figures for the endproduct models have been calculated for the natural rocks 25005, 25006, 25105 respectively.

$$a = X.\gamma$$

as a function of P,T and X. Thus, at any given temperature, the equilibrium fluid composition can be calculated for any isobaric univariant reaction.

The development of alternative models, has, in fact, already begun with the presentation of alternative chlorite data (Chapter 4) dependent upon the choice between ideal or MRK non-ideal mixing of gases (Holdaway 1976; figure 6:1 I). It is to be noted, even at this stage, that the two alternatives presented are not all-compassing, since the MRK non-ideal mixing model is only a first order development (de Santis et al 1974).

Comparison of the chlorite data, assuming ideal mixing of gases, with that derived from Fawcett and Yoder's (1966) experimental brackets, supports the ideal solution assumption implicit in linear interpolation of the data (Chapter 4). However, the non-ideal gas mixture chlorite data contains the possibility of a negative deviation from ideality in the aluminium substitution in chlorite:

$$VI_{Al}\ IV_{Al} = VI_{M}\ IV_{Si}$$

If this proves to be the case, it could be the explanation of the predominance of aluminous clinochlore as the chlorite in greenschists. Figure 6:2 represents a possible regular solvus constructed from the three data points available, the two endmembers from the present study (Chapter 4), and the chlorite data of Fawcett and Yoder (1966). Symmetry demands that ripidolite ('chl 3') shows the same deviation from ideality as clinochlore. Therefore the solvus

FIGURE 6:2

SYMMETRICAL ENERGY AND ENTROPY LOOPS FOR ALUMINOUS CHLORITES

Data sources:

Endmember data from present study; Chapter 4

*clinochlore ('chl 2') data from Fawcett and Yoder (1966)

Ch 1 - penninite

Ch 2 - clinochlore

Ch 3 - ripidolite/sheridanite

Ch 4 - amesite

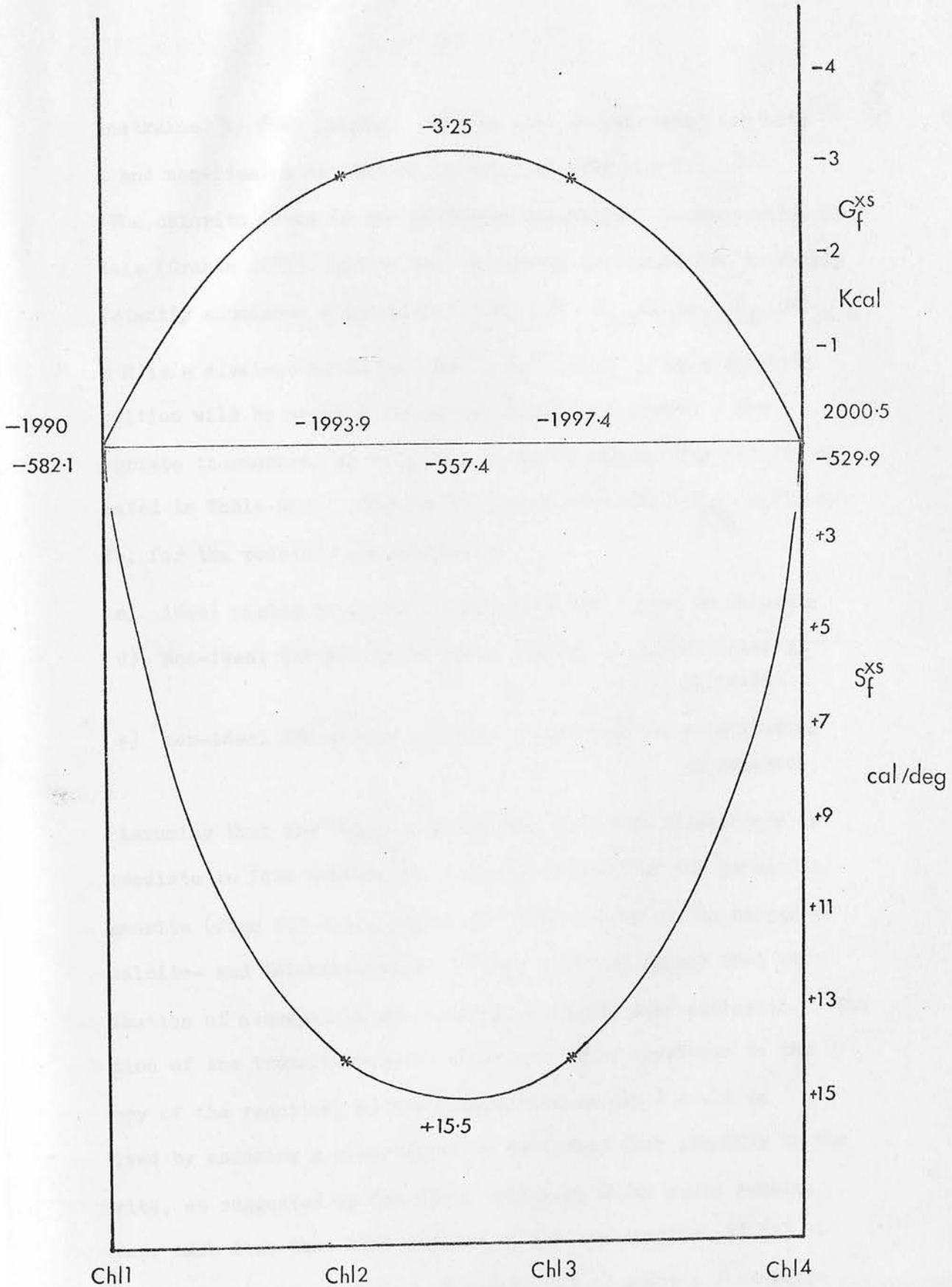
−4
−3
−2
−1
−3·25
G_f^{xs}
Kcal
2000·5
−1990
−1993·9
−1997·4
−582·1
−557·4
−529·9
+3
+5
+7
+9
+11
+13
+15
S_f^{xs}
cal/deg
+15·5
Ch1
Ch2
Ch3
Ch4

is constrained by four points. Models will be generated for both ideal and non-ideal substitution in chlorite (fig 6:1 II).

The chlorite found in the Dalradian greenschist metadolerites of Knapdale (Graham 1973), and in most metabasic greenschists, is fairly consistently aluminous clinochlore ('chl 2.5', $M_{9.5}Al_5Si_{3.5}O_{20}(OH)_{16}$ - where M is a divalent metal ion, Mg^{2+}, Fe^{2+} etc), so this chlorite composition will be assumed throughout the calculations. The appropriate thermochemical data for all three models (fig 5:3 II) is presented in Table 6:2. Figures 6:3 c,d,e show the $T\text{-}X_{CO_2}$ sections, at 5Kb, for the possible combinations:

c) ideal mixing of gases + ideal Al substitution in chlorite

d) non-ideal MRK mixing of gases + ideal Al substitution in chlorite

e) non-ideal MRK mixing of gases + non-ideal Al substitution in chlorite

Assuming that the $T\text{-}X_{CO_2}$ section for aluminous clinochlore is intermediate in form between the equivalent sections for penninite and amesite (figs 6:3 a,b), especially with regard to the shapes of the calcite- and dolomite-absent curves, it would appear that the combination of assumptions creating 6:3 d is the most realistic. The position of the tremolite-absent curve is highly sensitive to the entropy of the reaction, so its misposition in 6:3 d could be resolved by assuming a minor negative deviation from ideality in the chlorite, as suggested by the field evidence, which would remain, however, much less than that assumed in the construction of 6:3 e. The assumption of ideal mixing of gases (6:3 c) gives a reasonable

Table 6:2

Thermochemical data used in calculating $T-X_{CO_2}$ sections

Phase	$G_f^{1,298}$ cals	S_f^{298} cals/deg	$\bar{V}^{1,298}$ cal/bar
qtz	-204646	-43.616	+0.5423
zo*	-1552700	-319.5	3.262
zo+	-1556000	-330.2	3.262
trem*	-2775200	-582.92	6.5228
dol	-518734	-130.402	1.5377
cc	-269908	-62.65	0.8827
czo+	-1550800	-318.5	3.432
chlor+			
penninite			
id. gas	-1972000	-540.9	4.9425
non-id. gas	-1990000	-582.1	
amesite			
id. gas	-2007000	-534.2	
non-id. gas	-2000600	-529.9	
'chl 2.5'			
id. gas	-1989900	-538.9	
non-id. gas			
id. chlor	-1995660	-557.4	
non-id. chlor	-1998900	-543.3	

Sources:

* Zen (1972)

\+ Present work

Rest from Robie and Waldbaum (1968)

FIGURE 6:3

IRON-FREE T - X_{CO_2} MODELS

a) Experimental data

Penninite ('chl 1')

b) Experimental data

Amesite ('chl 4')

c) Aluminous clinochlore ('chl 2.5')

ideal mixing of gases

zoisite

d) MRK non-ideal mixing of gases

ideal Al substitution in chlorite

zoisite

(1) chlorite - zoisite - absent reaction; ideal mixing of gases

(2) chlorite - zoisite - absent reaction; non-ideal mixing of gases

(d) dolomite - absent reaction

(t) tremolite - absent reaction

(c) calcite - absent reaction

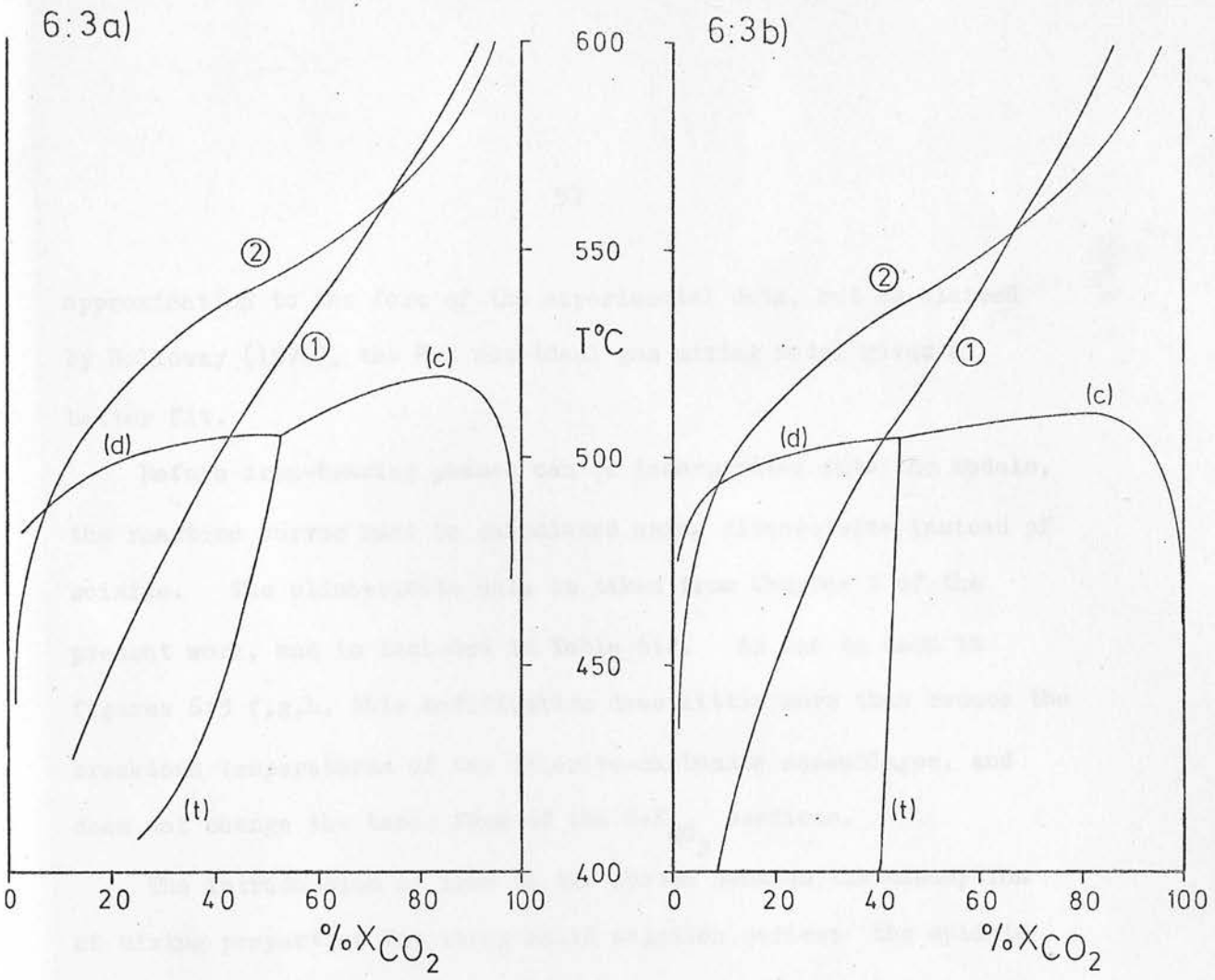
6:3a)
600
550
T°C
500
450
400
②
①
(c)
(d)
(t)
0
20
40
60
80
100
%X$_{CO_2}$

6:3b)
②
①
(c)
(d)
(t)
%X$_{CO_2}$

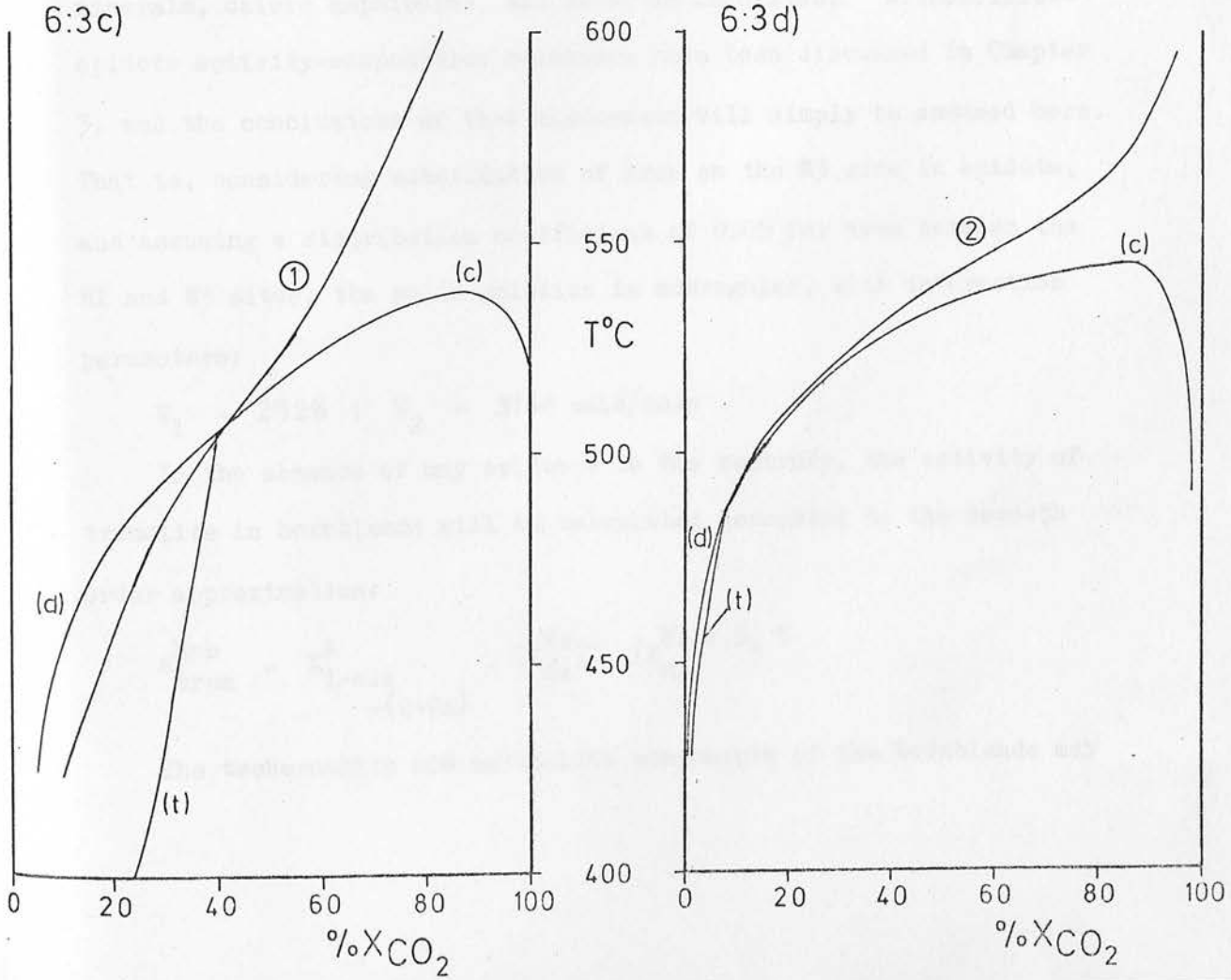
6:3c)
600
550
T°C
500
450
400
①
(c)
(d)
(t)
0
20
40
60
80
100
%X$_{CO_2}$

6:3d)
②
(c)
(d)
(t)
%X$_{CO_2}$

approximation to the form of the experimental data, but as claimed by Holloway (1976), the MRK non-ideal gas mixing model gives a better fit.

Before iron-bearing phases can be incorporated into the models, the reaction curves must be calculated using clinozoisite instead of zoisite. The clinozoisite data is taken from Chapter 3 of the present work, and is included in Table 6:2. As can be seen in figures 6:3 f,g,h, this modification does little more than reduce the breakdown temperatures of the chlorite-carbonate assemblages, and does not change the basic form of the T-X_{CO_2} sections.

The introduction of iron to the system demands the assumption of mixing properties for three solid solution series; the epidote minerals, calcic amphiboles, and Fe-Mg in chlorites. Clinozoisite-epidote activity-composition relations have been discussed in Chapter 3, and the conclusions of that discussion will simply be assumed here. That is, considering substitution of iron on the M3 site in epidote, and assuming a distribution coefficient of 0.05 for iron between the M1 and M3 sites, the solid solution is subregular, with interaction parameters:

$W_1 = 2928$; $W_2 = 3164$ cals/mole

In the absence of any evidence to the contrary, the activity of tremolite in hornblende will be calculated according to the zeroeth order approximation:

$$a^{hnb}_{trem} = X^{A}_{\substack{l\text{-}alk \\ -(2\text{-}Ca)}} \cdot (X^{M4}_{Ca})^2 \cdot (X^{M1,2,3}_{Mg})^5$$

The tschermakite and actinolite components of the hornblende may

FIGURE 6:3

IRON-FREE T - X_{CO_2} MODELS CONTD.

e) MRK non-ideal mixing of gases
non-ideal Al substitution in chlorite
zoisite

f) Ideal mixing of gases
clinozoisite

g) MRK non-ideal mixing of gases
ideal Al substitution in chlorite
clinozoisite

h) MRK non-ideal mixing of gases
non-ideal Al substitution in chlorite
clinozoisite

(1) chlorite - zoisite - absent reaction; ideal gas mixing

(2) chlorite - zoisite - absent reaction; non-ideal gas mixing

(d) dolomite - absent reaction

(t) tremolite - absent reaction

(c) calcite - absent reaction

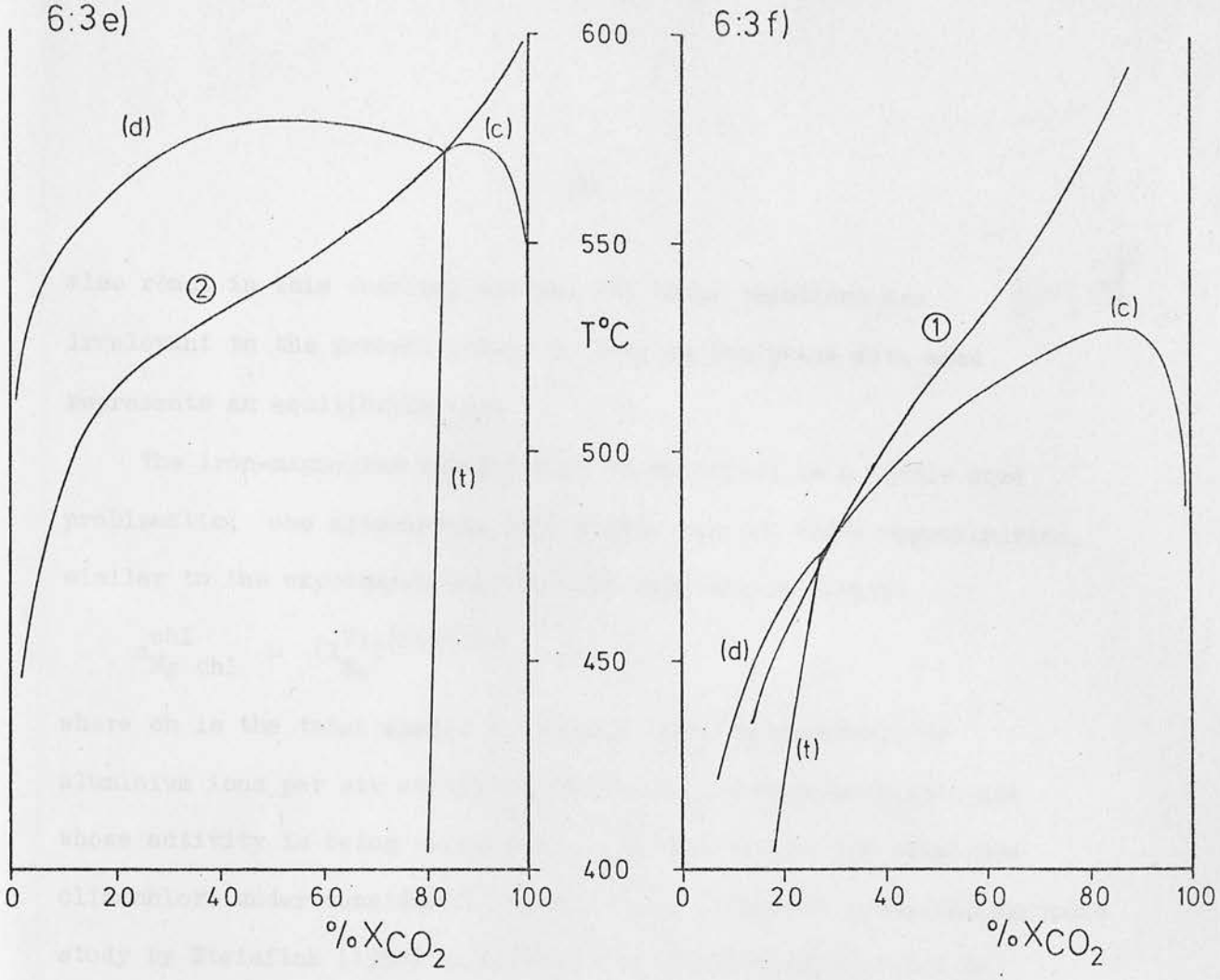
6:3 e)
(d)
(c)
②
(t)
600
550
T°C
500
450
400
0
20
40
60
80
100
%XCO_2

6:3 f)
①
(c)
(d)
(t)
0
20
40
60
80
100
%XCO_2

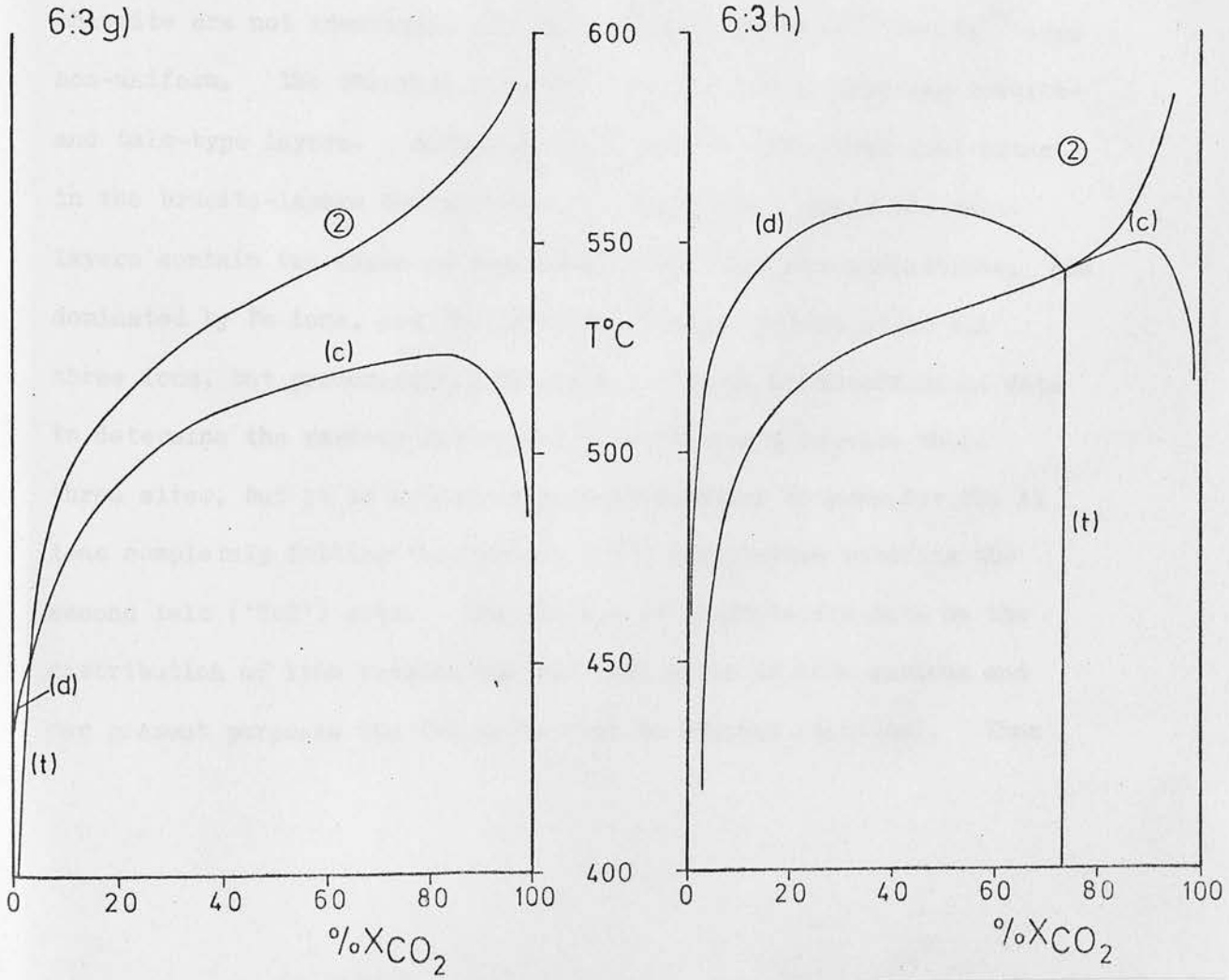
6:3 g)
②
(c)
(d)
(t)
600
550
T°C
500
450
400
0
20
40
60
80
100
%XCO_2

6:3 h)
②
(d)
(c)
(t)
0
20
40
60
80
100
%XCO_2

also react in this chemical system, but these reactions are irrelevant to the present study, so long as the phase data used represents an equilibrium set.

The iron-magnesium substitution in chlorites is a little more problematic; one alternative is a simple zeroeth order approximation, similar to the expression used for the amphibole activity:

$$a^{chl}_{Mg\ chl} = (X^{Vl}_{Mg})^{(6-ch/2)}$$

where ch is the total number (octahedral plus tetrahedral) of aluminium ions per six octahedral sites, in the endmember chlorite whose activity is being calculated. In the case of the aluminous clinochlore under consideration, ch = 2.5. However, a crystallographic study by Steinfink (1958) indicates that the octahedral sites in chlorite are not identical, and the distribution of Fe^{2+} and Mg^{2+} ions non-uniform. The chlorite structure consists of alternating brucite- and talc-type layers. According to Steinfink, the octahedral sites in the brucite-layers contain only Mg and Al ions, while the talc-layers contain two types of octahedral site, in equal proportions; one dominated by Fe ions, and the other containing, potentially, all three ions, but predominantly Mg and Fe. There are insufficient data to determine the various distribution coefficients between these three sites, but it is a reasonable approximation to consider the Al ions completely filling the brucite ('B') site before entering the second talc ('Tc2') site. The absence of quantitative data on the distribution of iron between the two talc sites is more serious and for present purposes the two sites must be assumed identical. Thus

FIGURE 6:4

NATURAL ROCK T - X_{CO_2} SECTIONS

a) ideal mixing of gases
one-site mixing in chlorite
rock 25005

b) ideal mixing of gases
one-site mixing in chlorite
rock 25006

c) ideal mixing of gases
one-site mixing in chlorite
rock 25105

d) ideal mixing of gases
two-site mixing in chlorite
rock 25005

(l) chlorite - epidote - absent reaction; ideal mixing of gases

(d) dolomite - absent reaction

(t) tremolite - absent reaction

(c) calcite - absent reaction

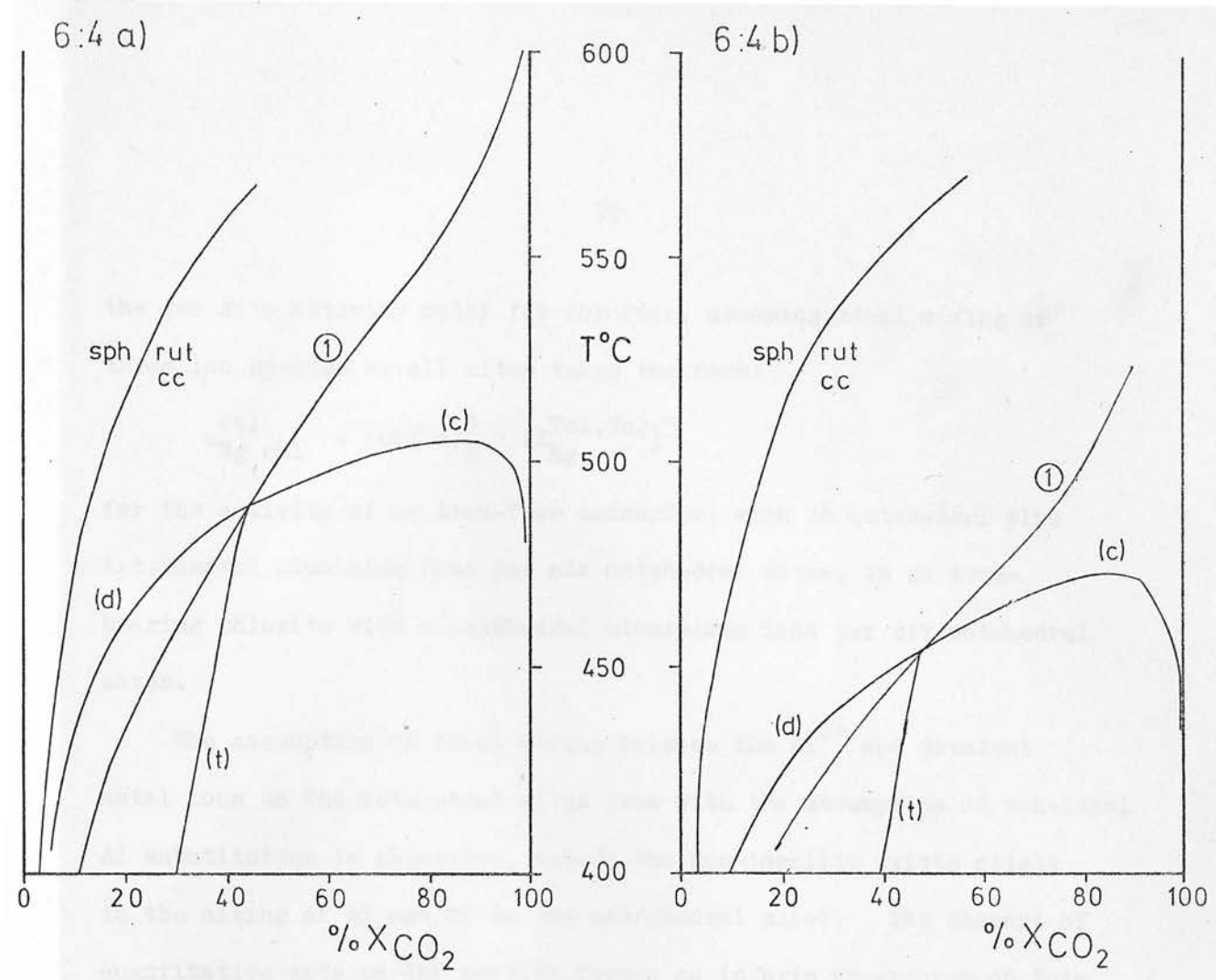
6:4 a)
sph
rut
cc
①
(c)
(d)
(t)
600
550
T°C
500
450
400
0
20
40
60
80
100
% X CO2

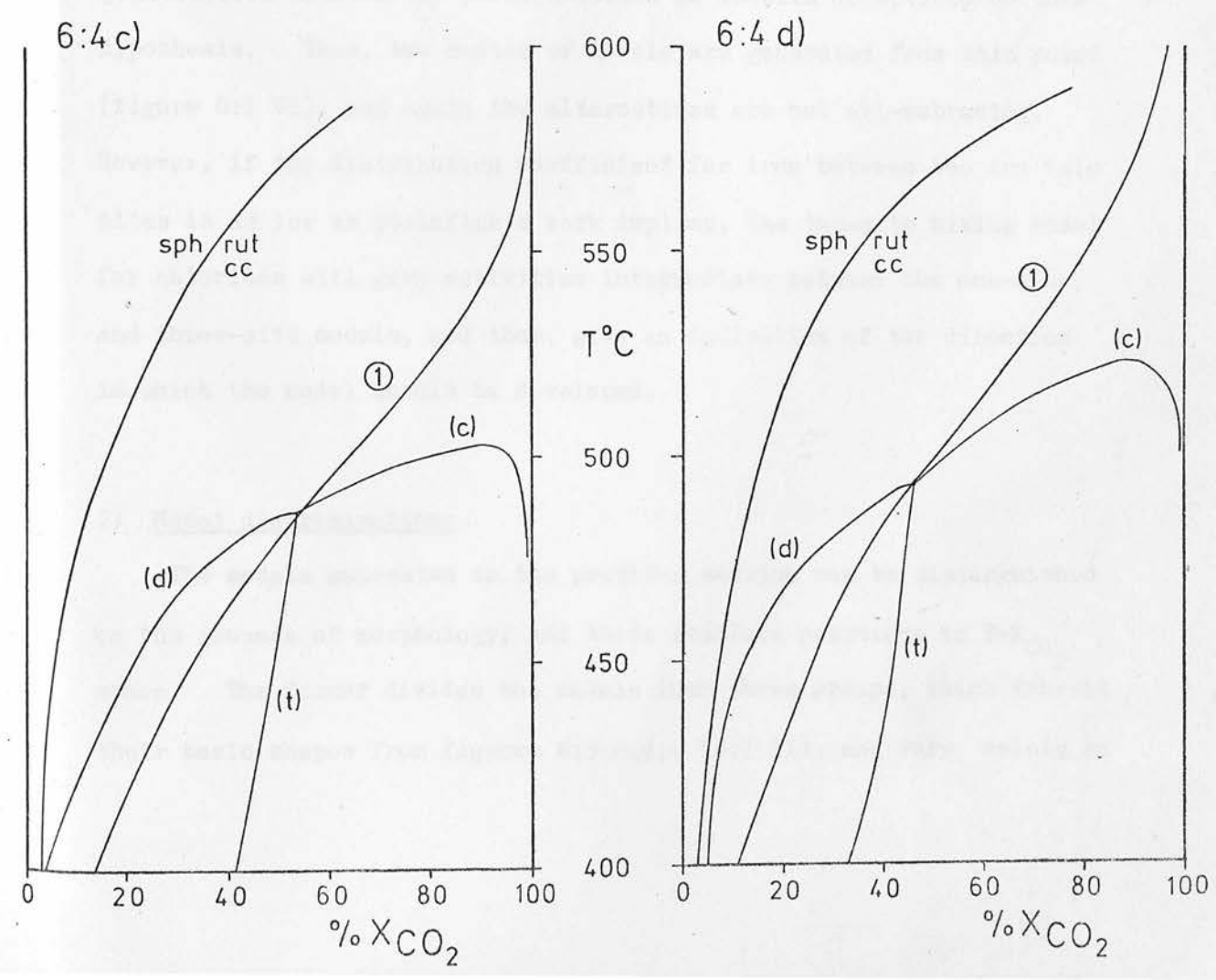
6:4 b)
sph
rut
cc
①
(c)
(d)
(t)
600
550
T°C
500
450
400
0
20
40
60
80
100
% X CO2

6:4 c)
sph
rut
cc
①
(c)
(d)
(t)
600
550
T°C
500
450
400
0
20
40
60
80
100
% X CO2

6:4 d)
sph
rut
cc
①
(c)
(d)
(t)
600
550
T°C
500
450
400
0
20
40
60
80
100
% X CO2

the two site activity model for chlorite, assuming ideal mixing of three ion species on all sites takes the form:

$$a^{chl}_{Mg\ chl} = (ch/2z)^3_B \cdot (X^{Tc1,Tc2}_{Mg})^3$$

for the activity of an iron-free endmember, with ch octahedral plus tetrahedral aluminium ions per six octahedral sites, in an iron-bearing chlorite with z octahedral aluminimum ions per six octahedral sites.

The assumption of ideal mixing between the Al^{3+} and divalent metal ions on the octahedral sites jars with the assumption of non-ideal Al substitution in chlorites, unless the non-ideality exists solely in the mixing of Al and Si on the tetrahedral sites. The absence of quantitative data on the problem forces an interim acceptance of this hypothesis. Thus, two series of models are generated from this point (figure 6:1 VI), and again the alternatives are not all-embracing. However, if the distribution coefficient for iron between the two talc sites is as low as Steinfink's work implies, the two-site mixing model for chlorites will give activities intermediate between the one-site, and three-site models, and thus, give an indication of the direction in which the model should be developed.

2) Model discrimination:

The models generated in the previous section can be distinguished on the grounds of morphology, and their absolute positions in $T\text{-}X_{CO_2}$ space. The former divides the models into three groups, which inherit their basic shapes from figures 6:3 c,d,e (6:1 II), and vary mainly in

FIGURE 6:4

NATURAL ROCK T - X_{CO_2} SECTIONS CONTD.

e) ideal mixing of gases
two-site mixing in chlorite
rock 25006

f) ideal mixing of gases
two-site mixing in chlorite
rock 25105

g) MRK non-ideal mixing of gases
ideal Al substitution in chlorite
one-site mixing in chlorite
rock 25005

h) MRK non-ideal mixing of gases
ideal Al substitution in chlorite
one-site mixing in chlorite
rock 25006

(1) chlorite - epidote - absent reaction; ideal gas mixing

(2) chlorite - epidote - absent reaction; non-ideal gas mixing

(d) dolomite - absent reaction

(t) tremolite - absent reaction

(c) calcite - absent reaction

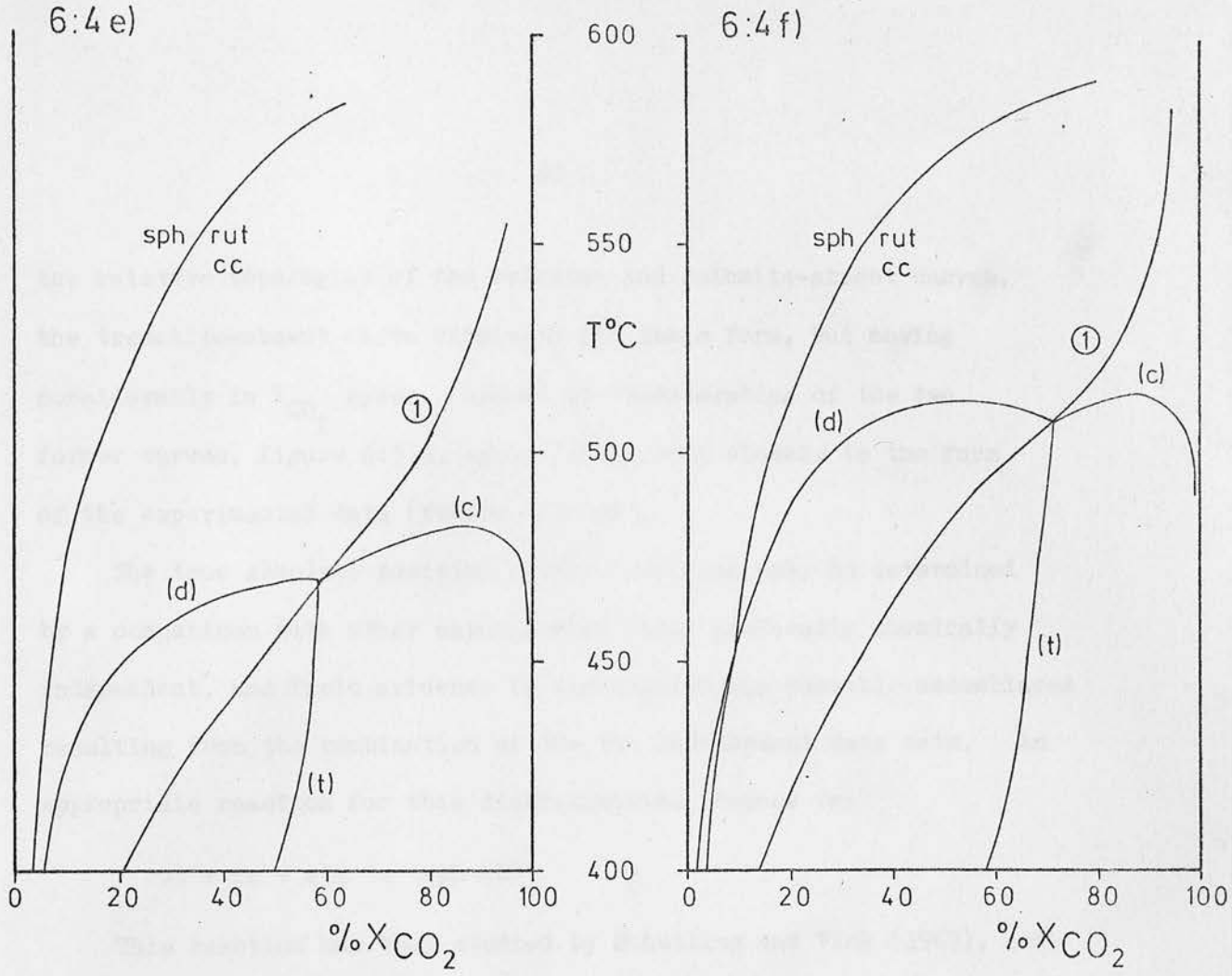
6:4 e)
sph
rut
cc
①
(c)
(d)
(t)
600
550
T°C
500
450
400
0
20
40
60
80
100
%XCO2

6:4 f)
sph
rut
cc
①
(c)
(d)
(t)
0
20
40
60
80
100
%XCO2

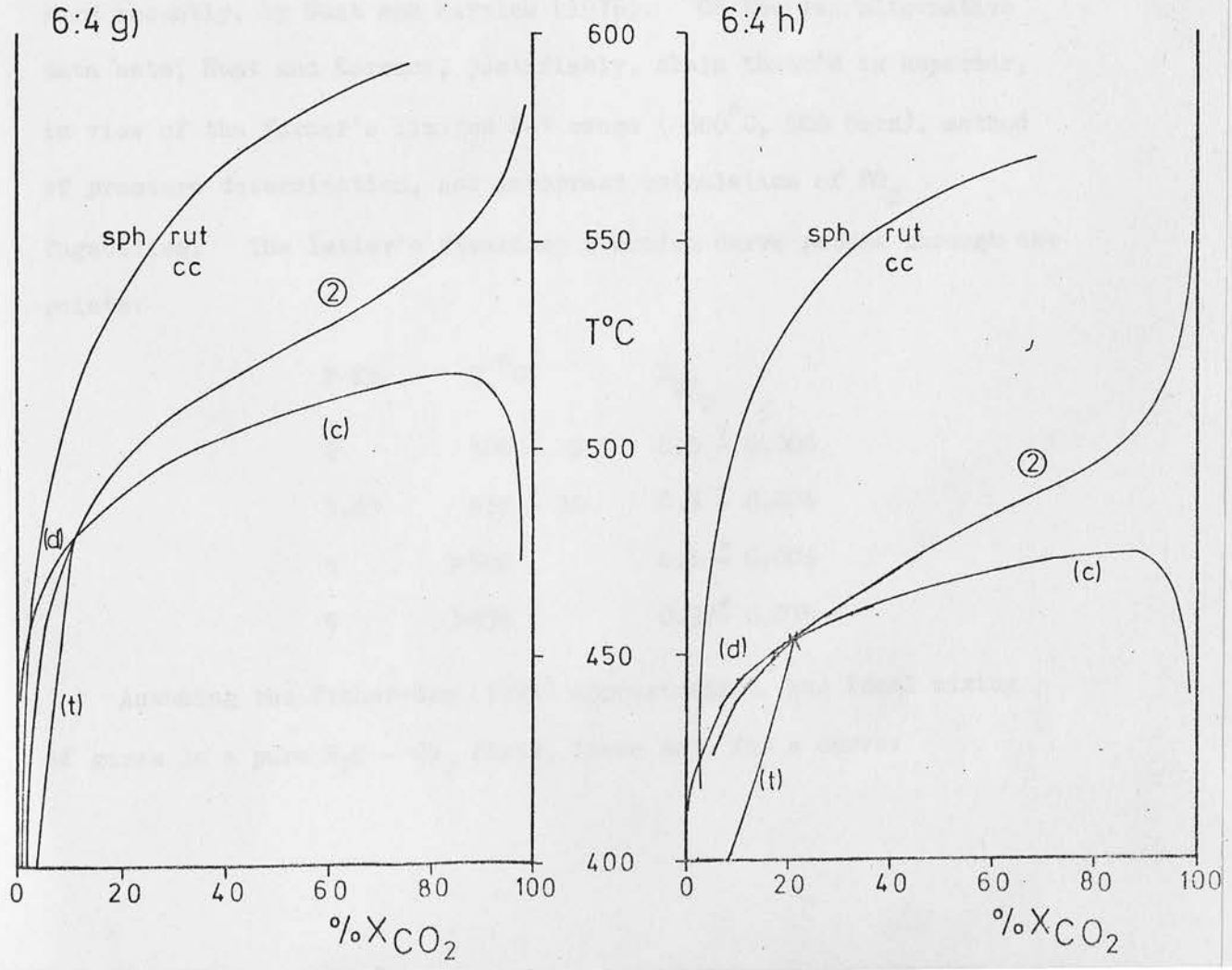
6:4 g)
sph
rut
cc
②
(c)
(d)
(t)
600
550
T°C
500
450
400
0
20
40
60
80
100
%XCO2

6:4 h)
sph
rut
cc
②
(c)
(d)
(t)
0
20
40
60
80
100
%XCO2

the relative topologies of the calcite- and dolomite-absent curves, the tremolite-absent curve retaining its basic form, but moving considerably in X_{CO_2} space. Based on consideration of the two former curves, figure 6:3 d, approximates most closely to the form of the experimental data (figure 6:3 a,b).

The true absolute position of the model can only be determined by a comparison with other experimental data, preferably chemically independent, and field evidence to distinguish the possible assemblages resulting from the combination of the two independent data sets. An appropriate reaction for this discrimination process is:

$$rut + cc + qtz = sph + CO_2$$

This reaction has been studied by Schuiling and Vink (1967), and, more recently, by Hunt and Kerrick (1976). Of the two alternative data sets, Hunt and Kerrick, justifiably, claim their's is superior, in view of the former's limited P-T range (500°C, 500 bars), method of pressure determination, and incorrect calculation of CO_2 fugacities. The latter's divariant reaction curve passes through the points:

P Kb	T °C	X_{CO_2}
2	500 ± 5	0.5 ± 0.006
3.45	535 ± 10	0.5 ± 0.006
5	>580	0.5 ± 0.006
5	>635	0.97 ± 0.035

Assuming the Fisher-Zen (1971) approximation, and ideal mixing of gases in a pure $H_2O - CO_2$ fluid, these data fit a curve:

FIGURE 6:4

NATURAL ROCK T - X_{CO_2} SECTIONS CONTD

i) MRK non-ideal mixing of gases
ideal Al substitution in chlorite
one-site mixing in chlorite
rock 25105

j) MRK non-ideal mixing of gases
ideal Al substitution in chlorite
two-site mixing in chlorite
rock 25005

k) MRK non-ideal mixing of gases
ideal Al substitution in chlorite
two-site mixing in chlorite
rock 25006

m) MRK non-ideal mixing of gases
ideal Al substitution in chlorite
two-site mixing in chlorite
rock 25105

(2) chlorite - epidote - absent reaction; non-ideal gas mixing

(d) dolomite - absent reaction

(t) tremolite - absent reaction

(c) calcite - absent reaction

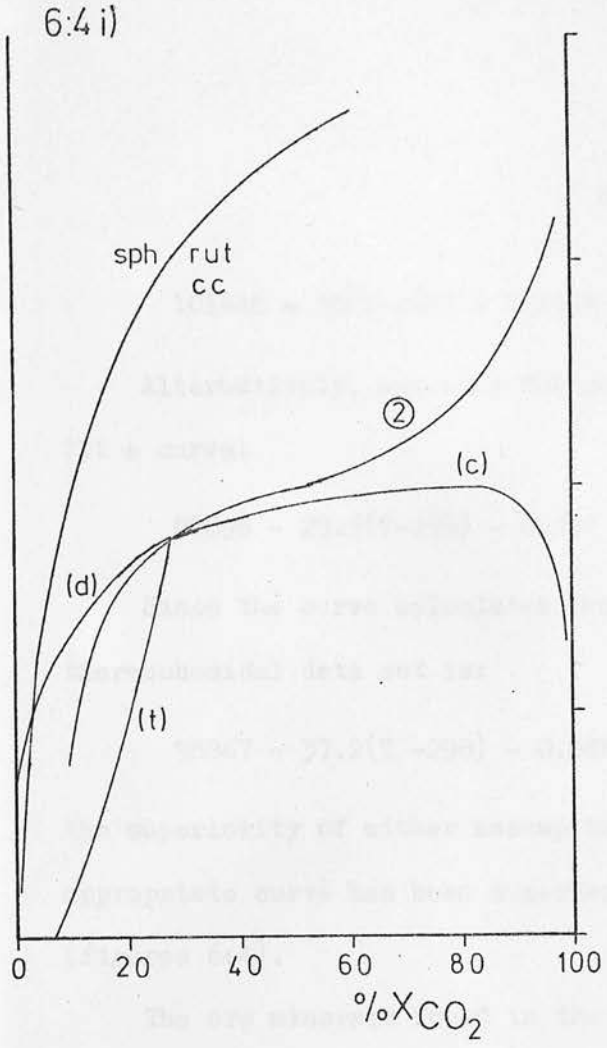
6:4 i)
sph
rut
cc
②
(c)
(d)
(t)
600
550
T°C
500
450
400
0
20
40
60
80
100
%XCO_2

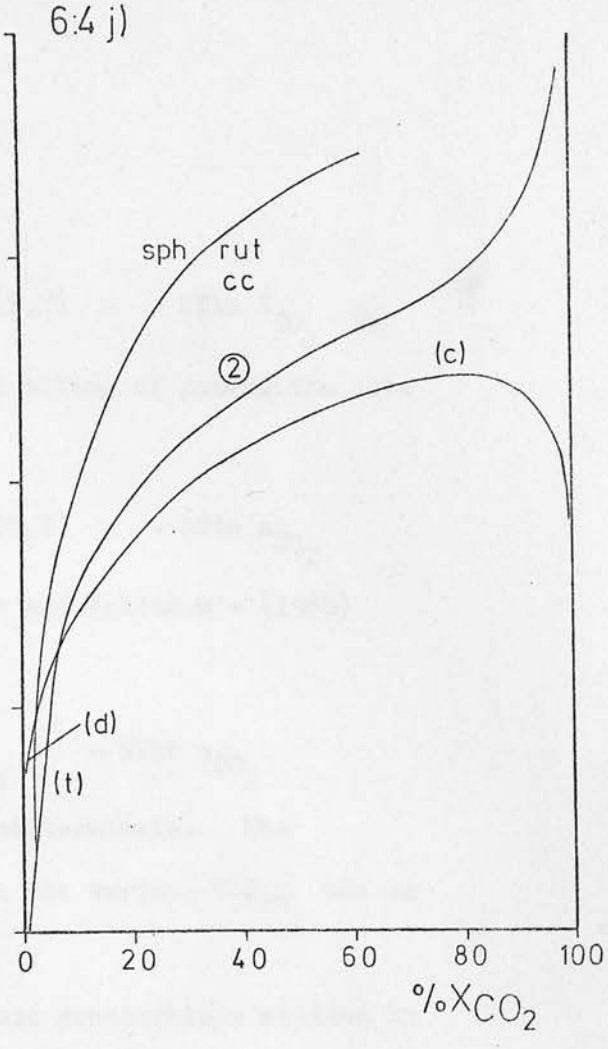
6:4 j)
sph
rut
cc
②
(c)
(d)
(t)
0
20
40
60
80
100
%XCO_2

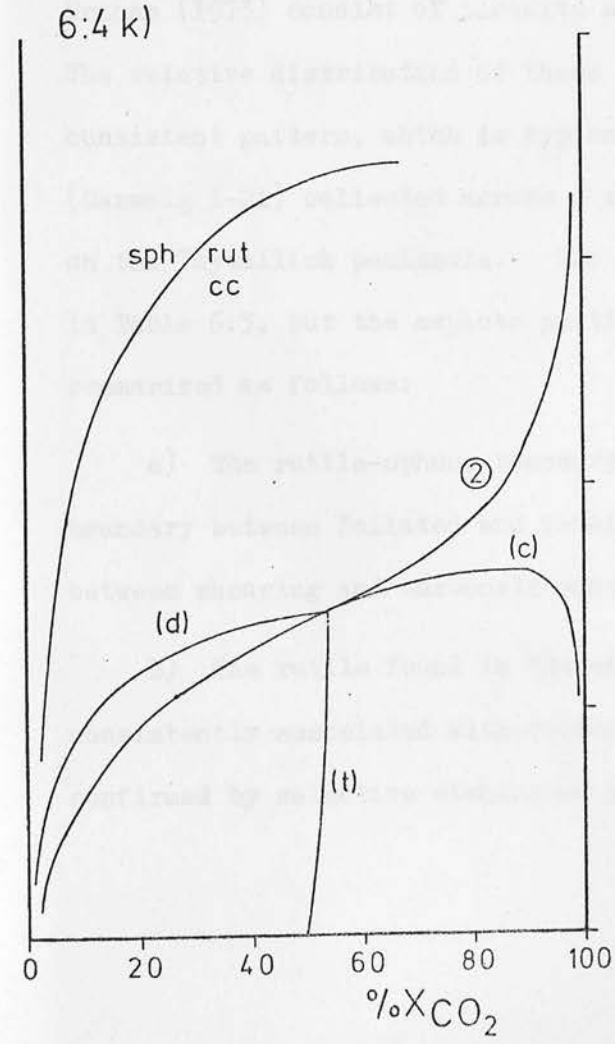
6:4 k)
sph
rut
cc
②
(c)
(d)
(t)
600
550
T°C
500
450
400
0
20
40
60
80
100
%XCO_2

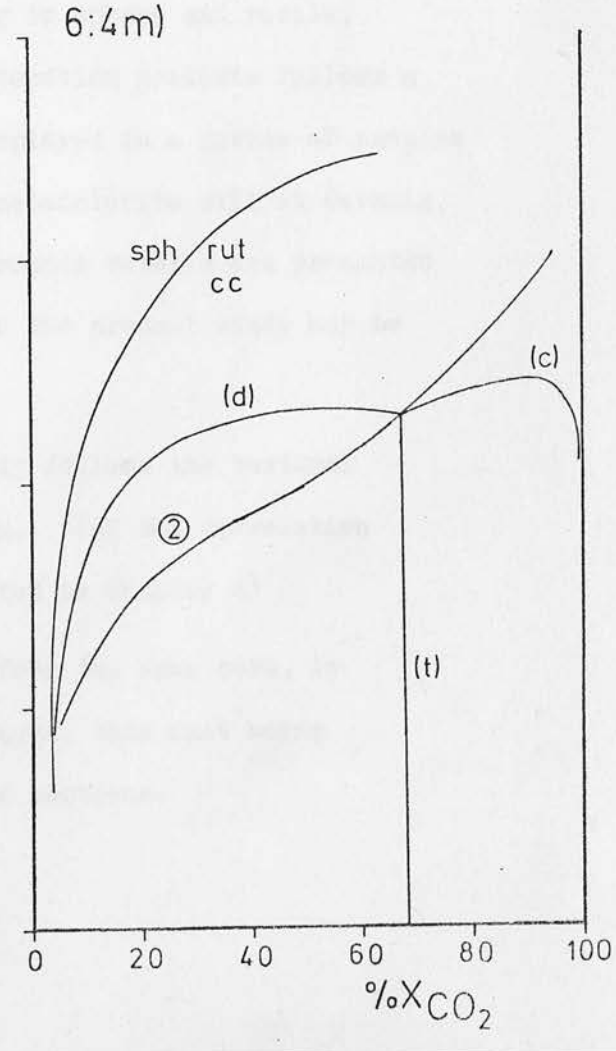
6:4 m)
sph
rut
cc
(c)
(d)
②
(t)
0
20
40
60
80
100
%XCO_2

$$101648 - 38(T-298) + 0.444P + G^{*}_{CO_2}(P,T) = - RT\ln X_{CO_2}$$

Alternatively, assuming MRK non-ideal mixing of gases, the data fit a curve:

$$97896 - 29.5(T-298) - 0.73P + G^{*}_{CO_2}(P,T) = - RT\ln a_{CO_2}$$

Since the curve calculated from Robie and Waldbaum's (1968) thermochemical data set is:

$$98867 - 37.2(T-298) - 0.54P + G^{*}_{CO_2} = - RT\ln a_{CO_2}$$

the superiority of either assumption is indeterminate. The appropriate curve has been superimposed on the various $T\text{-}X_{CO_2}$ models (figures 6:4).

The ore minerals found in the metabasic greenschists studied by Graham (1973) consist of ilmenite altering to sphene and rutile. The relative distribution of these two alteration products follows a consistent pattern, which is typically displayed in a series of samples (Carsaig 1-21) collected across a single metadolerite sill at Carsaig, on the Tayvallich peninsula. The petrographic details are presented in Table 6:3, but the aspects pertinent to the present study may be summarized as follows:

a) The rutile-sphene boundary closely follows the textural boundary between foliated and massive rock. (cf the correlation between shearing and carbonate content noted in Chapter 4)

b) The rutile found in the samples from the dyke core, is consistently associated with carbonate grains, this fact being confirmed by selective etching on polished sections.

FIGURE 6:4

NATURAL ROCK T - X_{CO_2} SECTIONS CONTD.

n) MRK non-ideal mixing of gases
non-ideal Al substitution in chlorite
one-site mixing in chlorite
rock 25005

p) MRK non-ideal mixing of gases
non-ideal Al substitution in chlorite
one-site mixing in chlorite
rock 25006

q) MRK non-ideal mixing of gases
non-ideal Al substitution in chlorite
one-site mixing in chlorite
rock 25105

r) MRK non-ideal mixing of gases
non-ideal Al substitution in chlorite
two-site mixing in chlorite
rock 25005

(2) chlorite - epidote - absent reaction; non-ideal gas mixing

(d) dolomite - absent reaction

(t) tremolite - absent reaction

(c) calcite - absent reaction

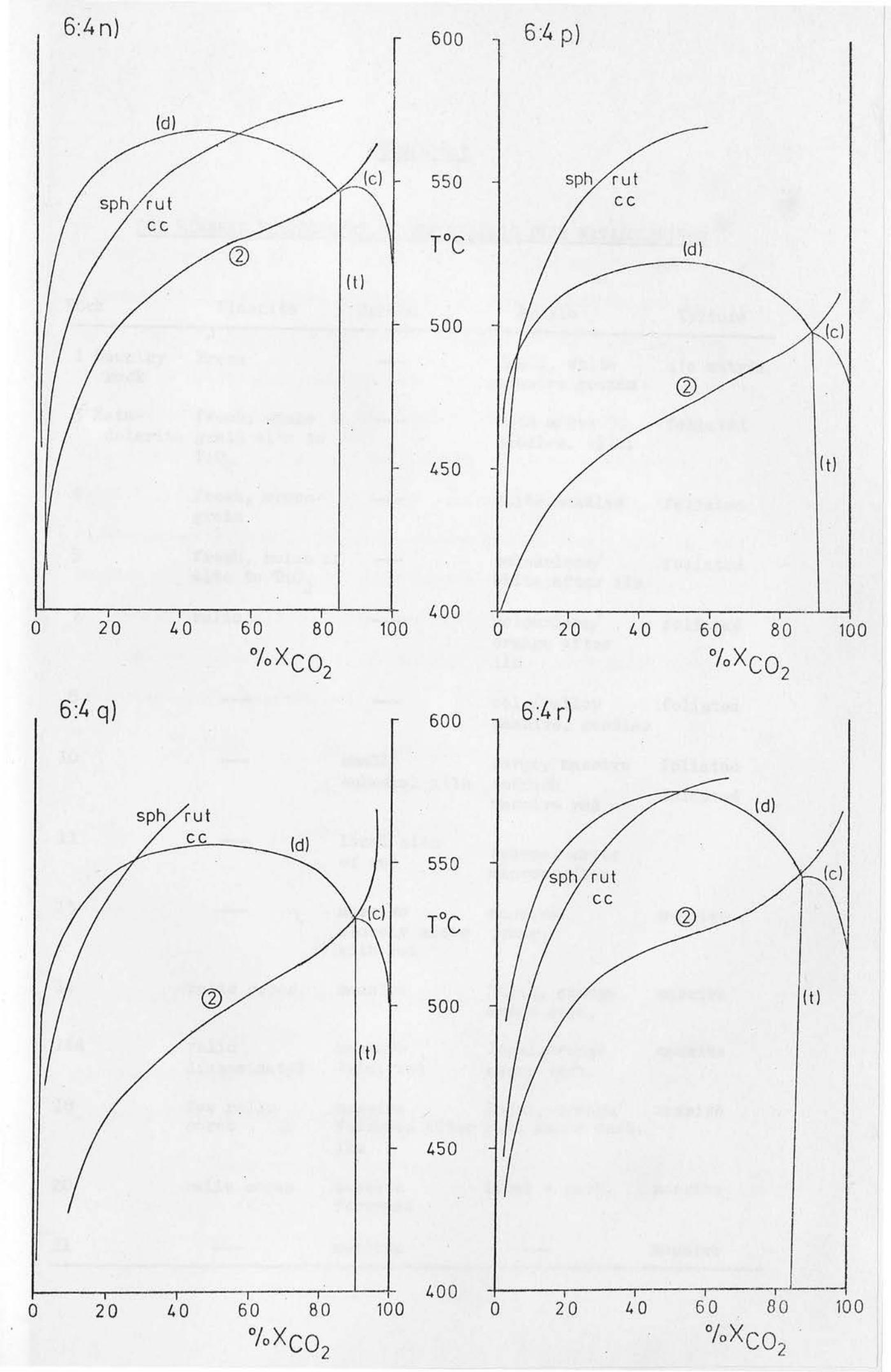
6:4 n)
(d)
sph
rut
cc
(c)
②
(t)
600
550
T°C
500
450
400
0
20
40
60
80
100
%XCO_2
6:4 p)
sph
rut
cc
(d)
(c)
②
(t)
0
20
40
60
80
100
%XCO_2
6:4 q)
sph
rut
cc
(d)
(c)
②
(t)
600
550
T°C
500
450
400
0
20
40
60
80
100
%XCO_2
6:4 r)
(d)
sph
rut
cc
(c)
②
(t)
0
20
40
60
80
100
%XCO_2

TABLE 6:3

ORE MINERAL PETROGRAPHY OF THE CARSAIG DYKE METADOLERITES

Rock	Ilmenite	Sphene	Rutile	Texture
1 Country rock	Fresh	---	Small, white massive grains	qtz matrix
3 Meta-dolerite	fresh, whole grain altn to TiO_2	---	Lots white needles, +lin.	foliated
4	fresh, cross-grain	---	white needles	foliated
5	fresh, relic of altn to TiO_2	---	colourless/ white after ilm	foliated
7	relic	---	colourless/ orange after ilm	foliated
8	---	---	col./yellow massive, needles	foliated
10	---	small euhedral xtls	large, massive reddish massive red +	foliated foliated
11	---	local altn of rut	sphene, white microneedles	
13	---	massive closely assoc with rut	massive orange	massive
14	relic cores	massive	local, orange assoc carb.	massive
16a	relic disseminated	massive ±ilm, rut	local, orange assoc carb.	massive
18	few relic cores	massive furrowed after ilm	local, orange/ red, assoc carb.	massive
20	relic cores	massive furrowed	local + carb.	massive
21	---	massive	---	massive

The change in colour of the TiO_2-phase may be simply the effect of changing grain size; alternatively it could be caused by a variation in the oxygen content of the phase, (Layton and Bagley 1965), cation impurities (Deer et al 1962), or the white TiO_2 may be another polymorph, e.g. anatase. If any of the latter three interpretations is correct, the implication is that two periods of TiO_2 growth have occurred. The texture of rock 11, with massive reddish TiO_2 associated with sphene, and small white TiO_2 needles disseminated throughout the rock, supports this view; however, the texture of rock 13 where it is uncertain whether sphene is altering to reddish TiO_2, or vice versa, casts doubt upon the hypothesis.

The ore minerals are found associated with carbonates in the following common assemblages:

chl - cc - sph

chl - cc - dol - rut

chl - dol - rut

ep - dol - rut

and at low grades

chl - dol - sph

Considered as representing a combination of the two sets of experimental data; Hunt and Kerrick's (1976) sphene-rutile study and the present mixed volatile model; the above assemblages indicate the following topological relationships:

a) the sphene-rutile curve remains to the water-rich side of the tremolite-absent curve.

FIGURE 6:4

NATURAL ROCK T - X_{CO_2} SECTIONS CONTD.

s) MRK non-ideal mixing of gases

Non-ideal Al substitution in chlorite

Two-site mixing in chlorite

rock 25006

t) MRK non-ideal mixing of gases

Non-ideal Al substitution in chlorite

Two-site mixing in chlorite

rock 25105

(2) chlorite - epidote - absent reaction; non-ideal mixing of gases
(d) dolomite - absent reaction
(t) tremolite - absent reaction
(c) calcite - absent reaction

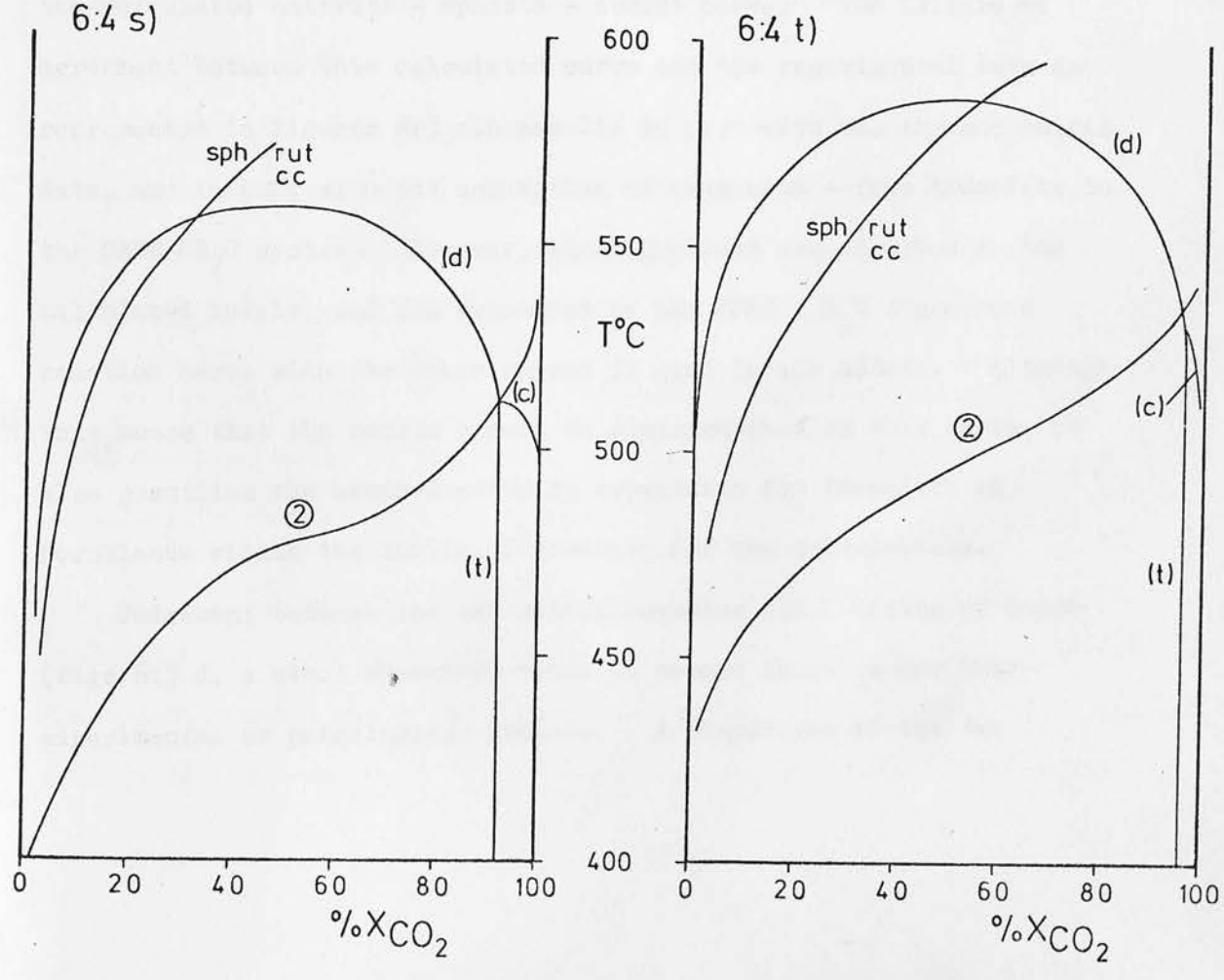

b) at low temperatures the sphene-rutile curve intersects the chlorite - epidote - absent curve

c) it follows from the above, and from a consideration of the intrinsic form of the curves in T-X_{CO_2} space (Greenwood 1967) that the sphene-rutile curve intersects the dolomite-absent curve at high temperatures.

These features definitely exclude the viability of the models represented in figures 6:4 a-f (ideal mixing of gases). Figures 6:4 k,m are also dubious, indicating a critical sensitivity to iron content in the model (MRK non-ideal, ideal chlorite - two site mixing), which is not apparent in the actual rocks.

The other external data by which the models could be judged is the calculated chlorite - epidote - absent curve. The failure of agreement between this calculated curve and the experimental data as represented in figures 6:3 a,b may lie in part with the thermochemical data, and in part with the assumption of aluminium - free tremolite in the CAMS - H_2O system. However, these problems are absorbed in the calculated models, and the agreement of the CFMS - H_2O degenerate reaction curve with the other curves is good in all models. Although this means that the models cannot be distinguished on this basis, it also justifies the assumed activity expression for tremolite in hornblende within the limits of accuracy for the calculations.

Judgement between the two models assuming ideal mixing of gases (figs 6:3 d, e etc.) therefore rests on common sense rather than experimental or petrological grounds. A comparison of the two

distinct topologies (e.g. figs 6:4 g and n) shows that the model assuming ideal chlorite approaches the experimental forms more closely, at least as far as the calcite- and dolomite-absent curves are concerned. As has been suggested before, a slight degree of non-ideality in the chlorite, intermediate between the two models, may improve the position of the tremolite-absent curve, and will certainly fit the field evidence of predominant aluminous clinochlore.

The conclusions regarding the various models may, therefore, be summarized as follows:

a) although the model assuming ideal mixing of gases fits the experimentally determined form of the isobaric invariant bundle reasonably well, it is rejected because it fails to predict the carbonate-ore mineral assemblages found in typical metabasic greenschists.

b) The model assuming MRK non-ideal mixing of gases, and strongly non-ideal chlorite is rejected because, although it successfully predicts the carbonate-ore mineral assemblages it does not have the form of the experimental data.

c) In the absence of a superior model, the MRK non-ideal mixing, ideal chlorite model is preferred, although a slight degree of non-ideality in the chlorite may be an improvement.

d) The difference between the one- and two-site models for Fe-Mg-Al mixing in chlorites is too small to distinguish them, although the two-site model may be more sensitive to variation in the iron content of the rock, than the real rocks are. However, neither model

has a very sound theoretical basis, and further crystallographic work on chlorites must be done before a reasoned model can be developed.

3) Geothermometry:

Two further checks on the absolute position of the mixed volatile model have been attempted, in the form of applications of established geothermometers to the Dalradian metabasalts. Both yielded reasonable temperatures, but neither was sufficiently reliable to contribute to the model discrimination procedure.

Co-existing Fe-Ti oxides (Buddington and Lindsley 1964) in rocks from the garnet zone plot on the very edge of the empirical diagram published by Buddington and Lindsley giving temperatures of $550 \pm 50^{\circ}C$ and oxygen fugacities around those imposed by the NNO buffer (Graham 1973).

Microprobe analyses (EDS) of two carbonate assemblages in metadolerites and country rock from Tayvallich and Carsaig, which are below the pelitic 'biotite isograd', and contain blue-green hornblende and stilpnomelane, have produced some very peculiar results. Dolomite occurs as rusty weathered porphyroblasts, and contains up to 25% $FeCO_3$, while calcite occurs in two distinct textures; one closely associated with the dolomite (as 'tongues' to the porphyroblasts) and the other as anhedral interstitial grains forming the rock matrix. Both textures of calcite contain a high proportion of iron, and virtually no magnesium. This absence of magnesium either denies the application of a two carbonate geothermometer

dependent on magnesium distribution, or indicates extremely low equilibration temperatures. Bickle and Powell (1977) have cast the two carbonate geothermometer in terms of a regular solution model, extracting interaction parameters W_{CaMg}; W_{CaFe}; and W_{CaMg} from experimental data. Using these interaction parameters, a geothermometer based on co-existing iron between calcite and dolomite can be established. For the reaction:

$$\underset{\text{dolomite}}{CaFe(CO_3)_2} = \underset{\text{calcite}}{CaFe(CO_3)_2}$$

assuming, as Bickle and Powell have done, that there is perfect ordering in the dolomite (M1, M2 sites), and perfect disorder in the calcite, and that Fe-Mg mixing is ideal, i.e. $W_{FeMg} = 0$; if X^{cc}_{Fe} and X^{cc}_{Mg} are both below 4%, the equilibrium equation can be simplified to the form:

$$(X^{cc}_{Fe}/X^{M1,dol}_{Fe}) = \exp(-W_{CaFe}/RT)$$

Bickle and Powell (1977) have calculated from the calcite-siderite experimental data of Goldsmith et al (1962), and Rosenberg (1963) that:

$$W_{CaFe} = 3800 \pm 100 \text{ cals}$$

Details of temperatures calculated are presented in Table 6:4. It is pertinent to note here that, in calc-pelites of the same metamorphic grade, to be found on Islay, the association kyanite plus pyrophyllite has been observed. At the ambient metamorphic pressure, in a purely aqueous fluid, these aluminosilicates co-exist at about

TABLE 6:4

TEMPERATURES CALCULATED FROM THE DISTRIBUTION OF IRON BETWEEN COEXISTING CARBONATES IN GREENSCHIST METADOLERITES, AND METAPELITE

$$(X_{Fe}^{cc} / X_{Fe}^{Ml,dol}) = \exp(-W_{CaFe} / RT)$$

Rock	%$FeCO_3$ in cc	%$FeCO_3$ in Ml in dol	T °C
69-200	1.9 av assoc dol	8.0*	(1060)
metadolerite		18.6*	565
		55.7*	290
		27.4 av of 3	420
	0.75 av interstitial	8.0*	(535)
		18.6*	
		55.7*	115
		27.4 av of 3	260
69-224b	2.0 av assoc dol	32.5 av of 3	420
metadolerite	0.75 av interstitial	32.5 av of 2	235
69-196	2.9 av	55.7 av of 4	375
metadolerite			
76-19	2.0 av	31.5 av of 5	420
metadolerite		21.1 av of 2	(540)

*single grain analysis

420°C (Haas and Holdaway 1973), however the presence of CO_2 will depress this equilibration temperature. (Burgess, Graham and Harte, in ppn).

In gross terms, the dolomite and calcite seem to have stopped equilibrating iron at around 420°C, but the interstitial calcite continued to lose iron to the surrounding chlorite as it cooled further, thus giving a spuriously low temperature. The low magnesium could be explained partly by preferential leaching of magnesium from the carbonates by hydrous fluids, below 400°C, and partly by the low initial magnesium content of the rock. However, a detailed explanation of these results would require a study of the field relations and petrogeny of these particular rocks. Due to the emphasis on the construction of a general greenschist model in this work, there has not been enough time to pursue this particular aspect further.

CHAPTER 7

ACTINOLITE - EDENITE SOLID SOLUTION - A PRELIMINARY STUDY

Introduction:

The general formula of an amphibole can be written: $WX_2Y_5X_8O_{22}(B)_2$ where W, X, Y, and Z represent ions on the sites A, M_4, $M_{1,2,3}$, and $Si_{1,2}$ with co-ordinations X, VIII-VI, VI and IV respectively, and B is OH, F, or Cl (Ernst 1968). In calcic amphiboles, the iron-magnesium substitution, on the M_1 and M_3 sites, is near ideal at greenschist-amphibolite temperatures. The other changes in calcic amphibole chemistry, in the prograde sequence from greenschist to amphibolite facies, can, at low pressures, be reduced to two basic, chemically distinct, substitutions, on the original actinolite molecule: $\square Ca_2(Fm)_5Si_8O_{22}(OH)_2$ ($\square$ represents the vacant 'A' site, and Fm, Mg^{2+} and Fe^{2+} ions:

1) $^{VI}_{Al}\ ^{IV}_{Al} \rightleftharpoons {}^{VI}_{Fm}\ ^{IV}_{Si}$ (tschermakite substitution on sites M_2, Si_2)

2) $^{X}_{Na}\ ^{IV}_{Al} \rightleftharpoons \square\ {}^{IV}_{Si}$ (edenite substitution on sites A, Si_2)

The sum effect of these two substitutions is to produce pargasitic hornblendes. At higher pressures, the edenite substitution is replaced by the richterite substitution:

3) $^{X}_{Na}\ ^{VIII}_{Na} \rightleftharpoons {}^{VIII}_{Ca}$ (on sites A, M_4)

which combines with the tschermakite substitution to produce barroisites.

Many workers have attempted empirical calibrations of these main substitutions with metamorphic grade (e.g. Binns 1965, Leake 1965a, Bard 1970), and also of some of the less extensive ones, notably the entry of titanium into the amphibole:

$$^{VI}Ti\,^{IV}Al \rightleftharpoons {}^{VI}Al\,{}^{IV}Si$$

which appears to be very sensitive to temperature.

Although these studies of natural amphiboles have not been successful in isolating the effects of the various substitutions, they have revealed some interesting correlations between them; e.g.

Leake (1965b) $^{VI}Al \leqslant 0.57\ {}^{IV}Al + 0.28$

Robinson et al (1971) A-site ions: $^{IV}Al \leqslant 0.6{:}1.4$

and the strong dependence of the edenite substitution upon the iron content of the amphibole (Graham 1974, inter alia). This empirical hierarchy of substitutions must have its basis in amphibole crystal chemistry. For example, Grapes et al (1977) have suggested that the relationship between A-site occupancy and tetrahedral aluminium, observed by Robinson et al, is due to sodium entering the A-site to relieve the stresses caused by expansion of the silicate lattice. If the sequence of cause and effect is traced, it should lead to a substitution which is dependent solely on external variables. Thus, if the degree of tschermakite substitution is controlled by the edenite substitution, as indicated by the above inequalities; the extent of the latter is, in turn, controlled by the Fe^{II}-Mg substitution. However, the Fe^{II}-Mg substitution appears to be independent of the pressure and temperature

of formation of most natural amphiboles, and to be determined by the bulk rock chemistry, and phase assemblage, alone. The first solid solution to be examined, experimentally, in isolation, therefore, is the edenite-actinolite series, treating pressure, temperature, and the iron content of the amphibole as external variables.

Experimental:

The edenite substitution can be isolated in the reaction:

trem + ab = eden + 4 qtz

This preliminary study has examined the reaction in the iron-free system, at 600°C, over the pressure range 3-10Kb, using both coldseal and internally heated pressure vessels. Pure natural quartz, and synthetic albite, hydrothermally recrystallized at 800°C, P_{H_2O} = 2Kb, for a week, were used; together with two tremolites (analyses Table 7:1). The phases were mixed in varying proportions covering the range Ab_2Amph_{10} to $Ab_{10}Amph_{10}$, with excess quartz. Since tremolite 1 contains about 10 mole % edenite, these mixtures of albite and amphibole are equivalent in bulk composition to a range of amphiboles, ed_3tr_7 to pure edenite with excess albite. Tremolite 2 contains a very small proportion of the richterite molecule, but if this is ignored the mixtures of albite and tremolite 2 are equivalent to amphiboles ranging from ed_2tr_8 to pure edenite.

Charges were sealed in platinum capsules, with excess water, and run for about one month. Run products were checked optically, and by XRD, to discover whether any albite remained. Critical runs were

TABLE 7:1

ANALYSES OF TREMOLITES USED TO STUDY THE REACTION:

trem + ab = eden + 4 qtz

wt%	Tremolite 1*	Tremolite 2**
SiO_2	57.76	58.12
Al_2O_3	0.64	0.05
TiO_2	0.05	0.03
Cr_2O_3	--	0.02
FeO	0.14	0.04 (total)
MnO	0.06	0.07
MgO	24.73	24.88
CaO	13.27	13.29
Na_2O	0.29	0.34
K_2O	0.09	0.17
H_2O	2.38	2.17***
F	0.28	--
TOTAL	99.67	99.18
	to 24 (O,OH,F)	to 22 (O) anhydrous
Si	7.84	8.05
Al	0.10	0.01
Fe(II)	0.02	--
Mn	0.01	0.01
Mg	5.03	5.13
Ca	1.94	1.97
Na	0.08	0.05
K	0.02	0.01
OH	2.14	2.00***
F	0.06	--

*Gouverneur Tremolite, collector A.E.J. Engel, wet chemical analysis A.E.J. Engel

**from Grant Institute Departmental Collection, locality unknown, probe analysis N.F. Best

***assumed, and backcalculated

rerun for a further 30 days, to confirm equilibrium, whilst charges in which albite had been totally consumed were rerun at lower pressures to reverse the reaction. Run data are presented in Table 7:2 and figure 7:1.

The data obtained so far are insufficient for numerical analysis, but the strong pressure dependence of the edenite substitution indicates that it may be developed into a valuable geobarometer.

Figure 7:1 P-X Diagram of experimental data for reaction:

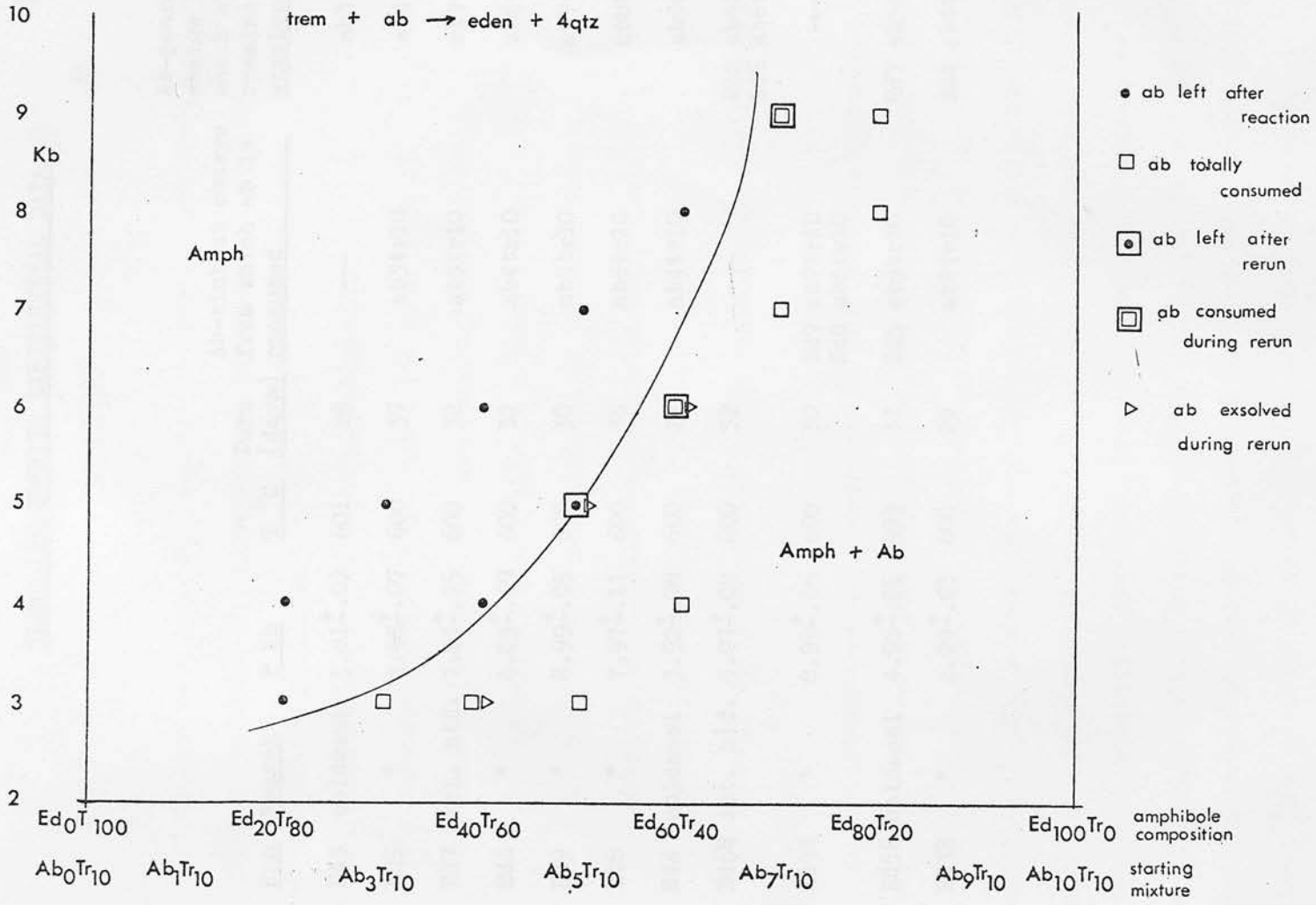

TABLE 7:2

TREMOLITE-EDENITE EXPERIMENTAL DATA

Run	Vessel	P Kb	T °C	Durn (days)	Ab-richest charge from which ab is consumed	Ab-poorest charge in which ab remains or exsolves
Ed3	coldseal	3.01±.02	601	26	---	ab3trl0
Ed5	"	4.98±.07	600	37	ab3trl0	ab5trl0
Ed7	int. htd.	7.04±.25	600	32	ab5trl0	ab7trl0
Ed6	"	6.03±.09	600	32	ab4trl0	ab6trl0
Ed9	"	8.99±.05	600	30	ab5trl0	ab7trl0
Ed8	"	7.97±.11	600	36	ab6trl0	ab8trl0
Ed4	coldseal	3.92±.08	600	27	ab4trl0	ab6trl0
Ed6R	int. htd.	5.97±.08	600	32	---	Ed8 ab6trl0 Ed6 ab6trl0
Ed9R	"	8.99±.05	600	30	Ed9 ab7trl0 Ed8 ab8trl0	---
Ed5R	coldseal	4.96±.05	599	31	Ed5 ab5trl0	Ed7 ab5trl0
Ed3R	"	2.99±.03	600	29	ab2trl0	Ed4 ab4trl0

CHAPTER 8

CONCLUSIONS

Looking back over the research covered in this thesis, the original statement of objectives, as expressed in the introduction seems somewhat grandiose:

> ".....the complete experimental definition of reaction relationships across the wide range of greenschist, epidote - amphibolite, and amphibolite facies mineral assemblages in metabasic rocks, and the simultaneous establishment of the temperature, pressure and fluid phase conditions for their respective stabilities"

However, it is hoped that a firm basis for further work has been constructed.

The thermochemical paramemters of the iron-free endmembers of the major phases in these metamorphic facies have been confirmed, and a start has been made in understanding the nature of the various solid solutions. The actual numerical data derived in the course of the research are summarized in Table 8:1. The techniques used to obtain the data on epidote, grossular, and even tremolite - edenite solid solutions are well - established (Wood 1975), and the work presented in this thesis is part of a necessary and inevitable compilation of data, made possible by these techniques. Further possible

TABLE 8:1

SUMMARY OF THE THERMOCHEMICAL DATA DERIVED IN THE COURSE OF THIS PROJECT

Phase	Source		$G_f^{1,298}$	S_f^{298}	$\bar{V}^{1,298}$
czo	Chap. 3		-1550800	-318.5	3.432
chlorite	Chap. 4				4.9425
ideal mixing		chl 1	-1972000	-540.9	
of gases		chl 4	-2007000	-534.2	
MRK non-ideal		chl 1	-1990000	-582.1	
mixing of gases		chl 4	-2000500	-529.9	

Solid solutions:

for binary pistacite-clinozoisite:-

$$RT \ln a_{cz}^{ep} = (1 + c)\, RT \ln X_{Al}^{M3} + (X_{Al}^{M3})^2 \, (W_1 + 2(X_{Al}^{M3})(W_2 - W_1))$$

$K_D^{M1-M3} = 0.05$

$c = (\ln X_{Fe}^{M3}) / (\ln X_{Al}^{M3})$

$W_1 = 2928$ cals

$W_2 = 3164$ cals

investigations, of the same nature, are suggested at every turn: more complete data on plagioclase solid solution, covering a range of P-T conditions, is required, and the reactions:

$$zo + ky + qtz = an + H_2O$$

$$gross + ky + qtz = an$$

used to study epidote solid solution (present work), and grossular-pyrope solid solution (Henson et al 1975), respectively, are suitable when considered in the NCAS - H_2O system. Once this data is available, it can be combined with the epidote data, and data on grossular-pyrope, and on grossular - almandine (Cressey, in ppn.) solid solution, to construct a geothermometer based on the reaction:

$$ep + ab + qtz = gross\text{-}gnt + plag + H_2O$$

studied in Chapter 2. Using this geothermometer, in conjunction with the amphibole-plagioclase geobarometer to be developed from the tremolite-edenite solid solution data, it should be possible to pinpoint the physical conditions of formation of any ep - plag - amph - qtz - gnt or - ky - bearing rock, which includes many, of various compositions, to be found in the upper greenschist, and epidote - amphibolite facies.

Excluding amphibole which has been discussed in the previous chapter, one major greenschist solid solution series remains outstanding for the lack of experimental attention it has received. Apart from investigation of various endmember breakdowns (Fawcett and Yoder, 1966; Hsu, 1968; and Staudigel and Schreyer, 1977), in at least one instance as unrestrained multivariant reactions, very little experimental work

on the chlorites has been attempted. The present study suggests that the two solid solutions (Fe - Mg, and Al - Si) should be examined separately, in conjunction with a study of ion distribution between apparently distinct crystallographic sites. One particularly important fruit of the Fe - Mg study would be an understanding of the distribution of iron between chlorite and other phases, notably amphibole. This changes to such an extent over the transition between the greenschist and amphibolite facies that the tie-lines between the coexisting phases reverse direction in AFM compositional space (Graham 1973, Harte and Graham 1975), so that it is probably a very sensitive indicator of the conditions of equilibration. However, as has been frequently stressed, throughout this work, it is more advantageous, in the long term, to study minerals individually, rather than, for example, to experiment directly on natural coexisting chlorites and amphiboles.

The potential collaboration between experimental petrologists or mineralogists, and crystallographers suggested above, has a much wider value than this one investigation, as is indicated by the present study on epidote solid solution (Chapter 3), and the proposed work on amphiboles (Chapter 7). Present work in this interdisciplinary field has accentuated the distribution of components between pairs of phases (Seifert pers. comm.), probably because this has the appeal of instant applicability to natural rocks. Again the total data to be derived empirically from the investigation of P-T-X dependent site occupancy in single phases would be much less. Before this is routinely possible, however, both experimental and crystallographic techniques

must be improved (Whittaker 1977).

The intention behind the development of the mixed volatile model was to deduce a general model for greenschist metamorphism, from observation of an assumed - typical example. The initial qualitative model (Harte and Graham 1975) was of wide applicability, successfully simulating assemblages found in the Dalradian, (Graham 1973), Vermont (Billings and White, 1950), and New Zealand (Cooper 1972), whilst the experimental determination was almost excessively general in employing extreme endmember chlorites. However the incorporation of mineral data to produce real rock models, in Chapter 6, necessarily reduced the field of application to the conditions prevalent during the formation of the Dalradian source rocks. Direct application of figures 6:4 to phase assemblages found in other regions where the greenschist facies is developed, is probably acceptable in practice, considering the relatively low degree of precision involved; however a superior technique would be to calculate the T-X_{CO_2} sections separately, using more appropriate mineral data, and treating Chapter 6 as a worked example. Even then the model is constrained by the pressure dependent stability limits of the mineral assemblages considered, and by the assumptions relating to fluid composition and hydrostatic pressure.

On a more constructive note, the mixed volatile model is being used in conjunction with physical data on the size of the various 'carbonate zones', in the Dalradian metadolerite dykes (Graham 1973, Harte and Graham 1975, Graham pers. comm.) in an application of the 'non-equilibrium thermodynamics' developed, in geological terms, by

Fisher (1977) to discover values for the diffusion rates of H_2O and CO_2 during metamorphism.

Perhaps the deepest conclusions of this project, that can be seen at present, are not the once-hoped-for array of P-T-X conditions to pigeonhole the various manifestations of greenschist metabasic metamorphism; but an appreciation of the extent and shortfalls in the thermochemical and crystal chemical data on minerals. It has also led to a doubt on the relative values of mineral data per se, and the use of that data to attach 'absolute' physical conditions of formation to rocks; particularly when anxiety to obtain the latter leads to a failure to complete a study of the former.

ACKNOWLEDGEMENTS

Foremost among those who have helped me see this thesis through to an end, is Ben Harte, whose sensitive supervision has managed to keep the project rooted in reality, even though, at times, it seemed to be drifting away from geology altogether. Second only to Ben, in helpfulness, has been Colin Graham, whose own thesis laid much of the foundation for the present work, and whose critical faculties have frequently been exercised, to, I hope, our mutual benefit, in the integration of two somewhat different approaches to the same problems.

The oral traditions of experimental petrology, I learnt from Cameron Begg, Cliff Ford, and Phil Spencer, to whom I am greatly indebted.

Many people have been generous in supplying, sometimes beautiful, mineral specimens for use as experimental fodder: Peder Aspen, Curator of the Grant Institute Museum, John Dixon, Colin Graham and Tim Heaton, University of Edinburgh; Michael Raith, Mineralogisch-Petrologisches Institut, Kiel and A.E.J. Engel, Geophysical Lab., Washington, who supplied the sample of Gouverneur Tremolite, through the agency of Ben Harte. I am also indebted to D.H. Eggler, and T.C. Hoering, of the same establishment, who produced gas chromatography analyses of some of my mixed volatile samples, again through the agency of my supervisor. John Holloway, University of Arizona, sent microfiche copies of his MRK gas mixing computer programme, and specimen output. Use of the Microscan V electron microprobe, in Edinburgh, was learnt, and performed under the supervision of Pete Hill.

The typing of this slim volume was done quickly and efficiently by Lesley Marshall.

Finally, I must thank Prof. M.J. O'Hara for use of the high pressure experimental equipment and Prof. G.Y. Craig for use of the general facilities of the department, during my stay in Edinburgh. The research was performed during the tenure of a 3 year Natural Environment Research Council studentship.

Buddington, A.F., and Lindsley, D.H. (1964) 'Iron-titanium oxide minerals and synthetic equivalents'
J. Petrol. 5 p 310-357

Chinner, G.A., Smith, J.V., and Knowles, C.R. (1969) 'Transition metal contents of Al_2SiO_5 polymorphs'
Am. J. Sci. 267A p 96-113

Cooper, A.F. (1972) 'Progressive metamorphism in metabasites, Haast Schists, New Zealand'
J. Petrol. 13 p 457-92

Deer, W.A., Howie, R.A., and Zussman, J. (1962) 'Rock-forming Minerals: Vols. I - V' Longmans London

Dollase, W.A. (1971) 'Crystal structure refinements of epidote, allanite and hancockite'
Am. Miner. 56 p 447-64

---------- (1973) 'Mössbauer spectra and iron distribution in the epidote group minerals'
Zeits. Krist. 138 (Buerger-Festband) p 41-63

Enns, T., Scholander, P.F., and Bradstreet, E.D. (1965) 'Effect of hydrostatic pressure on the solubility of gases in water'
J. Phys. Chem. 69(1) p 389-91

Ernst, W.G. (1968) 'Amphiboles' Springer-Verlag, Berlin-Heidelberg-New York

Eskola, P., (1915) 'On the relations between the chemical and mineralogical composition in the metamorphic rocks of the Orijärvi region'
Bull. Comm. geol. Finlande No. 44

---------- (1939) 'Die metamorphen Gesteine'
p 263-407 in 'Die Enststehung der Gesteine' eds. Barth, T.F.W., Correns, C.W., and Eskola, P. Springer; Berlin

Fawcett, J.J., and Yoder, H.S. (1966) 'Phase relations of chlorites in the system MAS - H_2O'
Am. Miner. 51 p 353-80

Ferry, J.M. (1976) 'P,T, f_{CO_2} and f_{H_2O} during metamorphism of calcareous sediments in the Waterville-Vassalboro Area, South-Central Maine'
Contr. Miner. Petrol. 57 p 119-43

Fisher, G.W. (1977) 'Non-equilibrium thermodynamics in metamorphism'
p381-403 in 'Thermodynamics in Geology' ed. Fraser, D.G. D. Reidel Publ. Co. Dordrecht - Holland and Boston - USA

Fisher, J.R., and Zen, E-An (1971) 'Thermochemical calculations for hydrothermal phase equilibria data, and the free energy of H_2O'
Am. J. Sci. 270 p 293-314

Ford, C.E., (1972) 'Temperature measurement and distribution in 'Tuttle' hydrothermal pressure vessels'
J. Phys. E5 p 457-60

Fyfe, W.S., (1960) 'Hydrothermal synthesis and determination of equilibrium between minerals in the subliquidus region'
J. Geol. 68 p 553-66

Glassley, W. (1974) 'A model for phase equilibria in the prehnite-pumpellyite facies'
Contr. Miner. Petrol. 43 p 317-32

Goldsmith, J.R., Graf, D.L., Witters, J., and Northrop, D.A. (1962) 'Studies in the system $CaCO_3$ - $MgCO_3$ - $FeCO_3$'
J. Geol. 70 p 659-88

Graham, C.M. (1973) 'Chemical petrology of Dalradian metabasites from Knapdale, Argyll'
Edinburgh Univ. Ph. D. Thesis (unpublished)

Graham, C.M. (1974) 'Metabasite amphiboles of the Scottish Dalradian'
Contr. Miner. Petrol. 47 p 165-85

Grapes, R.H., Hashimoto, Seiji, and Miyashito, Sumio (1977) 'Amphiboles of a metagabbro - amphibolite sequence, Hidaka metamorphic belt, Hokkaido'
J. Petrol. 18 p 285-318

Greenwood, H.J. (1962) 'Metamorphic reactions involving two volatile components'
Yb. Carnegie Instn. Wash. 61 p 82-85

Greenwood, H.J. (1967) 'Experimental studies in the system CMS-H_2O-CO_2'
p 542-67 in 'Researches in Geochemistry: Vol II'
ed. Abelson, P.H. Wiley; New York

Guggenheim, E.A. (1949) 'Thermodynamics: An advanced treatment for chemists and physicists' North-Holland Publ. Co.; Amsterdam

Haas, H., and Holdaway, M.J. (1973) 'Equilibria in the system Al_2O_3 - SiO_2 - H_2O, involving the stability limits of pyrophyllite and thermodynamic data of pyrophyllite'
Am. J. Sci. 273 p 449-64

Harte, B. (1976) 'Determination of a pelite petrogenetic grid for the Eastern Scottish Dalradian'
Yb. Carnegie Instn. Wash. 75 p 438-46

Harte, B., and Graham, C.M. (1975) 'Graphical analysis of greenschist to amphibolite facies mineral assemblages in metabasalts'
J. Petrol. 16 p 347-70

Hashimoto, M. (1972) 'Reactions producing actinolite in basic metamorphic rocks'
Lithos 5 p 19-31

Helgeson, H.C. (1969) 'Thermodynamics of hydrothermal systems at elevated temperatures and pressures'
Am. J. Sci. 267 p 729-804

Hensen, B.J., Schmidt, R., and Wood, B.J. (1975) 'Activity - composition relationships of pyrope - grossular garnet'
Contr. Miner. Petrol. 51 p 161-6

Holdaway, M.J. (1965) 'Regionally metamorphosed basic rocks in the Klamath Mountains, North California'
Am. Miner. 50 p 953-77

---------- (1966) 'Hydrothermal stability of clinozoisite plus quartz'
Am. J. Sci. 264 p 643-67

---------- (1972) 'Thermal stability of Al-Fe epidote as a function of oxygen fugacity and iron content'
Contr. Miner. Petrol. 37 p 307-40

Holloway, J.R. (1976) 'Fugacity and activity coefficients of molecular species in fluids at high pressures and temperatures'
Yb. Carnegie Instn. Wash. 75 p 771-5

Howells, S. (1976) Unpublished Ph D Thesis, Edinburgh University

Howells, S., and O'Hara, M.J. (1975) 'Palaeogeotherms and the diopside-enstatite solvus'
Nature 254 p 406-408

Hsu, L.C. (1968) 'Selected phase relationships in the system Al-Mn-Fe-Si-O-H; a model for garnet equilibria'
J. Petrol. 9 p 40

Hunt, J.A., and Kerrick, D.A. (1976) 'The stability of sphene: Experimental redetermination and geologic implications' Geochim. Cosmochim. Act. 41 p 279-88

Jasmund, K., and Schaffer, R. (1972) 'Experimentelle Bestimmung der P-T-Stabilitatsbereiche in der Mischkristallreihe Tremolit-Tschermakit' Contr. Miner. Petrol. 34 p 101-15

Johannes, W. (1969) 'An experimental investigation of the system MS-H_2O-CO_2' Am. J. Sci. 267 p 1083-104

Langer, K., and Raith, M. (1974) 'Infrared spectra of Al-Fe(III) - epidotes and zoisites: $Ca_2(Al_{1-p}Fe^{3+}_p)\ Al_2O(OH)\ (Si_2O_7)\ (SiO_4)$ Am. Miner. 59 p 1249-58

Layton, W., and Bagley, A.S. (1965) 'The nature and the estimation of titanium in rutile concentrates' Aust. Inst. of Min. & Metal. 215 p 37-46

Leake, B.E. (1965a) 'The relationship between composition of calciferous amphibole and grade of metamorphism' p 229-319 in 'Controls of Metamorphism' eds. Pitcher, W.S., and Flynn, G.W.; Oliver and Boyd; Edinburgh and London

Leake, B.E. (1965b) 'The relationship between tetrahedral aluminium and the maximum octahedral aluminium in natural calciferous and subcalciferous amphiboles' Am. Miner. 50 p 843-51

Liou, J.G. (1973) 'Synthesis and stability relations of epidote' J. Petrol. 14 p 381-413

Liou, J.G., Kuniyoshi, S., and Ito, K. (1974) Experimental studies of the phase relations between greenschist and amphibolite in a basaltic system' Am. J. Sci. 274 p 613-32

Macgregor, I.D. (1974) 'The system MAS: solubility of Al_2O_3 in enstatite for spinel and garnet peridotite compositions' Am. Miner. 59 p 110-9

Metz, P., and Trommsdorf, V. (1968) 'On phase equilibria in metamorphosed siliceous dolomite' Contr. Miner. Petrol. 18 p 305-9

Miyashiro, A. (1958) 'Regional metamorphism of the Gosaisyo-Takanuki district of the Central Abukuma plateau' J. Fac. Sci. Tok. Univ. Sec. II 11 p 219-72

----------(1968) 'Metamorphism of mafic rocks' P 799-834 in 'Basalts: the Poldervaart Treatise on rocks of basaltic composition' eds. Hess, H.H., and Poldervaart, A. Interscience; New York

Newhall, D.H., Abbot, L.H., and Dunn, R.A. (1963) 'A redetermination of the freezing pressure of mercury using improved apparatus and techniques' in 'High pressure measurement' eds. Giardini, A.A., and Lloyd, E.C.; Butterworths; Washington

Newton, R.C. (1966) 'Some calc-silicate phase relations' Am. J. Sci. 264 p 204-22

Nitsch, K. (1971) 'Stabilitatsbeziehungen von prehnit - und pumpellyit-haltigen paragenesen' Contr. Miner. Petrol. 30 p 240-60

Orville, P.M. (1972) 'Plagioclase cation exchange equilibria with aqueous chloride solution, in the presence of quartz' Am. J. Sci. 272 p 234-72

Powell, R. (1974) 'A comparison of some mixing models for crystalline silicate solid solutions' Contr. Miner. Petrol. 46 p 265-74

Raith,M. (1976) 'The Al-Fe(III) epidote miscibility gap in a metamorphic profile through the Penninic Series, in the Tauern Window'
Contr. Miner. Petrol. 57 p 99-117

Robie, R.A., and Waldbaum, D.R. (1968) 'Thermodynamic properties of minerals and related substances at 298.15 K (25.0 °C) and one atmosphere pressure, and at higher temperatures'
U.S. Geol. Surv. Bull. 1259

Robinson, P., Ross, M., and Jaffe, H.W. (1971) 'Composition of the anthophyllite-gedrite series, and a comparison of the gedrite-hornblende and the anthophyllite-gedrite solvi'
Am. Miner. 56 p 1005-41

Rosenberg, P.E. (1963) 'Subsolidus relations in the system $CaCO_3$ - Fe CO_3'
Am. J. Sci. 261 p 683-90

de Santis, R., Breedvelde, G.F.J., and Prausnitz, J.M. (1974) 'Thermodynamic properties of aqueous gas mixtures'
Ind. & Eng. Chem. Process. Des. Dev. 13 p 374-7

Schuiling, R.D., and Vink, B.W. (1967) 'Stability relations of some titanium minerals (sphene, perovskite, rutile, anatase)'
Geochim. Cosmochim. Act. 31 p 2399-411

Skippen, G.B. (1971) 'Experimental data for reactions in siliceous marbles'
J. Geol. 79 p 457-81

Slaughter, J., Kerrick, D.M., and Wall, V.J. (1975) 'Experimental and thermodynamic study of equilibria in the system CMS-H_2O-CO_2'
Am. J. Sci. 275 p 143-162

Staudigel, H., and Schreyer, W. (1977) 'Upper thermal stability limit of clinochlore at 10-35 Kb P_{H_2O}'
Contr. Miner. Petrol. 61 p 187-98

Steinfink, H. (1958) 'Crystal structure of chlorite I'
Act. Cryst. 11 p 191-4

Storre, B., and Nitsch, K. (1972) 'Die reaktion: 2 zoisit + CO_2 = anorthit + calcit + H_2O'
Contr. Miner. Petrol. 35 p 1-10

Strens, R.G.J. (1965) 'Stability and relations of the Al-Fe epdiotes'
Miner. Mag. 35 p 464-75

Tilley, C.E. (1923) 'The petrology of the metamorphosed rocks of the Start area (South Devon)'
Q.J. Geol. Soc. Lond. 79 p 172-204

---------- (1938) 'The status of hornblende in low grade metamorphic zones of greenschists'
Geol. Mag. 75 p 497-511

Thompson, A.B. (1974) 'Gibbs' energies of aluminous minerals'
Contr. Miner. Petrol. 48 p 123-6

Thompson, J.B. (1957) 'The graphical analysis of mineral assemblages in pelitic schists'
Am. Miner 42 p 842-58

Turner, F.J. (1968) 'Metamorphic petrology: mineralogical and field aspects'
McGraw-Hill; New York

de Waard, D. (1959) 'Anorthite content of plagioclase in basic and pelitic crystalline schists, as related to metamorphic zoning, in the Usu Massif, Timor'
Am. J. Sci. 257 p 553-62

Wagman, D.D., Kilpatrick, J.E., Taylor, W.J., Pitzer, K.S., and Rossini, F.D. (1945) 'Heats, free energies and equilibrium constants of some reactions involving O_2,H_2,C,CO,CO_2, and CH_4'
U.S. Nat. Bur. Stand. Res. Pap. 1634, J. Res. Nat. Bur. Stand. 34

Watts, B.J. (1973a) 'Relationships between fluid-bearing and fluid-absent invariant points, and a petrogenetic grid for a greenschist facies assemblage, in the system CMAS-H_2O-CO_2'
Contr. Miner. Petrol. 40 p 225-38

---------- (1973b) 'Fluid-bearing and fluid-absent invariant points in the system CMAS-H_2O-CO_2 for a greenschist facies assemblage; a correction and some further implications'
Contr. Miner. Petrol. 47 p 153-64

Whittaker, E.J.W. (1977) 'Determination of atomic accupancies'
p 99-114 in 'Thermodynamics in Geology' ed. Fraser, D.G.
D. Reidel Publ. Co. Dordrecht - Holland and Boston - USA

Wiebe, R., and Gaddy, V.L. (1939) 'Pressure solution of CO_2 in water'
J. Am. Chem. Soc. 61 p 315-8

Wood, B.J. (1975) 'Thermodynamic modelling of experimental data'
Fortschr. Miner. 52 p 21-45

Wyllie, P.J., (1962) 'The petrogenetic model, an extension of Bowen's petrogenetic grid'
Geol. Mag 99 p 558-69

Yoder, H.S. (1952) 'The MAS-H_2O system, and the related metamorphic facies'
Am. J. Sci. (Bowen Vol.) p 569-627

Zen, E-An (1966) 'Construction of P-T diagrams for multicomponent systems after the method of Schreinemakers' - a geometric approach'
U.S. Geol. Surv. Bull. 1225

---------- (1969) 'Free energy of formation of pyrophyllite from hydrothermal data: values, discrepancies and implications'
Amer. Miner. 54 p 1592-606

---------- (1971) 'Comments on the thermodynamic constants and hydrothermal stability relations of anthophyllite', Am. J. Sci. 270 p 136-50

---------- (1972) 'Thermodynamic data on 10 Al-bearing minerals' Amer. Miner. 57 p 524-53